DOE/NV/0000939-19

Radiological and Environmental Monitoring at the Clean Slate I and III Sites, Tonopah Test Range, Nevada, With Emphasis on the Implications for Off-site Transport

prepared by

Steve A. Mizell, Vic Etyemezian, Greg McCurdy, George Nikolich,
Craig Shadel, and Julianne J. Miller

submitted to

Nevada Field Office
National Nuclear Security Administration
U.S. Department of Energy
Las Vegas, Nevada

September 2014

Publication No. 45257

Nevada System of Higher Education

Available for sale to the public from:

U.S. Department of Commerce
National Technical Information Service
5301 Shawnee Rd.
Alexandria, VA 22312
Phone: 800.553.6847
Fax: 703.605.6900
Email: orders@ntis.gov
Online ordering: http://www.osti.gov/ordering.htm

Available electronically at http://www.osti.gov/bridge

Available for a processing fee to the U.S. Department of Energy and its contractors, in paper, from:

U.S. Department of Energy
Office of Scientific and Technical Information
P.O. Box 62
Oak Ridge, TN 37831-0062
Phone: 865.576.8401
Fax: 865.576.5728
Email: reports@adonis.osti.gov

DOE/NV/0000939-19

Radiological and Environmental Monitoring at the Clean Slate I and III Sites, Tonopah Test Range, Nevada, With Emphasis on the Implications for Off-site Transport

prepared by

Steve A. Mizell, Vic Etyemezian, Greg McCurdy, George Nikolich,
Craig Shadel, and Julianne J. Miller

Division of Hydrologic Sciences
Desert Research Institute
Nevada System of Higher Education

Publication No. 45257

submitted to

Nevada Field Office
National Nuclear Security Administration
U.S. Department of Energy
Las Vegas, Nevada

September 2014

The work upon which this report is based was supported by the U.S. Department of Energy under Contract #DE-NA0000939. Approved for public release; further dissemination unlimited.

THIS PAGE LEFT INTENTIONALLY BLANK

ABSTRACT

In 1963, the U.S. Department of Energy (DOE) (formerly the Atomic Energy Commission [AEC]) implemented Operation Roller Coaster on the Tonopah Test Range (TTR) and an adjacent area of the Nevada Test and Training Range (NTTR) (formerly the Nellis Air Force Range [NAFR]). Operation Roller Coaster consisted of four tests in which chemical explosions were detonated in the presence of nuclear devices to assess the dispersal of radionuclides and evaluate the effectiveness of storage structures to contain the ejected radionuclides. These tests resulted in the dispersal of plutonium over the ground surface downwind of the test ground zero (GZ). Three tests—Clean Slate I, II, and III—were conducted on the TTR in Cactus Flat. The fourth, Double Tracks, was conducted in Stonewall Flat on the NTTR.

The Desert Research Institute (DRI) installed two monitoring stations in 2008, Station 400 at the Sandia National Laboratories (SNL) Range Operations Center (ROC) and Station 401 at Clean Slate III. Station 402 was installed at Clean Slate I in 2011 to measure radiological, meteorological, and dust conditions. The monitoring activity was implemented to determine if radionuclide contamination in the soil at the Clean Slate sites was being transported beyond the contamination area boundaries. Some of the data collected also permits comparison of radiological exposure at the TTR monitoring stations to conditions observed at Community Environmental Monitoring Program (CEMP) stations around the NTTR.

Annual average gross alpha values from the TTR monitoring stations are higher than values from the surrounding CEMP stations. Annual average gross beta values from the TTR monitoring stations are generally lower than values observed for the surrounding CEMP stations. This may be due to use of sample filters with larger pore space because when glass-fiber filters began to be used at TTR Station 400, gross beta values increased. Gamma spectroscopy typically identified only naturally occurring radionuclides. The radionuclides cesium-134 and -137 were identified in only two samples at each station collected in the weeks following the destruction of the nuclear power reactor in Fukushima, Japan, on March 11, 2011.

Observed gamma energy values never exceeded the local background by more than 4 μR/h. The higher observed gamma values were coincident with wind from any of the cardinal directions, which suggests that there is no significant transport from the Clean Slate contamination areas. Annual average daily gamma values at the TTR stations are higher than at the surrounding CEMP stations, but they are equivalent to or just slightly higher than the background estimates made at locations at equivalent elevations, such as Denver, Colorado. Winds in excess of approximately 15 mph begin to resuspend soil particles and create dust, but dust generation is also affected by soil temperature, relative humidity, and soil water content. Power curves provide good predictive equations for dust concentration as a function of wind speed. However, winds in the highest wind speed category occur infrequently.

ACKNOWLEDGEMENTS

The authors wish to express their appreciation to Dr. Jeff Daniels for his assistance interpreting the radiological results obtained for the air particulate samples and the ambient gamma radiation observations reported by the PIC instrumentation. Dr. Daniels also provided information on background radiological exposures in the continental United States that helped put the observations into context. Ms. Nicole Damon contributed her expertise in document publication and helped to ensure a clear, consistent presentation of the report. Several DRI faculty provided technical reviews of the document that facilitated a clear and substantial presentation of the monitoring observations.

CONTENTS

LIST OF FIGURES

LIST OF TABLES

LIST OF ACRONYMS

AEC	Atomic Energy Commission
CAU	Corrective Action Units
CEMP	Community Environmental Monitoring Program
CS I	Clean Slate I
CS III	Clean Slate III
DOE	Department of Energy
DRI	Desert Research Institute
FEM	Federal Equivalent Methods
FIDLER	field instrument for the detection of low-energy radiation
FRM	Federal Reference Methods
GOES	Geostationary Operational Environmental Satellite
GZ	ground zero
LLW	low-level waste
NAAQS	National Ambient Air Quality Standards
NAFR	Nellis Air Force Range
NCRP	National Council on Radiation Protection and Measurements
NNSA/NFO	National Nuclear Security Administration, Nevada Field Office
NNSS	Nevada National Security Site
NTS	Nevada Test Site
NTTR	Nevada Test and Training Range
OSHA	Occupational Safety and Health Agency
PIC	pressurized ionization chamber
PoR	period of record (of data collection)
ROC	Range Operations Center
RH	relative humidity
SNL	Sandia National Laboratories
SSW	south southwest
TTR	Tonopah Test Range
TDR	time domain reflectometry
WRCC	Western Regional Climate Center
WNW	west northwest

LIST OF MEASUREMENT UNITS

Bq/m^3	Becquerel per cubic meter
keV	kiloelectron volt
fCi/m^3	femtoCurie per cubic meter = 1 x 10-15 Curie per cubic meter
pCi/g	picoCurie per gram = 1 x 10-12 Curie per gram
µCi/ml	microCurie per milliliter = 1 x 10-6 Curie per milliliter
$\mu g/m^2$	microgram per square meter
ft	feet
m	meter
µm	micrometer
in	inch
cm	centimeter
km	kilometer
mi	mile
lpm	liters/minute
cfm	cubic feet/minute
yd	yard

THIS PAGE LEFT INTENTIONALLY BLANK

INTRODUCTION

In May and June 1963, the U.S. Department of Energy (DOE) (formerly the Atomic Energy Commission [AEC]) implemented Operation Roller Coaster to evaluate the radionuclide dispersal in the event that nuclear devices were subjected to chemical explosions during storage or transit (Dick *et al.*, 1963; Johnson and Edwards, 1996). Operation Roller Coaster consisted of four tests: Double Tracks, which was conducted in the northwest corner of the Nevada Test and Training Range (NTTR) (formerly the Nellis Air Force Range [NAFR]) in Stonewall Flat, and Clean Slate I, II, and III, which were conducted on the Tonopah Test Range (TTR) in Cactus Flat. Both test areas are southeast of Tonopah in Nye County, Nevada (Figure 1). Double Tracks, which is approximately 14 miles west-southwest of monitoring Station 400, is not shown on Figure 1 and is beyond the west edge of Figure 2. The emphasis of monitoring efforts documented in this report is on the TTR Clean Slate sites.

The Clean Slate tests were intended to evaluate the capability of weapons storage bunkers to contain some of the radionuclide material dispersed in a chemical explosion. These tests involved one device containing plutonium and several simulated devices containing uranium (Dick *et al.*, 1963; Johnson and Edwards, 1996). For each test, data collection was distributed along arcs within a quarter-circle -shaped area emanating from the test ground zero (GZ) and centered along a radius extending from GZ to the south or southeast (Dick *et al.*, 1963; Johnson and Edwards, 1996), the expected downwind directions.

As anticipated, the destruction of nuclear devices as a result of chemical explosions in the Operation Roller Coaster tests caused plutonium and uranium to be scattered over the land surface downwind of GZ. Most of the contaminated debris and soil fell within 2,500 ft (762 m) of GZ, but some soil was spread to distances of up to 10 miles (16 km) downwind (Barnett *et al.*, 1964). Post-test surveys using mobile low-energy gamma detection techniques in conjunction with analytical chemistry methods were used to rapidly delineate surface contamination boundaries (Dick *et al.*, 1963). Concentrations of plutonium greater than 1 $\mu g/m^2$ were mapped at each test location. Following the Clean Slate I test, a long, narrow field of plutonium concentrations greater than 1 $\mu g/m^2$ encompassed an arc of approximately 12° at 34,000 ft (10,363 m), even though the plume extended an undetermined distance beyond 34,000 ft (10,363 m). The plume was oriented in a generally south-southeasterly direction. Plutonium concentrations greater than 100 $\mu g/m^2$ were mapped to a distance of approximately 1,800 ft (549 m) (Dick *et al.*, 1963).

The plutonium distribution (greater than 1 $\mu g/m^2$) resulting from the Clean Slate II test extended more than 12,500 ft (3,800 m) downrange from GZ. It covered an arc somewhat greater than 120° to a distance of 5,000 feet. At a distance of 12,500 ft (3,800 m), the arc narrowed to approximately 30° and was oriented in a southeasterly direction. The area of highest concentration (greater than 100 $\mu g/m^2$) covered an arc of approximately 20° and extended about 4,600 ft (1,400 m) in a southeasterly direction from GZ (Dick *et al.*, 1963). Although the pattern at Clean Slate III was not quite as wide as the plutonium distribution pattern at Clean Slate II, it was similar. The highest concentrations (greater than 100 $\mu g/m^2$) at Clean Slate III extended approximately 5,800 ft (1,768 m) downrange from GZ in a southeasterly direction. The plume of greater than 1 $\mu g/m^2$ was oriented in the same direction and extended more than 12,500 ft (3,800 m) downrange (Dick *et al.*, 1963).

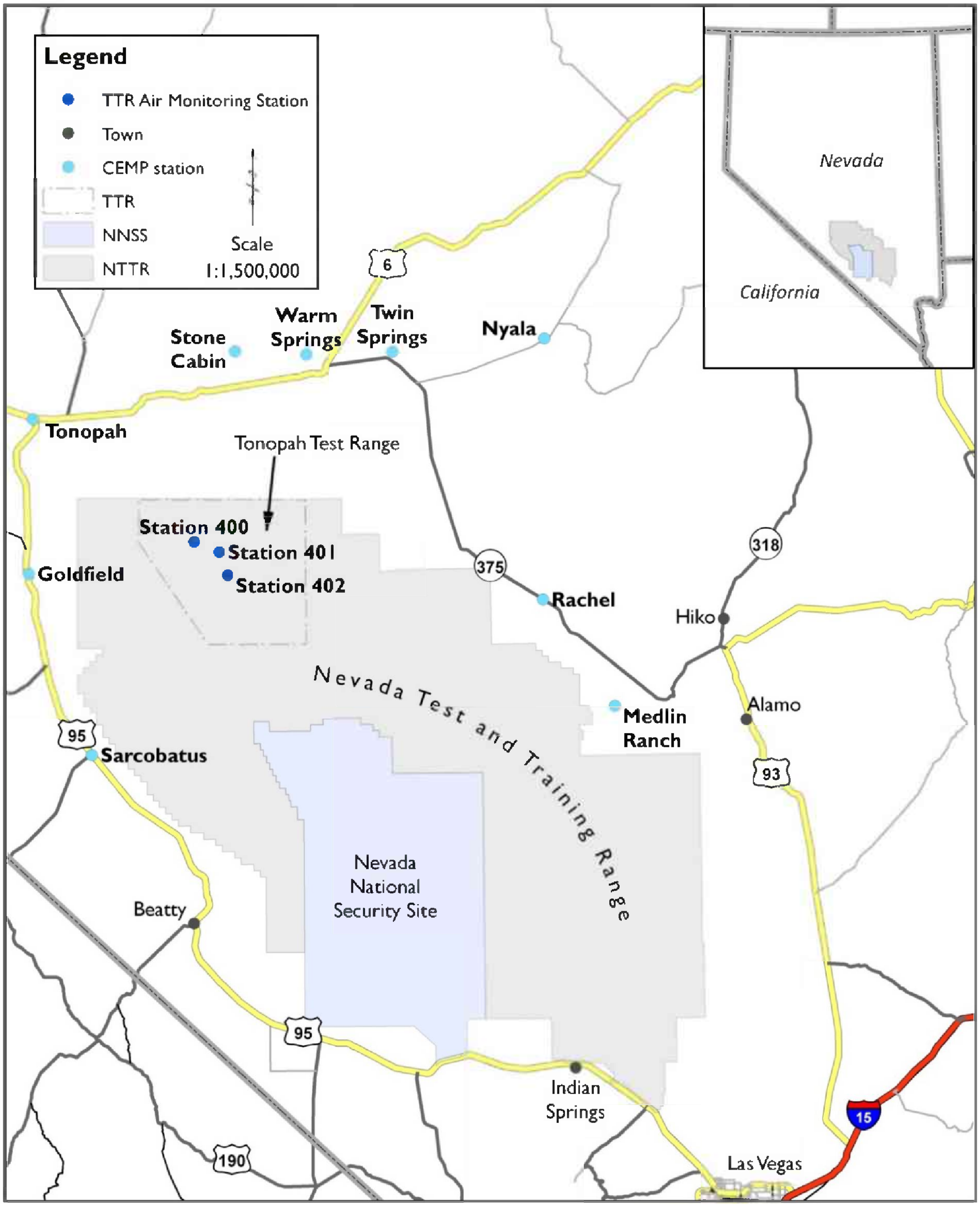

Figure 1. The Tonopah Test Range (TTR) is located at the north end of the Nevada Test and Training Range (NTTR) in southern Nevada.

Figure 2. The TTR environmental monitoring stations are located on the south side of the Sandia National Laboratory (SNL) compound and at the north ends of the Clean Slate I and III contamination areas.

The initial post-test cleanup at each location involved disposing the contaminated debris in the crater generated at GZ, scraping the surface soil around GZ to a depth of several inches, and placing the soil material in the pit or mounding it over the contaminated debris. The mound of contaminated materials was covered with additional soil, and then compacted and watered (Johnson and Edwards, 1996). Based on soil survey data collected using a handheld field instrument for the detection of low-energy radiation (FIDLER) meter supplemented with an analytical analysis of soil samples, the GZ disposal area was fenced to delineate the extent of plutonium concentrations greater than or equal to 1,000 $\mu g/m^2$ (Culp *et al.*, 1997). In 1973, following a subsequent pedestrian survey that also used a FIDLER instrument, a second fence was constructed at the approximate limit of 40 pCi/g of plutonium (Culp *et al.*, 1997). The area delineated by the second fence is shown in Figure 2 by the light blue polygons. Interim corrective actions were performed at Clean Slate I in 1997. These remediation activities reduced the levels of transuranic (plutonium) contamination in the soil to levels less than or equal to 400 pCi/g (SNL, 2011). Corrective actions other than the post-test cleanup have not yet been performed at Clean Slate II and III. Although plutonium concentrations are reported in these surveys, it is most likely that the surveys were conducted with the intent of detecting americium.

Weapons-grade plutonium consists chiefly of plutonium-239 (^{239}Pu), but other isotopes, including ^{241}Pu, are typically present as well. Upon decay, ^{239}Pu releases an alpha particle and a 17keV gamma ray (Kathren, 1984; NARP, 2005), but both of these decay products are difficult to detect. The alpha particle is low energy, will only travel approximately 4 cm (1.5 in) through air, and can be stopped by a thin layer of dust or a sheet of paper (NARP, 2005). Background signals in the same energy range make measuring the 17keV gamma ray highly uncertain (NARP, 2005). Field surveys for plutonium typically rely instead on the decay signal of americium-241 (^{241}Am), a daughter product of ^{241}Pu (NARP, 2005). As ^{241}Am decays to neptunium-237, it releases a 60keV gamma ray that is more easily detected than the decay energies of ^{239}Pu (Kathren, 1984). Estimates of plutonium concentrations are made based on the relative concentrations of plutonium and americium in either the source material or analytical determinations of coincident soil samples.

Aerial surveys of Operation Roller Coaster contamination areas were conducted in 1977 (EG&G, 1979, as reported in Culp *et al.*, 1997) and 1993 (Proctor and Hendricks, 1995). These surveys used gamma detectors to identify americium-241 (^{241}Am) and coincident soil sample analyses to estimate the plutonium concentration. Based on the 1977 survey, the total area of diffuse plutonium for all Operation Roller Coaster sites was estimated to be 20 x 10^6 m^2 (4,942.11 acres) (Duncan *et al.*, 2000). The 1993 survey estimated the maximum concentration at the Clean Slate I GZ to be between 200 pCi/g and 400 pCi/g. At Clean Slate II and III, the maximum concentrations at GZ were reported to be greater than 2,000 pCi/g. This survey also reported plutonium concentrations between 200 pCi/g and 400 pCi/g outside the outer perimeter fence at Clean Slate I and II. At Clean Slate III, plutonium concentrations outside the outer perimeter fence approached 200 pCi/g (Proctor and Hendricks, 1995).

Plutonium released in the environment has a strong tendency to attach to small soil particles (Tamura, 1974, 1975, 1976). Tamura (1974) noted that the highest concentrations of plutonium in the analyzed samples were associated with medium-sized silt (5 µm to 20 µm) particles. He also reported that plutonium associated with coarse silt (20 µm to 50 µm) and fine sand (50 µm to 125 µm) particles were significant because these size fractions made up the greater percentage of the soil sample. The potential for plutonium transport of plutonium by water runoff, wind resuspension, and saltation is enhanced because of the attachment to soil particles. These processes can move plutonium from the original point of deposition and perhaps beyond the administrative control boundaries of a contamination site. Plutonium resuspension with fine soil particles presents an additional hazard associated with human inhalation.

As part of the Environmental Management Operations Soils Activity, the Department of Energy (DOE), National Nuclear Security Administration, Nevada Field Office (NNSA/NFO), requested that the Desert Research Institute (DRI) construct, deploy, and maintain environmental monitoring stations at selected locations on the TTR. The objectives of the monitoring effort are: (1) to evaluate whether there is wind transport of radiological contaminants from the Soils Corrective Action Units (CAUs) associated with Operation Roller Coaster, and if so, under what conditions it occurs and (2) to assess the likely dose exposure for personnel working in the general area.

In 2008, DRI installed monitoring equipment at the Sandia National Laboratories (SNL) Range Operations Center (ROC) and at the Clean Slate III contamination area. A third station was deployed at Clean Slate I in 2011. These stations have been operated continuously by DRI since installation. This report presents the monitoring observations over the period of data collection (from installation to the end of calendar year 2012) and draws initial conclusions regarding the monitoring objectives. This report includes sections on: (1) methodology, in which monitoring station design and data collection parameters are delineated; (2) meteorology, where observed weather conditions are presented; (3) a radiological assessment of airborne particulates that describes the results of the radiological analysis of airborne dust; (4) an assessment of gamma radiation exposure in which observations of ambient gamma radiation conditions are reported; and (5) an evaluation of soil transport by wind suspension and saltation and the relationship between wind speed and the movement of soil particulates. Intuitively, wind is the mechanism most likely to move contaminated soil particles outside the boundaries of the contamination areas. However, wind transport may be limited by other environmental conditions. Measurements of radiological characteristics of airborne particulates and ambient radiation provide a direct observation of the radiological conditions outside of the contamination areas.

METHODOLOGY

Plutonium was the primary radionuclide released during the Clean Slate tests. Because plutonium has a tendency to attach to fine soil particles when released on the ground surface, wind-driven resuspension of contaminated dust is a likely mechanism for plutonium transport and redistribution beyond the delineated administrative boundaries of the soil contamination areas. Additionally, suspension of inhalable, plutonium-contaminated dust creates a significant potential human health risk. Therefore, the radiological analysis of airborne soil particulates is the fundamental observation made in order to assess the significance of wind redistribution of contaminated soil at and downwind of the Clean Slate sites. However, atmospheric dust suspension is subject to a variety of meteorological and environmental parameters, including wind speed and direction; precipitation, relative humidity, and soil moisture; and air and soil temperature. These parameters are measured at each monitoring station. Solar radiation and barometric pressure are collected to enhance the understanding of meteorological conditions. Airborne-particle size is determined to ascertain the concentration of inhalable dust and saltation events are monitored to indicate their significance. The fundamental design of these stations is similar to the design of the stations used in the Community Environmental Monitoring Program (CEMP) (NSTec, 2012). Table 1 lists the parameters measured and approximate date of initial data collection at each of the three monitoring stations.

Table 1. Radiological, meteorological, and environmental sensors deployed at the TTR air monitoring stations.

Instrument/Measurement	Station 400	Station 401	Station 402
Wind speed	5/27/2008	6/10/2008	5/18/2011
Wind direction	5/27/2008	12/22/2009	5/18/2011
Precipitation	5/27/2008	12/22/2009	5/18/2011
Temperature	5/27/2008	6/10/2008	5/18/2011
Relative humidity	5/27/2008	6/10/2008	5/18/2011
Solar radiation	5/27/2008	NA	5/18/2011
Barometric pressure	5/27/2008	NA	5/18/2011
Soil temperature	5/27/2008	12/22/2009	5/18/2011
Soil moisture content	5/27/2008	12/22/2009	5/18/2011
Airborne-particle size profiler	5/27/2008	6/10/2008	5/18/2011
Airborne-particle collector	5/27/2008	7/30/2008	8/23/2011
Saltation senor	NA	8/x/2011	8/x/2011
Gamma radiation PIC	5/27/2008	12/22/2009	12/15/2011
Data logger	5/27/2008	6/10/2008	5/18/2011
GOES transmitter	5/27/2008	12/22/2009	5/18/2011

NA = sensors not installed, data not collected.

Station 400 was installed in May 2008 at the SNL ROC. Station coordinates are given in Table 1. The ROC, adjacent TTR airfield, and surrounding work area are downwind of the Clean Slate contamination sites when winds are out of the south-southeast, which is one of the two dominant wind directions through the area. These facilities are 8 km to 9 km (5 mi to 6 mi) from the Clean Slate contamination sites, so they are the closest, regularly manned work locations in a dominant downwind direction. Station 400 was originally located just north of the center of the SNL compound, approximately 145 m (159 yd) west-northwest of the ROC. In 2012, the station was moved approximately 200 m (220 yd) to the southeast at the request of SNL. In the new location, Station 400 is approximately 90 m (98 yd) south of the ROC near the southeast corner of the SNL compound (Figure 2). Sandia National Laboratories provides line power to operate the equipment at Station 400, which consists of a meteorological tower and air sampling equipment installed on a 2.1 m x 4.3 m (7 ft x 14 ft) trailer (Figure 3).

Stations 401 (installed in June 2008) and 402 (installed in May 2011) are located at the demarcation fences on the north perimeters of the Clean Slate III and Clean Slate I sites, respectively (Figure 2). These locations were chosen because they place the monitoring instrumentation in proximity to the contamination sites and on the downwind side of the sites during south-southeast winds, which are one of the two dominant wind directions through the area. Wind data for the Tonopah Airport (Engelbrecht *et al.*, 2008) was used to determine the original downwind station locations. Data collected since station installation have confirmed that the stations are downwind of the Clean Slate sites (see the discussion below in the section summarizing meteorological observations). Both Stations 401 and 402 are battery powered and the batteries are continuously recharged by solar panels. Table 2 gives the coordinates for these monitoring stations. At Stations 401 and 402 the air samplers, solar panels, and the batteries are on trailers. This arrangement requires that the meteorological towers be installed on freestanding tripods that are separate from the trailer (Figures 4 and 5).

Table 2. Location coordinates for the TTR Air Monitoring stations.

Station	Latitude	Longitude	Elevation (ft)
Station 400 – original	37° 47’ 15” N	116° 45’ 26” W	5,525
– current	37° 47’ 10” N	116° 45’ 21” W	5,534
Station 401	37° 45’ 39” N	116° 40’ 58” W	5,390
Station 402	37° 42’ 33” N	116° 39’ 32” W	5,387

Figure 3. Station 400 is a trailer-mounted radiological and meteorological measurement system located near the Range Operations Center (ROC) at the SNL compound on the TTR.

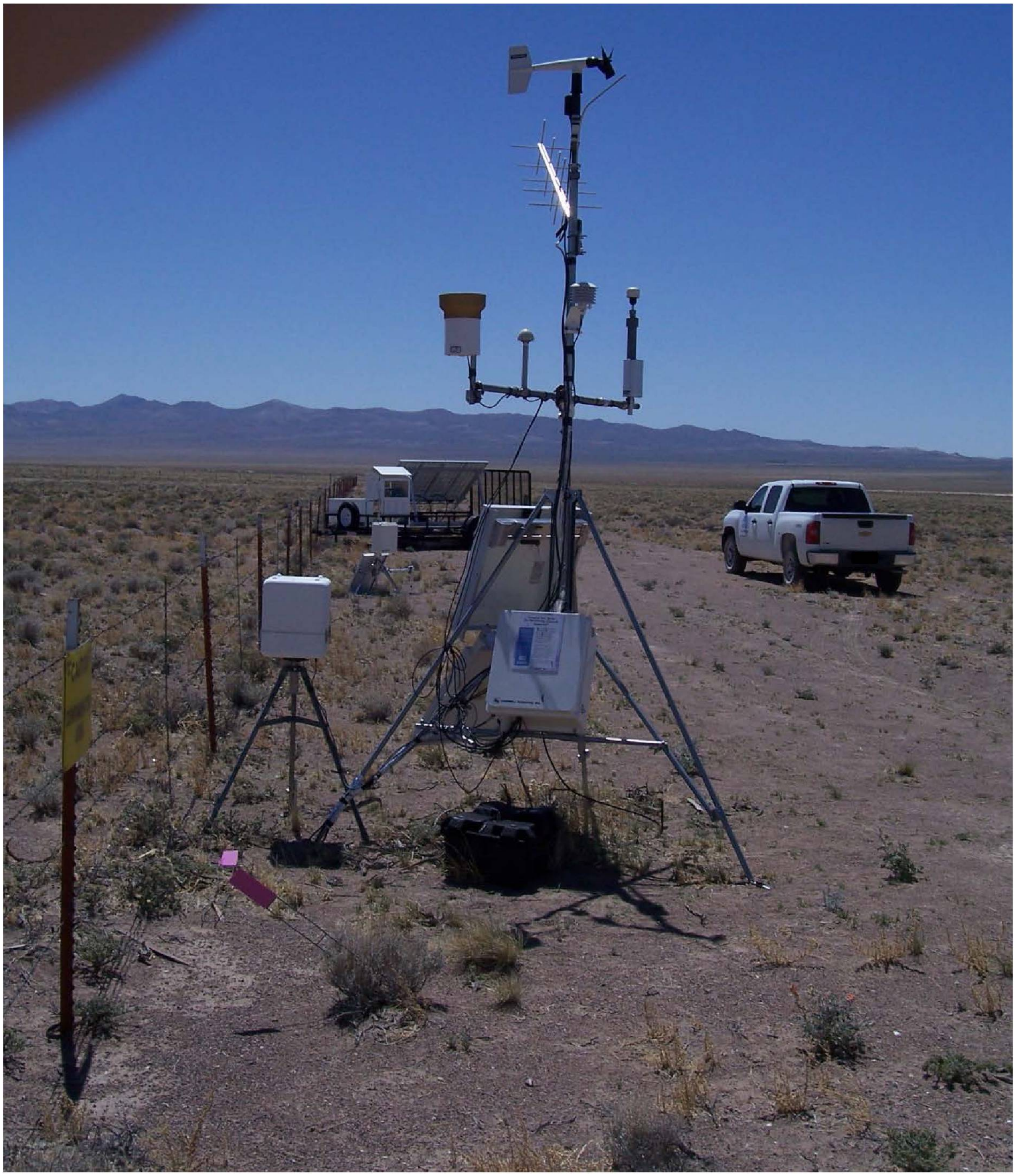

Figure 4. The solar powered air sampler, saltation sensor, and meteorological tower (background, center, and foreground, respectively) at Station 401 are located along the north fence that bounds the Clean Slate III contamination area.

Figure 5. The solar powered air sampler, saltation sensor, and meteorological tower (center right, foreground left, and center left, respectively) at Station 402 are located along the north fence that bounds the Clean Slate I contamination area.

Suspended, airborne particulates are collected on 10 cm (4 in) diameter glass-fiber filters (pore size: 0.3 µm) and cellulose-fiber filters (pore size: 20 to 25 µm) using Hi-Q™ continuous-flow, low-volume air samplers. Initially, cellulose filters were used at all three TTR monitoring stations. Glass filters were deployed at Station 400 beginning in March 2011. This change was made to ensure that the inhalable fraction of airborne particulates was being collected (Hartwell, 2014, written communication). This change was made coincidently with the destruction of the reactor in Fukushima, Japan, which enhanced data collection following the reactor destruction. Glass filters were deployed at Stations 401 and 402 in April 2013 to complete the transition from cellulose filters. Air is drawn through the filters at a rate of approximately 0.05663 m^3 (2 ft^3) per minute. The Hi-Q™ equipment is designed to maintain this flow rate as dust gathers on the filter. The total volume of air passed through the filter and the total hours of operation are recorded as filters are retrieved and new filters are deployed every two weeks. Beginning in February 2011, filters have been weighed before and after deployment to determine the mass of particulates collected. Sample mass was not determined prior to February 2011. The filters are accumulated and periodically delivered to the Radiological Services Laboratory (RSL) at the University of Nevada, Las Vegas, for gross alpha, gross beta, and gamma spectral analyses. If the gamma spectral analysis indicates the presence of ^{241}Am, which could suggest the presence of plutonium particles, samples are submitted for alpha spectral analysis. (To date, the gamma spectroscopy analysis has not indicated the presence of americium, so alpha spectroscopy analysis has not been performed.)

Gamma radiation is measured using a Reuter-Stokes pressurized ionization chamber (PIC) instrument. The PIC detector is used because it responds instantaneously to gamma energy emissions and because of its sensitivity, which may detect low-level, ambient exposures that go undetected by other monitoring methods. The instantaneous response of the PIC is expected to help resolve the timing of high radiological assessments in the particulate samples collected every two weeks. The PIC detectors are typically deployed to detect changes in ambient gamma radiation due to human activities. In the absence of such activities, the detectors will respond to ambient or natural gamma radiation, which varies among locations as a result of differences in altitude (cosmic radiation) and in the natural radioactivity in the soil and geological material (terrestrial radiation) at the instrumentation site (UNSCEAR, 2000).

Readings from the PICs were observed to fluctuate widely between negative and positive values immediately following power surges that cycled instruments on and off. Additionally, PIC readings reflected gamma sources periodically used in the field to check instrument performance. Data subject to these affects were identified in quality control examinations and removed from the data sets before analysis. The early PIC data record (May 21, 2008 to December 31, 2008) from Station 400 (not shown in the accompanying graphics) was considered excessively erratic and was removed from the data set prior to analysis. The period of erratic values was assumed to result from start-up problems with instrument deployment and management. Therefore, the period of record (PoR) and the data available for analysis varied among the stations.

The PIC, meteorological, and environmental sensors are programed to make measurements every three seconds. Average, maximum, minimum, and total values as appropriate to the measured parameter for each consecutive 10-minute period are recorded in the on-site data logger. Ten-minute values are downloaded approximately every two weeks. After recovery, they are transmitted electronically to the Western Regional Climate Center (WRCC), which performs a quality control review. Following quality confirmation, the 10-minute data are released to a topic specialist for analysis. Average, maximum, minimum, and total 3-second values are also computed for each 60-minute period. These 60-minute observations are transmitted via the Geostationary Operational Environmental Satellite (GOES) to WRCC once each hour. Sixty-minute observations are primarily used to monitor instrument performance remotely.

SUMMARY OF SITE METEOROLOGICAL CONDITIONS

During nearly five years of data collection at TTR stations 400 and 401 and 18 months of data collection at Station 402, the highest observed temperature was approximately 38 °C (100 °F) and the lowest observed temperature was approximately -25 °C (-13 °F) (Table 3). Definitions of summary meteorological parameters are provided in Appendix A. Monthly summaries of measured meteorological parameters are presented in Appendix B.

Temperature data collected at the three TTR monitoring stations gives evidence of consistent nighttime temperature inversions. Both the monthly average and maximum of daily maximum temperatures at all three monitoring stations are very similar (Appendix C, Figure C-1 and C-3). However, despite an elevation difference of only approximately 46 m (150 ft) between Station 400, on the alluvial slope, and Stations 401 and 402, on the valley floor, the monthly extreme minimum temperatures are typically almost 5 °C colder at Stations 401 and 402 (Figure C-2). This difference in monthly extreme minimum temperatures indicates the presence of colder air on the valley floor. Figures C-2 through C-4, indicate that these nighttime temperature inversions are persistent throughout the year.

For the period May 2008 through December 2012, the annual average precipitation at Stations 400 and 401 was 98.87 mm (3.89 in) and 138.69 mm (5.46 in), respectively (Table 4). During the period of record at Station 402 (May 2011 through December 2012), the annual average precipitation was 94.15 mm (3.71 in) (Table 4). The difference between the maximum and minimum annual precipitation at Station 400 was only 3.05 mm (0.12 in) during the period of data collection. At Stations 401 and 402, this difference was 85.34 mm (3.36 in) and 109.98 mm (4.33 in), respectively. Maximum monthly and maximum daily precipitation at Stations 401 and 402 was significantly greater than the values reported for Station 400 (Table 4). Precipitation may be received in any month. However, at least one of the summer months is likely to have no precipitation. June is the month most frequently reported with zero precipitation (Appendix B, Tables B-1, B-2, and B-3). Additionally, the significant differences in precipitation amounts recorded at the three stations (Table 4), at every timescale, suggest considerable spatial variability in the distribution of precipitation.

Table 3. Summary of temperature (degrees Celsius) extremes observed at TTR monitoring stations (Tables B-1, B-2, and B-3).

Air Temperature	Station 400		Station 401		Station 402[1]	
	Temperature	Date	Temperature	Date	Temperature	Date
Annual Average	11.5		10.4		10.4	
Highest Average of Daily Maximums	33.2	July 2009	33.2	July 2010	33.0	Aug. 2011
Highest of Daily Maximums	37.3	July 11, 2012	37.9	July 3, 2012	38.3	July 11, 2012
Lowest Average of Daily Minimums	-9.3	Dec. 2009	-12.2	Dec. 2009	-11.3	Dec., 2011
Lowest of Daily Minimums	-21.7	Dec. 9, 2009	-25.3	Dec. 9, 2009	-18.9	Jan. 7, 2012

1 = Station 402 was operational from May 2011 through December 2012.

Table 4. Summary statistics for precipitation (mm) at Stations 400, 401, and 402 (Tables B-1, B-2, and B-3).

Precipitation	Station 400		Station 401		Station 402	
	Precipitation	Date	Precipitation	Date	Precipitation	Date
Annual Average	98.87		138.69		94.15	
Maximum Annual	99.83	2009	155.45	2009	191.01	2012
Minimum Annual	96.78	2011	70.11	2011	81.03[1]	2011
Maximum Monthly	32.77	July 2011	45.21	July 2012	93.22	July 2012
Maximum Daily[2]	16.76	Sept. 11, 2012	33.78	Sept. 11, 2012	64.26	July 23, 2012

1 = Station 402 was operational only from May through December in 2001.
2 = Daily precipitation values are not published in this report.

Table 5 indicates that the average wind speeds at each of the TTR monitoring stations reach the upper range of a light wind, 2.2 m/s to 3.1 m/s (5 mph to 7 mph) on the U.S. Weather Bureau scale of wind speed (http://www.windows2universe.org/earth/Atmosphere/wind_speeds.html accessed June 30 2014); maximum monthly average wind speeds at 4 m/s to 5 m/s (9 mph to 11 mph) are only slightly higher than the annual and long-term averages. However, peak gusts may reach the category of a strong wind, 11.2 m/s to 13.9 m/s (25 mph to 31 mph) (Table 5 and Tables B-1, B-2, and B-3). The strongest winds may occur during any time of the year and are typically associated with either winter/spring frontal storms or summer thunderstorms. Appendix B lists the observed monthly average and maximum wind speeds for the period of record at each monitoring station.

Table 5. Summary statistics for wind speed (m/s) at Stations 400, 401, and 402 (Tables B-1, B-2, and B-3).

Wind	Station 400		Station 401		Station 402	
	Speed	Date	Speed	Date	Speed	Date
Period of Record Mean	3.1		3.2		3.1	
Highest Annual Mean	3.4		3.4		3.1	
Maximum Monthly Average	4.4	June	4.4	May	5.1	May
Peak Wind Gust	23.5	Apr. 20, 2010	25.4	Apr. 20, 2010	27.0	Sept. 24, 2011

Examination of wind roses for each of the TTR monitoring stations (Figure 6A, left column) reveals that winds are most frequently from the south and southeast or the west and northwest. Winds from the east and northeast are least common at Stations 400 and 401, whereas winds from the west and west-southwest are least common at Station 402. The wind rose pattern at Station 401 appears to be rotated slightly clockwise relative to the wind roses at Station 400 and Station 402. Station 402 has a significantly higher frequency of light winds (<8 mph) from the northeast. In Figure 6A, the wind roses in the left column are derived from the period of record observations at each station, whereas wind roses in the right column depict conditions for June 1, 2011, through December 31, 2012, the period of record for Station 402. Comparison of the period or record and short-term wind roses indicates that the general wind patterns are similar. However, the June 2011 through December 2012 wind roses indicate that winds with a southerly orientation were more common than indicated in the PoR wind roses at Stations 400 and 401. The increase in frequency of the southerly oriented winds between June 2011 and December 2012 was generally accompanied by a decrease in the frequency of winds with northerly and northwesterly orientations. Wind roses representing summer (April through September) and winter (October through March) are presented in Figure 6B. Although the winds from the dominant directions (north and northwest or south and southeast) are common in both summer and winter, the southerly winds appear to be stronger and more frequent in the summer and the northerly winds seem to be stronger and more frequent in the winter.

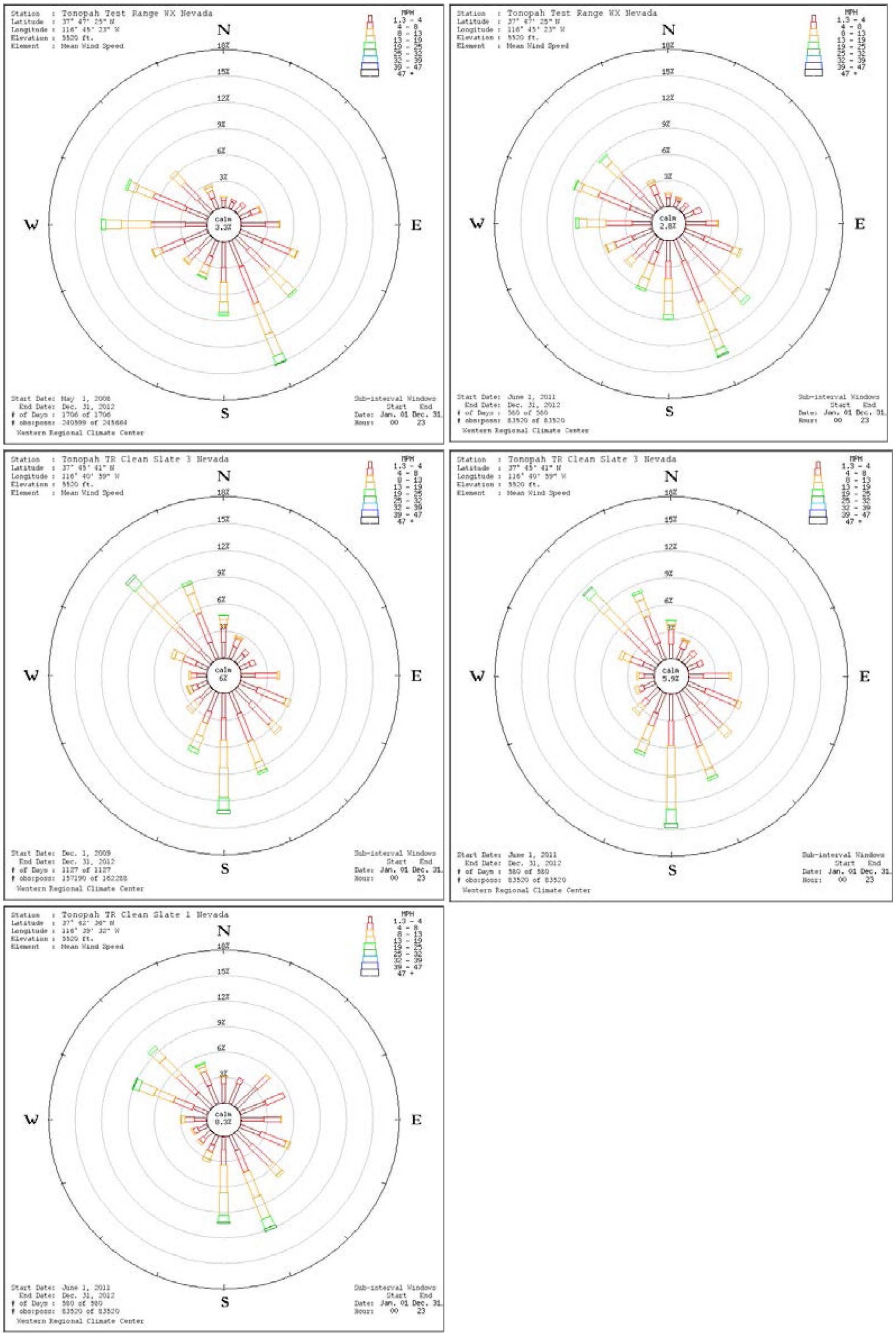

Figure 6A. Wind roses for the Stations 400 (top), 401 (middle), and 402 (bottom) based on 10-minute mean wind speed and 10-minute wind vector directions for all hours of the day during the period of record (left column) and the common period (June 1, 2011 through December 31, 2012) (right column). At Station 402, the common period is the period of record.

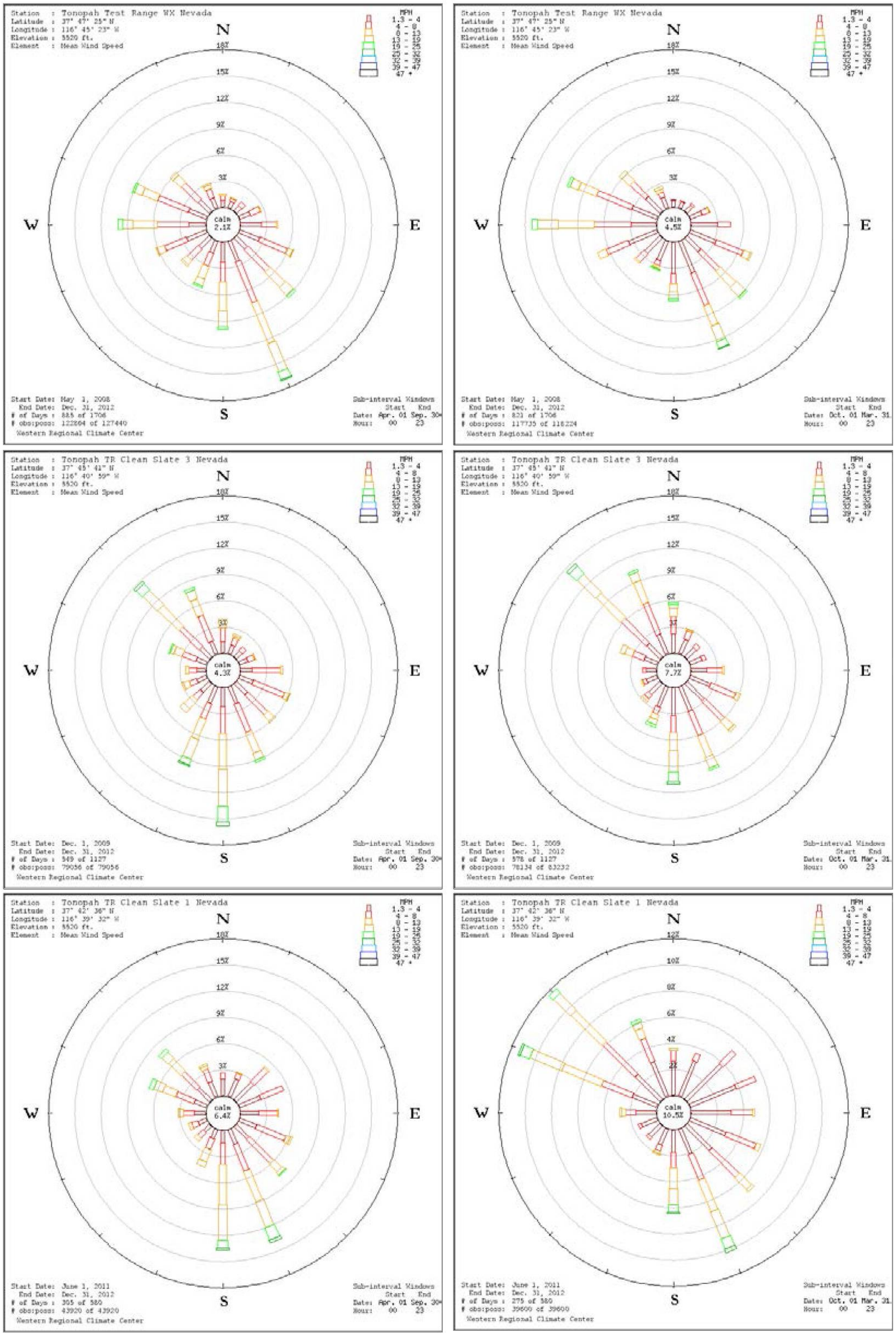

Figure 6B. April through September (left column) and October through March (right column) wind roses for Stations 400 (top), 401 (middle), and 402 (bottom) using 10-minute mean wind speed and 10-minute wind vector directions and all hours of the day during the period of record at each station.

A comparison of daytime and nighttime wind roses (Figure 6C) reveals noticeable differences. The range of observed wind speeds and the orientation of the higher wind speeds are similar for both the daytime and nighttime hours. However, the frequency of light breezes is significantly higher at night. Additionally, the lighter nighttime breezes tend to have a different orientation than the lighter daytime breezes. At Station 400, the nighttime wind rose indicates a slight increase in the frequency of winds from the west-southwest relative to the daytime wind rose. At Stations 401 and 402, the nighttime breezes have an easterly orientation much more frequently than the daytime breezes. These diurnal variations in wind speed and orientation suggest that the daytime winds are dominated by synoptic patterns (atmospheric pressure systems with horizontal dimensions typically ranging from 600 miles [1,000 km] to 1,550 miles [2,500 km]), whereas the nighttime winds are dominated by the weaker drainage flow patterns influenced by local topography.

Figure 6D compares the 10-minute average and 10-minute peak wind speeds at each station. There is little or no difference in the frequency of orientation of the average and peak wind speeds. These wind roses indicate that each site exhibits similar major wind characteristics, but that the detail characteristics are slightly different. In summary, the strongest and most frequent winds at each site occur from the south/southeast or west/northwest and have an approximately equal likelihood of occurring during the night or day; lighter breezes predominately occur at night and frequently come from nondominant directions; southerly oriented winds appear to occur somewhat more frequently during the summer, whereas northwesterly oriented winds appear to be slightly more common during the winter. These general conditions appear to characterize both typical wind conditions and gust conditions.

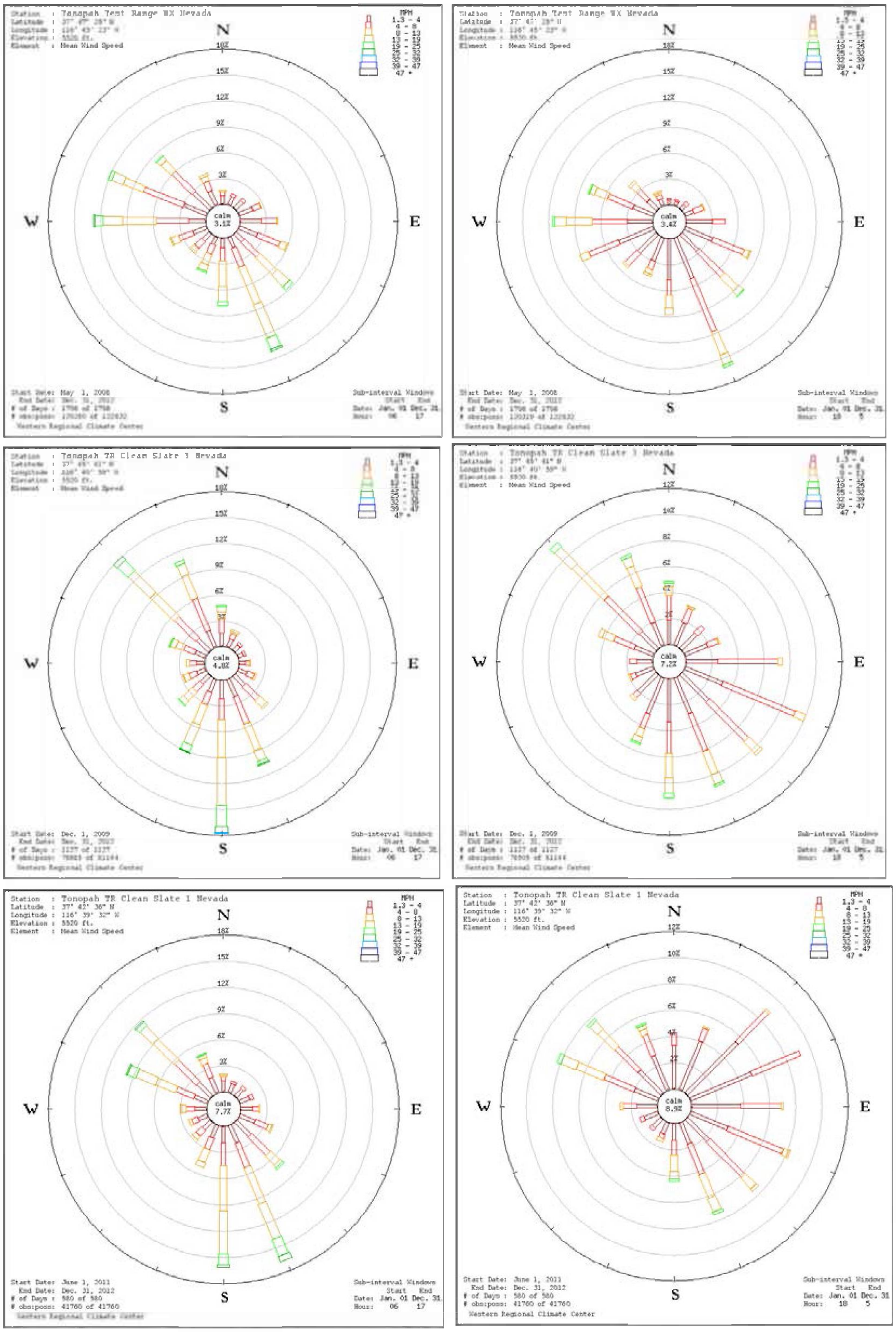

Figure 6C. Daytime (left column) and nighttime (right column) wind roses for Stations 400 (top), 401 (middle), and 402 (bottom) using 10-minute mean speed and 10-minute wind vector directions for the period of record at each station.

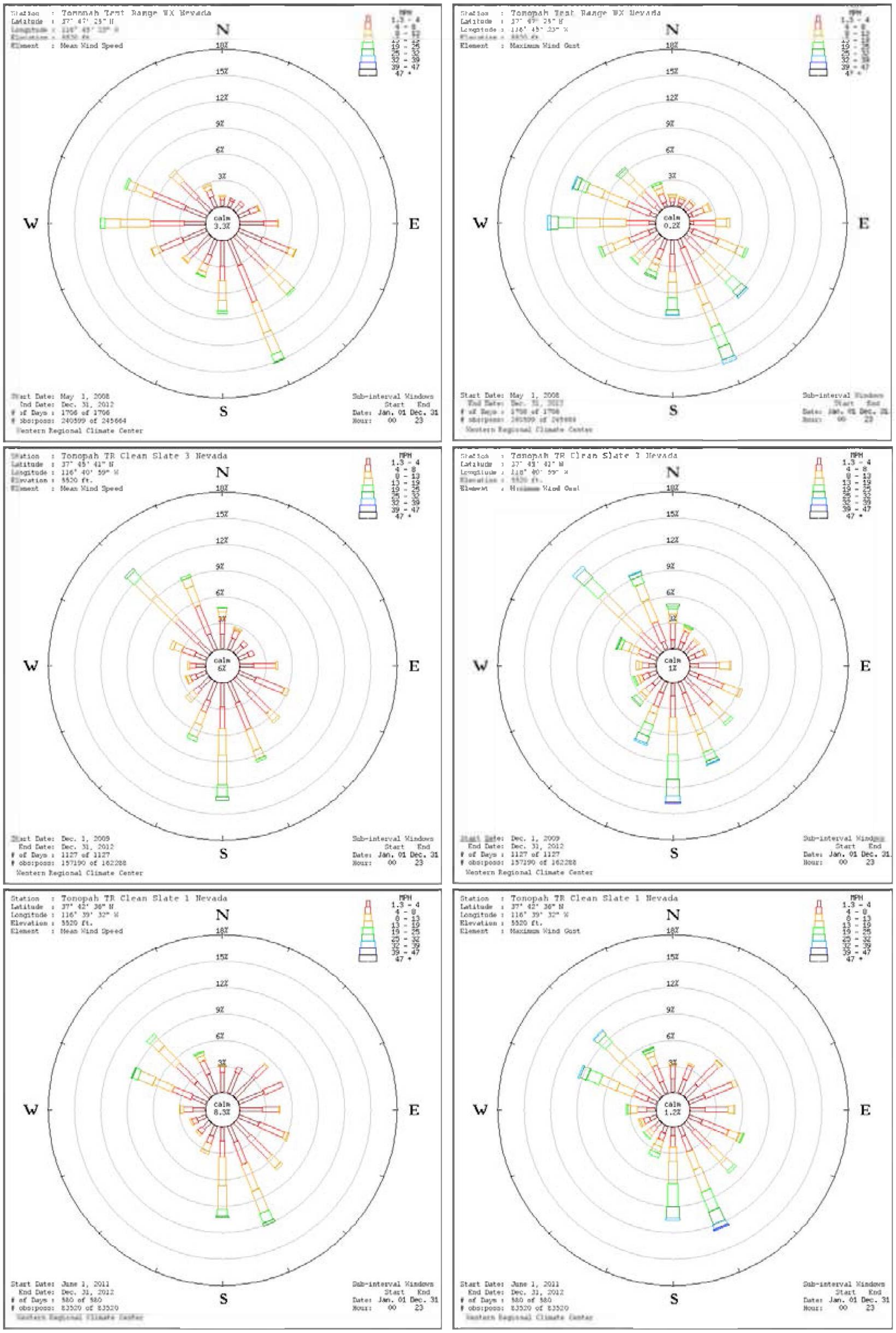

Figure 6D. Comparison of 10-minute mean wind speed (left column) and 10-minute maximum gust (right column) wind roses for Stations 400 (top), 401 (middle), and 402 (bottom) based on 10-minute wind vector directions for the period of record at each station.

Observed station humidity values are typical of Great Basin/southwest desert environments that experience extended periods of extremely dry conditions. Table RH summarizes relative humidity observations. All the monitoring stations frequently recorded single-digit humidity at almost any time of the year. High humidity was also frequently recorded with associated winter/spring synoptic storms and summer/fall monsoon storms. Monthly values of relative humidity are available in Appendix B. Table BP summarizes barometric pressure observations at the TTR monitoring stations. Monthly values of barometric pressure are included in Appendix B.

Table RH. Summary of relative humidity (%) extremes observed at TTR monitoring stations (Table B-1, B-2, and B-3).

	Station 400		Station 401		Station 402[1]	
	Humidity	Date	Humidity	Date	Humidity	Date
Annual Avg Maximum	94		92		92	
Annual Avg Minimum	8		7		7	
Maximum Monthly	100	multiple	97	multiple	100	multiple
Minimum Monthly	3	July 2012	1	June 2008	0	multiple

1 = Station 402 was operational from May 2011 through December 2012.

Table BP. Summary of barometric pressure (mbar) extremes observed at TTR monitoring stations (Table B-1, B-2, and B-3).

	Station 400		Station 401[1]		Station 402[2]	
	Pressure	Date	Pressure	Date	Pressure	Date
Annual Average	831.72				NA	
Maximum Avg Monthly	836.70	Jan. 2009			839.10	Sep. 2012
Minimum Avg Monthly	827.40	Apr. 2010			831.00	May 2011

1 = Barometric pressure is not collected at Station 401.
2 = Station 402 was operational from May 2011 through December 2012.
NA = not available.

As mentioned in the Methodology section, monitoring stations were originally located to observe conditions downwind of the Clean Slate surface contamination sites in one of the dominant wind directions based on meteorological conditions described for the Tonopah airport by Engelbrecht *et al.* (2008). In Figure 6E, the observed wind roses for Stations 401 and 402 are centered at the station location and overlaid on the outline of the adjacent Clean Slate surface contamination areas, which are depicted by the long narrow polygons outlined in red that extend toward the southeast. The wind roses in Figure 6E show that dominant southerly winds do not parallel the orientation of the Clean Slate III contamination area. The southerly winds cross the contamination area at an angle of approximately 45° and have a fetch of approximately 2,218 ft (676 m) across the contamination area as they approach Station 401. The southerly fetch across Clean Slate III could be increased to approximately 3,168 ft (966 m) by positioning the monitoring station at the northeast apex of the Clean Slate III contamination area boundary. At Station 402 the fetch of dominant south-southeasterly winds that are approximately aligned with the contamination area at Clean Slate I is approximately 1,848 ft (563 m). The length of fetch for south-southeasterly winds at this station could be increased to approximately 2,270 ft (692 m) by moving the station to the northeast apex of the contamination area. If the monitoring stations were moved as suggested to increase the fetch length across the respective contamination areas, the dominant winds from the south would no longer cross GZ, the area of highest surface contamination, as they approach the monitoring station at either location. Therefore, the current positions of both Stations 401 and 402 are considered the most appropriate for assessing the effects of wind-generated migration of contaminated soil particles.

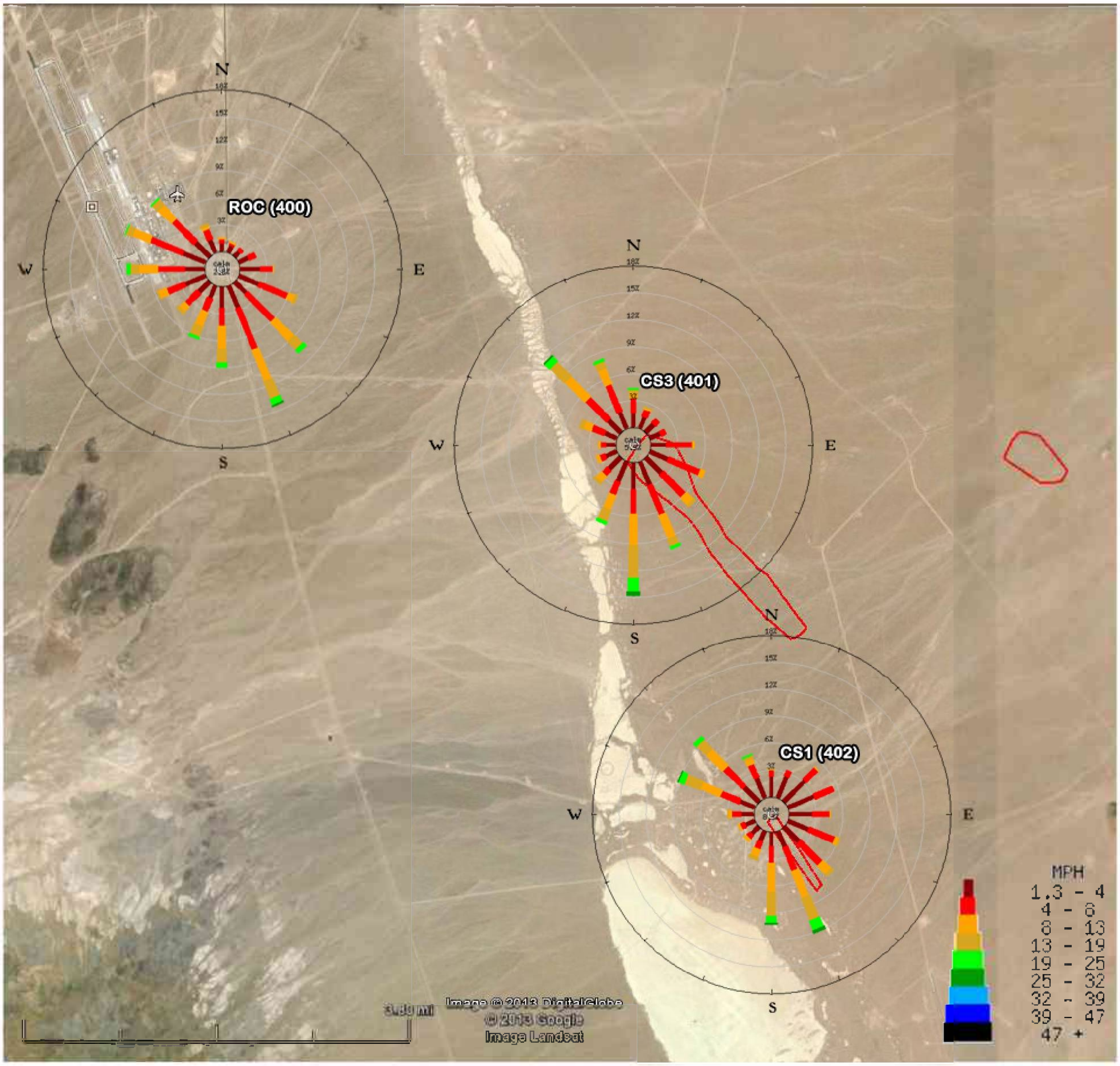

Figure 6E. Wind roses derived for each TTR monitoring station for the period June 1, 2011 to December 31, 2012 are positioned at the station location showing that southerly oriented winds blow across significant portions of the Clean Slate I and III surface contamination sites, which are depicted by elongate southeasterly trending polygons outlined in red.

RADIOLOGICAL ASSESSMENT OF AIRBORNE PARTICULATES

The most direct approach to assessing the potential for wind transport of radionuclides from the Clean Slate contamination areas is to measure the radiological characteristics of suspended dust, so air sampling equipment was installed at Stations 400 and 401 in 2008 and at Station 402 in 2011. Initially, cellulose-fiber filters were used to collect dust samples. With pore sizes between 20 µm and 25 µm, these filters passed the smaller dust particles. As concern about human inhalation of contaminated dust increased, the need to use filters with a smaller pore size was recognized and the cellulose filters were replaced with glass filters. The glass filters, which have a pore size of 0.3 µm, collect most of the inhalable PM_{10} material in addition to the larger suspended particles. The glass filters were first deployed at Station 400 on March 23, 2011. Deployment of glass filters at Station 400 occurred immediately following the tsunami-induced reactor accident in Fukushima, Japan. Glass filters were not deployed at Stations 401 and 402 until April 2013.

Particulates collected on the filters were submitted for gross alpha, gross beta, and gamma spectroscopy analyses. Figures 7 and 8 show the biweekly results for gross alpha and gross beta analyses, respectively. Visual inspection of these figures suggests that gross alpha and gross beta values for Station 400 are higher than for either Stations 401 or 402. Correlation analysis substantiates this observation. The multiplying factors in the correlation equations that estimate Station 401 and 402 values based on Station 400 data are less than one (Table 6 and 7), which indicates that values at Station 400 are generally larger than at the other two stations. When the gross alpha and gross beta results for Stations 400 and 401 were separated into pre- and post-March 23, 2011 collections, the correlation coefficients rose (Table 6 and 7). The increase was slight to moderate for the gross alpha comparison, but it was quite substantial for the gross beta comparisons. The correlation equation relating Stations 401 and 402 indicates that gross alpha and gross beta values at Station 402 are larger than at Station 401. Summary statistics of the gross alpha and gross beta analyses are presented in Tables 8 and 9. As suggested in the time series plots (Figures 7 and 8), the annual means for gross alpha and gross beta are highest for Station 400.

Separating the gross alpha data based on the filter used to collect the sample suggests that the gross alpha measured on cellulose filter samples declined over time (Figure 9), but the values measured on glass filter samples increased. At Station 401, the trend in gross alpha measurements appears to be declining, whereas the short record at Station 402 suggests an increasing trend. Similar analysis of the gross beta data (Figure 10) suggests that both the cellulose-filter and glass-filter samples exhibit declining trends. Additionally, declining trends are suggested in the Station 401 and 402 gross beta records. The gross alpha and gross beta data may offer a hint of a seasonal pattern in which higher values appear to occur during the fall and early winter and lower values occur during the spring and summer. However, this pattern has not been quantified.

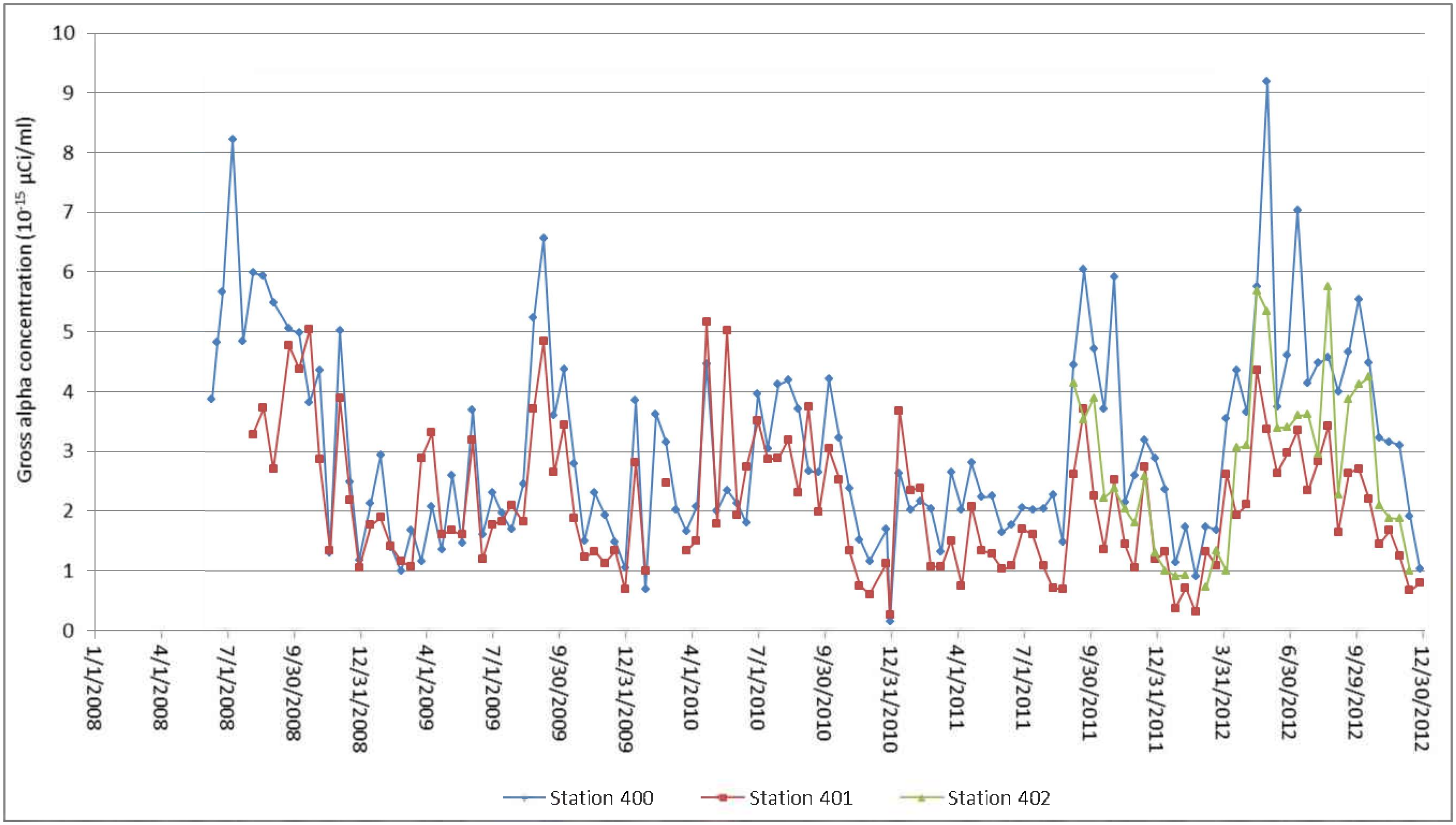

Figure 7. Gross alpha results for air-particulate samples collected from the TTR monitoring stations for the period of record. Sample collection at Station 400 converted from cellulose to glass filters around March 23, 2011.

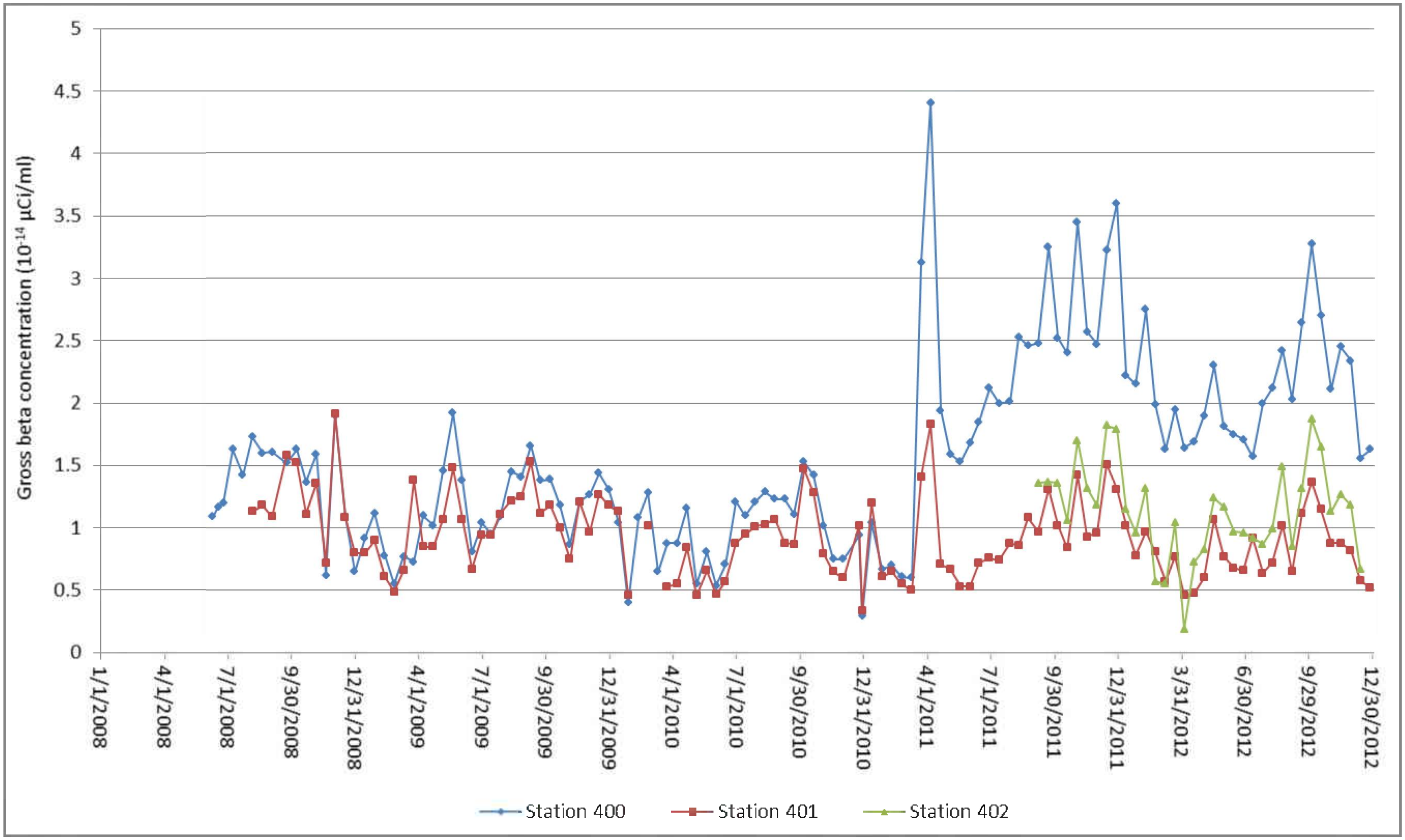

Figure 8. Gross beta results for air particulate samples collected from the TTR monitoring stations for the period of record. Sample collection at Station 400 converted from cellulose to glass filters around March 23, 2011.

Table 6. Correlation equations for gross alpha data from Stations 400, 401, and 402.

Data collection interval	Correlation equation	Correlation coefficient
June 2008 through Dec. 2012[1]	Station 401 gross alpha = 0.5121(Station 400 gross alpha) + 0.5957	0.51
June 2008 through Mar. 2011[2]	Station 401 gross alpha = 0.6426(Station 400 gross alpha) + 0.57	0.59
Mar. 2011 through Dec. 2102[3]	Station 401 gross alpha = 0.4777(Station 400 gross alpha) + 0.24	0.73
Aug. 2011 through Dec. 2012[4]	Station 402 gross alpha = 0.6529(Station 400 gross alpha) + 0.1998	0.61
Aug. 2011 through Dec. 2012	Station 402 gross alpha = 1.22(Station 401 gross alpha) + 0.1747	0.68

[1] Collection interval represents entire period of record presented in this report.
[2] Collection interval represents period of record when both stations were deployed with a cellulose filter.
[3] Collection interval represents period of record when Station 400 was deployed with a glass filter.
[4] Collection interval represents period of record when Station 402 was deployed.

Table 7. Correlation equations for gross beta data from stations 400, 401, and 402.

Data collection interval	Correlation equation	Correlation coefficient
June 2008 through Dec. 2012[1]	Station 401 gross beta = 0.1955(Station 400 gross beta) + 0.617	0.22
June 2008 through Mar. 2011[2]	Station 401 gross beta = 0.7637(Station 400 gross beta) + 0.1161	0.76
Mar. 2011 through Dec. 2102[3]	Station 401 gross beta = 0.4203(Station 400 gross beta) – 0.0635	0.85
Aug. 2011 through Dec. 2012[4]	Station 402 gross beta = 0.5939(Station 400 gross beta) - 0.2314	0.76
Aug. 2011 through Dec. 2012	Station 402 gross beta = 1.2706(Station 401 gross beta) - 0.0031	0.81

[1] Collection interval represents entire period of record presented in this report.
[2] Collection interval represents period of record when both stations were deployed with a cellulose filter.
[3] Collection interval represents period of record when Station 400 was deployed with a glass filter.
[4] Collection interval represents period of record when Station 402 was deployed.

Table 8. Summary statistics of gross alpha results for Tonopah Test Range monitoring data.

Station 400

Year	Number of samples	Gross alpha concentration (x10^{-15} µCi/ml [3.7 x 10^{-5} Becquerel (Bq)/m^3])			
		Mean	Standard Deviation	Maximum	Minimum
2008	16	4.57	1.78	8.21	1.19
2009	26	2.40	1.34	6.56	1.00
2010	26	2.64	1.16	4.46	0.16
2011	26	2.74	1.25	6.04	1.32
2012	26	3.69	1.92	9.19	0.92
Pre-March 2011	73	2.94	1.60	8.21	0.16
Post-March 2011	47	3.34	1.71	9.19	0.92
PoR	120	3.09	1.65	9.19	0.16

Station 401

Year	Number of samples	Gross alpha concentration (x10^{-15} µCi/ml [3.7 x 10^{-5} Becquerel (Bq)/m^3])			
		Mean	Standard Deviation	Maximum	Minimum
2008	11	3.20	1.32	5.04	1.05
2009	26	2.02	0.99	4.84	0.69
2010	24	2.33	1.27	5.16	0.27
2011	26	1.71	0.85	3.72	0.70
2012	26	2.01	1.06	4.36	0.32
PoR	113	2.13	1.13	5.16	0.27

Station 402

Year	Number of samples	Gross alpha concentration (x10^{-15} µCi/ml [3.7 x 10^{-5} Becquerel (Bq)/m^3])			
		Mean	Standard Deviation	Maximum	Minimum
2008	0	Not installed	Not installed	Not installed	Not installed
2009	0	Not installed	Not installed	Not installed	Not installed
2010	0	Not installed	Not installed	Not installed	Not installed
2011	9	2.66	0.98	4.15	1.30
2012	24	2.80	1.56	5.76	.73
PoR	33	2.76	1.42	5.76	.73

NOTES: Bq = Becquerel; m^3 = cubic meter; µCi/ml = microCurie per milliliter; TTR = Tonopah Test Range; glass-fiber filters at Station 400 retain particulates greater than 0.3 µm; cellulose-fiber filters at Stations 401 and 402 retain particulates greater than 20 µm.

Table 9. Summary statistics of gross beta results for Tonopah Test Range monitoring data. Equipment at Station 402 was not installed until late 2011.

Station 400

Year	Number of samples	Gross beta concentration (x10^{-14} µCi/ml [3.7 x 10^{-4} Becquerel (Bq)/m^3])			
		Mean	Standard Deviation	Maximum	Minimum
2008	16	1.36	0.37	1.90	0.62
2009	26	1.16	0.32	1.92	0.55
2010	26	0.96	0.32	1.53	0.30
2011	26	2.18	0.99	4.40	0.60
2012	26	2.09	0.43	3.27	1.56
PoR	120	1.57	0.75	4.40	0.30

Station 401

Year	Number of samples	Gross beta concentration (x10^{-14} µCi/ml [3.7 x 10^{-4} Becquerel (Bq)/m^3])			
		Mean	Standard Deviation	Maximum	Minimum
2008	11	1.22	0.35	1.91	0.72
2009	26	1.02	0.27	1.53	0.49
2010	24	0.81	0.29	1.47	0.34
2011	26	0.94	0.35	1.83	0.50
2012	26	0.80	0.23	1.37	0.46
PoR	113	0.93	0.32	1.91	0.34

Station 402

Year	Number of samples	Gross beta concentration (x10^{-14} µCi/ml [3.7 x 10^{-4} Becquerel (Bq)/m^3])			
		Mean	Standard Deviation	Maximum	Minimum
2008	0	Not installed	Not installed	Not installed	Not installed
2009	0	Not installed	Not installed	Not installed	Not installed
2010	0	Not installed	Not installed	Not installed	Not installed
2011	9	1.44	0.27	1.82	1.06
2012	25	1.04	0.36	1.87	0.19
PoR	34	1.14	0.38	1.87	0.19

NOTES: Bq = Becquerel; m^3 = cubic meter; µCi/ml = microCurie per milliliter; TTR = Tonopah Test Range; glass-fiber filters at Station 400 retain particulates greater than 0.3 µm; cellulose-fiber filters at Stations 401 and 402 retain particulates greater than 20 µm. Equipment at Station 402 was not installed until late 2011.

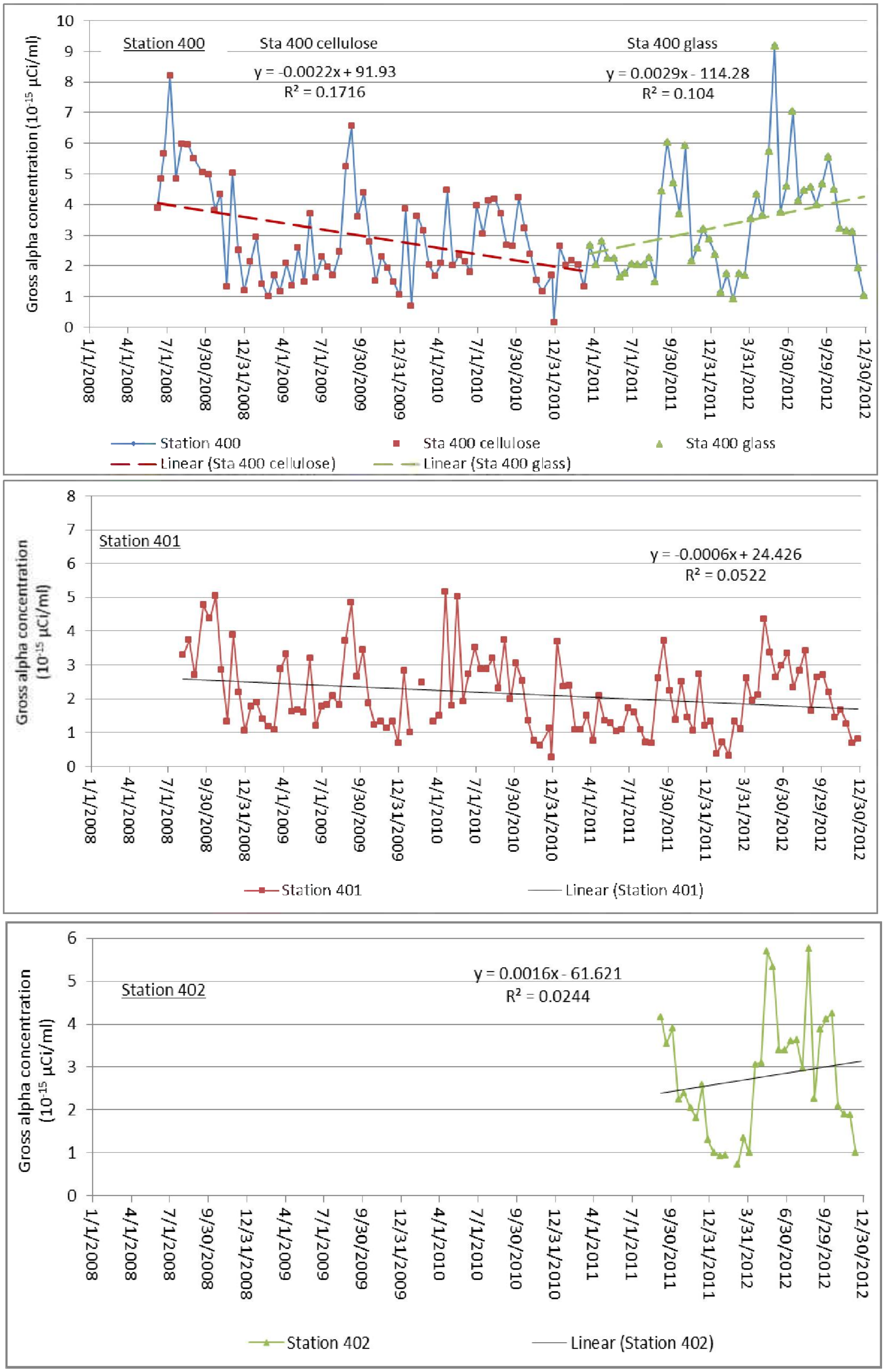

Figure 9. Temporal trends for gross alpha on suspended particulates vary from station to station.

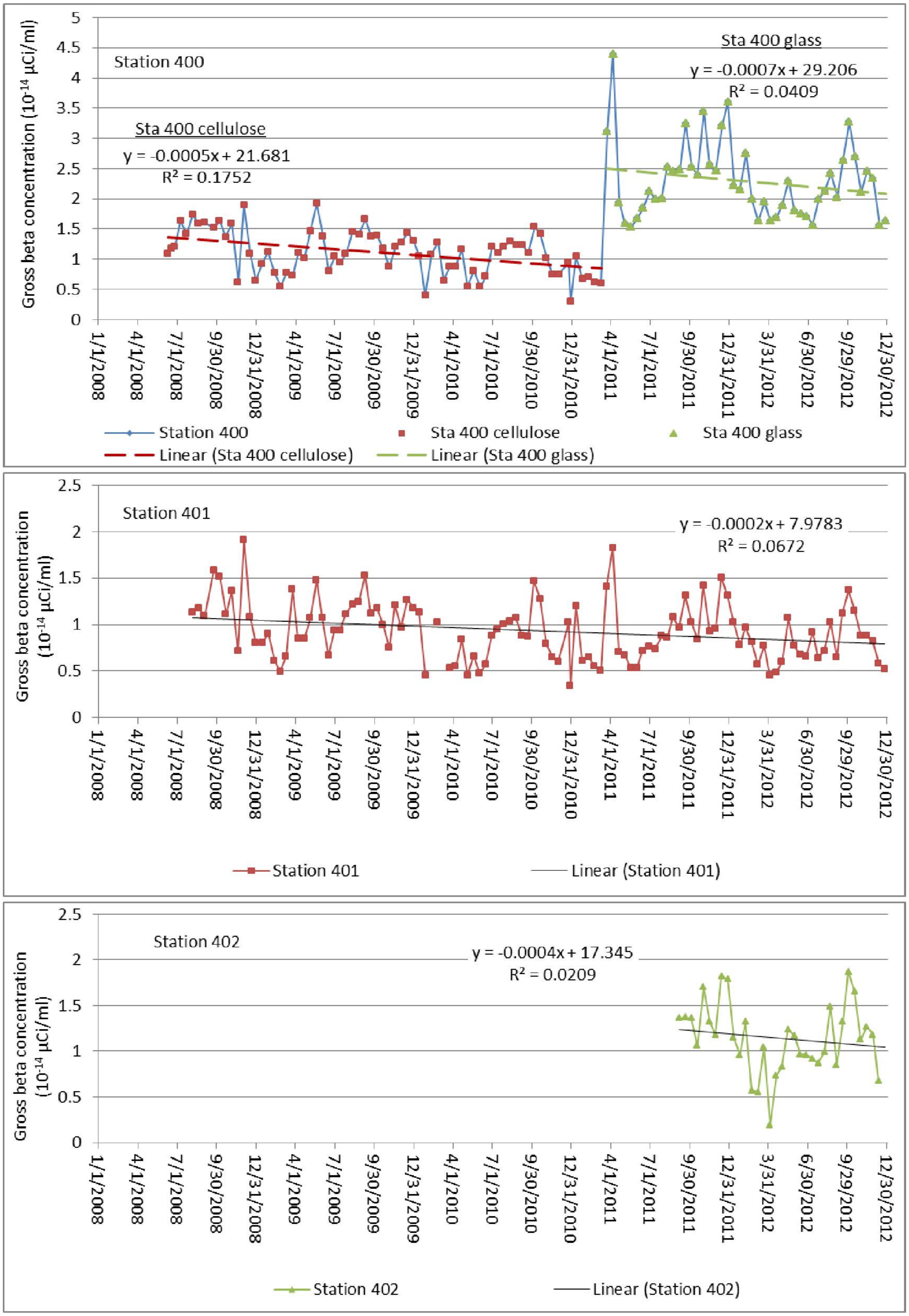

Figure 10. Temporal trends for gross beta on suspended particulates vary from station to station.

Figures 9 and 10 strongly suggest that there are differences in the gross alpha and gross beta measurements associated with the cellulose and glass filters. The gross beta values for samples collected on the glass filters are noticeably higher than the values measured on samples collected on cellulose filters. Comparing the mean values of all gross alpha and gross beta measurements for the two filter types further emphasizes this pattern. The mean of gross alpha values for glass-filter samples is 3.34×10^{-15} µCi/ml compared to 2.94×10^{-15} µCi/ml for the cellulose-filter samples. Similarly, the glass-filter samples give a gross beta mean of 2.29×10^{-14} µCi/ml, whereas the cellulose-filter samples produce a mean of 1.10×10^{-14} µCi/ml. The higher concentrations for the glass-filter samples are most likely due to the retention of smaller suspended particles. Although plutonium has not been detected in the samples from the TTR stations, the work of Tamura (1974, 1975, and 1976) may be instructive. In evaluating the association between plutonium and native soils from the Nevada National Security Site (NNSS) (formerly the Nevada Test Site [NTS]), Tamura (1974) noted that the highest concentrations of plutonium were attached to medium-silt-sized (5 µm to 20 µm) particles. This is the particle size range that was included in the suspended particulates samples when the collection filters were changed from cellulose to glass. Therefore, it is likely that the increase in gross alpha and gross beta values noted with the change to glass filters is due to both the increase in suspended particulates retained in the samples and the preferential attachment of radionuclides to the smaller particles incorporated in the samples by the glass filters.

The DOE-sponsored CEMP data collection produces gross alpha and gross beta observations similar to those collected at the TTR monitoring stations. Mean gross alpha and gross beta determinations for the CEMP stations (DOE, 2009; 2010; 2011; 2012; 2013) that surround the TTR (Figure 1) are presented in Tables 10 and 11. Comparing the TTR data to the CEMP data indicates that the mean annual gross alpha values at the TTR stations exceed the mean annual gross alpha at all of the surrounding CEMP stations in every year except 2011. In 2011, mean annual gross alpha for TTR Station 401 ranked lower than the CEMP Sarcobatus station but higher than all other CEMP stations surrounding the TTR. The annual mean gross alpha values for the TTR stations were between 25 percent and 100 percent greater than the highest of the surrounding CEMP station values. The reason for this difference has not been determined. Because the gamma spectroscopy analyses have not indicated the presence of ^{241}Am, which suggests plutonium, it is unlikely that plutonium is the cause for the higher gross alpha values.

The mean annual gross beta values at the TTR stations are lower than the corresponding CEMP values with two exceptions. The 2011 mean annual gross beta value for Station 400 falls in the middle of the range of values reported for the surrounding CEMP stations and the 2012 mean annual gross beta value for Station 400 was just below the Sarcobatus Flat mean annual value, the highest of the surrounding CEMP stations, in 2012. Glass filters have been used in the CEMP air sampling equipment throughout the CEMP program. The use of glass filters at Station 400 in March 2011 resulted in an increased collection of smaller particles and may explain the change in ranking of TTR Station 400 mean annual gross beta observations.

Table 10. Annual mean gross alpha determinations for seven CEMP stations that surround the TTR (DOE, 2009; 2010; 2011; 2012; 2013).

Sampling Location	Gross alpha concentration (10^{-15} µCi/ml)			
	2009	2010	2011	2012
TTR Station 400	2.48	2.66	2.57	3.69
TTR Station 401	2.07	2.32	1.74	2.01
TTR Station 402	NA	NA	2.65	2.80
Goldfield	0.97	1.08	1.05	1.05
Nyala Ranch	0.65	1.17	1.03	1.03
Rachel	0.92	1.18	1.03	1.03
Sarcobatus Valley	1.64	1.88	1.83	1.83
Stone Cabin Ranch	0.83	1.04	0.91	0.91
Tonopah	1.07	1.03	1.08	1.08
Twin Springs Ranch	0.85	1.25	0.95	0.95

NA = data not available.

Table 11. Annual mean gross beta determinations for seven CEMP stations that surround the TTR (DOE, 2009; 2010; 2011; 2012; 2013).

Sampling Location	Gross beta concentration (10^{-14} µCi/ml)			
	2009	2010	2011	2012
TTR Station 400	1.18	0.97	2.18	2.09
TTR Station 401	1.03	0.82	0.94	0.81
TTR Station 402	NA	NA	1.44	1.04
Goldfield	1.88	1.63	2.09	1.88
Nyala Ranch	1.67	1.81	2.21	1.53
Rachel	1.85	1.78	2.24	1.87
Sarcobatus Valley	2.04	1.86	2.32	2.11
Stone Cabin Ranch	1.65	1.50	1.80	1.74
Tonopah	1.81	1.54	2.12	1.82
Twin Springs Ranch	1.88	1.85	2.06	1.81

NA = data not available.

Gamma spectroscopy identified eight radionuclides in the TTR air particulate samples. Table 12 lists the radionuclides and the frequency of their occurrence. Cesium-134 and cesium-137 were both identified in two samples collected during March 2011. The concentration of cesium isotopes in the TTR samples was reported at values less than 2×10^{-14} µCi/ml. Samples collected by the CEMP that operates monitoring stations throughout southern Nevada and western Utah also showed cesium in the air samples collected in March 2011 (DOE, 2012). These cesium detections are associated with worldwide fallout from the reactor accident in Fukushima, Japan, on March 11, 2011 (DOE, 2012). With the exception of these cesium detections, all radionuclides identified in the gamma spectroscopy analyses are naturally occurring. Beryllium-7, the most frequently identified gamma emitter, appears in more than 80 percent of the samples from each of the monitoring stations. Lead-210 is the second most common gamma emitter, occurring in between 47 percent and 69 percent of the samples. At Station 400 and 401, potassium-40 is the third most frequently identified gamma emitter. However, at Station 402, protactinium-234m is the third most commonly identified gamma source. Because americium-241 was not detected in the gamma spectroscopy analyses, no alpha spectroscopy analyses were performed. Spectroscopy data suggest that gamma emitting radionuclides associated with airborne particulates at the TTR monitoring stations are similar to the conditions observed at surrounding CEMP stations.

The TTR and surrounding CEMP gross beta and gamma spectroscopy observations are of similar magnitude. Although gross alpha values for the TTR stations are higher than values reported for the surrounding CEMP stations, the failure to detect americium-241 in the gamma spectroscopy analysis suggests that plutonium is not the likely source of the alpha emissions. Therefore, there is no evidence of radionuclide-contaminated soil particulates being transported from the Clean Slate I or Clean Slate III sites.

The 1975 and 1987 reports from the National Council on Radiation Protection and Measurements (NCRP) estimated that the average concentration of long-lived gross alpha activity in air was 2 fCi/m3 (2×10^{-15} µCi/ml) and that the average concentration of long-lived gross beta activity in air was 20 fCi/m3 (2×10^{-14} µCi/ml). The gross alpha activity is primarily due to the decay of polonium-210, which is a decay product of radon, in conjunction with other naturally occurring radionuclides. Lead-210, bismuth-210 (both decay products of radon), and other naturally occurring radionuclides generate the gross beta value. Variations in the observed concentrations of gross alpha and gross beta are dependent on atmospheric (barometric) pressure, atmospheric mixing, temperature, soil moisture, and the “age” of the radon. The mean annual gross alpha and gross beta values observed at the TTR monitoring stations generally approximate these NCRP averages. Therefore, it appears that radiation exposure at the TTR monitoring stations is similar to average exposure levels for the United States.

Table 12. Number of occurrences of specific isotopes determined by gamma spectroscopy. (PoR = period of record of data collection at each station.)

Station 400

Year	2008	2009	2010	2011	2012	PoR
Number of samples	17	26	25	26	26	120
Beryllium-7 (Be-7)	16	23	16	22	26	103 (86%)
Potassium-40 (K-40)	16	2	1	7	5	31 (26%)
Lead-210 (Pb-210)	16	12	12	23	20	83 (69%)
Lead-212 (Pb-212)	3	0	0	0	0	3 (3%)
Bismuth-214 (Bi-214)	3	0	1	1	0	5 (4%)
Protactinium-234m (Pa-234m)	0	1	0	0	3	4 (3%)
Cesium-137 (Cs-137)	0	0	0	2[1]	0	2 (2%)
Cesium-134 (Cs-134)	0	0	0	2[1]	0	2 (2%)

Station 401

Year	2008	2009	2010	2011	2012	PoR
Number of samples	12	26	24	25	26	113
Beryllium-7 (Be-7)	11	25	14	21	21	92 (81%)
Potassium-40 (K-40)	11	2	2	3	3	21 (19%)
Lead-210 (Pb-210)	10	12	8	14	9	53 (47%)
Lead-212 (Pb-212)	4	0	0	0	0	4 (4%)
Bismuth-214 (Bi-214)	3	0	1	1	0	5 (4%)
Protactinium-234m (Pa-234m)	0	0	0	2	1	3 (3%)
Cesium-137 (Cs-137)	0	0	0	2[1]	0	2 (2%)
Cesium-134 (Cs-134)	0	0	0	2[1]	0	2 (2%)

Station 402

Year	2008	2009	2010	2011	2012	PoR
Number of samples	Not installed	Not installed	Not installed	9	25	34
Beryllium-7 (Be-7)	Not installed	Not installed	Not installed	9	22	31 (91%)
Potassium-40 (K-40)	Not installed	Not installed	Not installed	1	0	1 (3%)
Lead-210 (Pb-210)	Not installed	Not installed	Not installed	6	13	19 (56%)
Lead-212 (Pb-212)	Not installed	Not installed	Not installed	0	3	3 (9%)
Bismuth-214 (Bi-214)	Not installed	Not installed	Not installed	0	3	3 (9%)
Protactinium-234m (Pa-234m)	Not installed	Not installed	Not installed	3	1	4 (12%)
Cesium-137 (Cs-137)	Not installed	Not installed	Not installed	0[2]	0	0 (0%)
Cesium-134 (Cs-134)	Not installed	Not installed	Not installed	0[2]	0	0 (0%)

[1] Cesium detections coincide with the reactor accident in Fukushima, Japan, which was associated with the tsunami of March 2011

[2] Station 402 was deployed in April 2011 after the Fukushima accident.

GAMMA RADIATION EXPOSURE ASSESSMENT

Gamma radiation has a range of several hundred feet in air (NSTec, 2010). Therefore, the PIC reports gamma radiation within a sphere of detection. Approximately half of this sphere of detection is in air and has an effective radius of several feet. The lower half of the sphere is below ground and has a smaller effective radius because of the solid particles that make up the soil. Additionally, because the PIC instrumentation is located at the radionuclide-contaminated area boundary, half of the land surface included in the sphere of influence is inside and the other half is outside of the contaminated area. Therefore, values of gamma radiation reported by the PIC instrumentation reflect the influence of both the uncontaminated and contaminated areas surrounding the instrument. Under perfectly static conditions in this setting, the reported values of gamma radiation are expected to be somewhat higher than the values that would be observed if the PIC were completely surrounded by an area of uncontaminated land.

Pressurized ionization chamber instrumentation is typically used to monitor ambient gamma radiation levels and to detect occasions when the gamma observations significantly exceed the natural background levels. In assessing potential radiological exposure to the public from low-level waste (LLW) transported by trucks, Gertz (2001, as reported in Miller *et al.*, 2005) assumed a background of 50 μR/h when observations were made at LLW disposal sites on the Nevada National Security Site (NNSS). Miller *et al.* (2005) estimated that the background gamma for each truck that entered the PIC array near Mercury, Nevada. They calculated the background for the 12-hour (daytime or nighttime) portion of the day that the truck arrived as the average of the maximum gamma values observed during each 2-minute period plus one standard deviation. Miller *et al.* (2005) observed that maximum background gamma values for the 2-minute observation intervals ranged from 9 to 40 μR/h, but they typically fell within the range of 10 to 15 μR/h. All average 10-minute gamma values from the TTR monitoring stations are above the range of typical background values and below the upper extreme background value (40 μR/h) observed by Miller *et al.* (2005) and the 50 μR/h background value assumed by Gertz (2001).

The PIC instruments were then installed at the Clean Slate I and III sites in the expectation that atmospheric transport of radionuclide-contaminated soil from these sites might be detected in the gamma observations due to the increased amount of contaminated dust entrained in the surrounding air. Additionally, observation of gamma radiation during periods of time when there is no known strong source influence indicates the ambient radiation exposure at the monitoring stations adjacent to the Clean Slate contamination areas. A PIC is deployed at the SNL ROC as a comparison for the PIC results at the Clean Slate sites.

In order to identify notably high gamma values, the range of normal background gamma values was established as the mean value for the period of record at each monitoring station plus or minus 3 μR/h. Because high gamma values are of interest, only the high limit is considered in the following discussion. The mean plus 3 μR/h value is adopted from the DOE CEMP where it is used to determine when notifications of high gamma observations are sent (G. McCurdy, verbal communication, February 2014). The period of record mean gamma value for each station is given in Table 13. Figures 11, 12, and 13 display the observed 10-minute average gamma values for each monitoring station.

Table 13. Approximately four years of data are included in the PIC assessment and analysis.

Station	400	401	402
Start-up date time	1/1/2009 0000	12/16/2009 1240	12/14/2011 1430
End of current analysis period	12/31/2012 2350	12/31/2012 2350	12/31/2012 2350
Possible 10-minute intervals	209895	157180	55209
Actual 10-minute intervals used in analysis	208690	157159	55202
Average 10-minute gamma for PoR (μR /h)	19.52	21.32	18.16
Background (μR /h)	22.52	24.32	21.16
# of occasions observed gamma > background	47	85	5

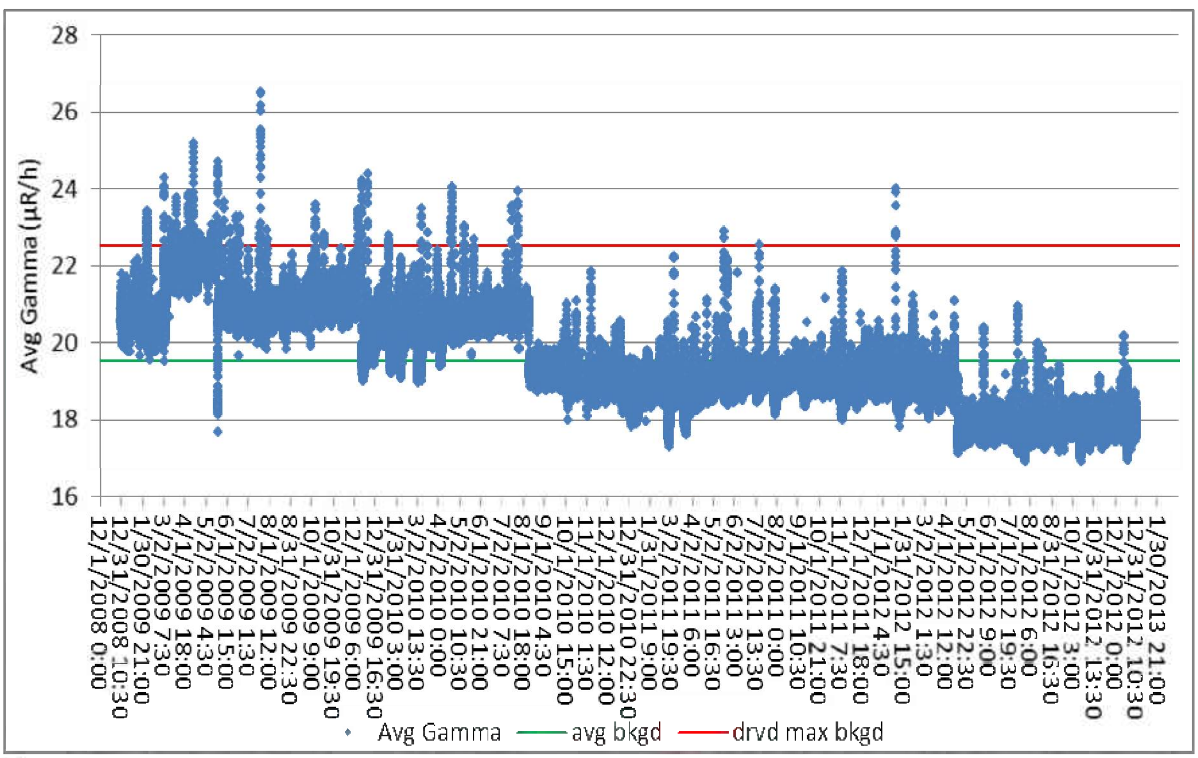

Figure 11. At Station 400 average 10-minute gamma values (blue dots) ranged between 16.93 and 26.50 μR/h over the period of record. The mean value (green line) and mean + 3 μR/h (red line) are also shown.

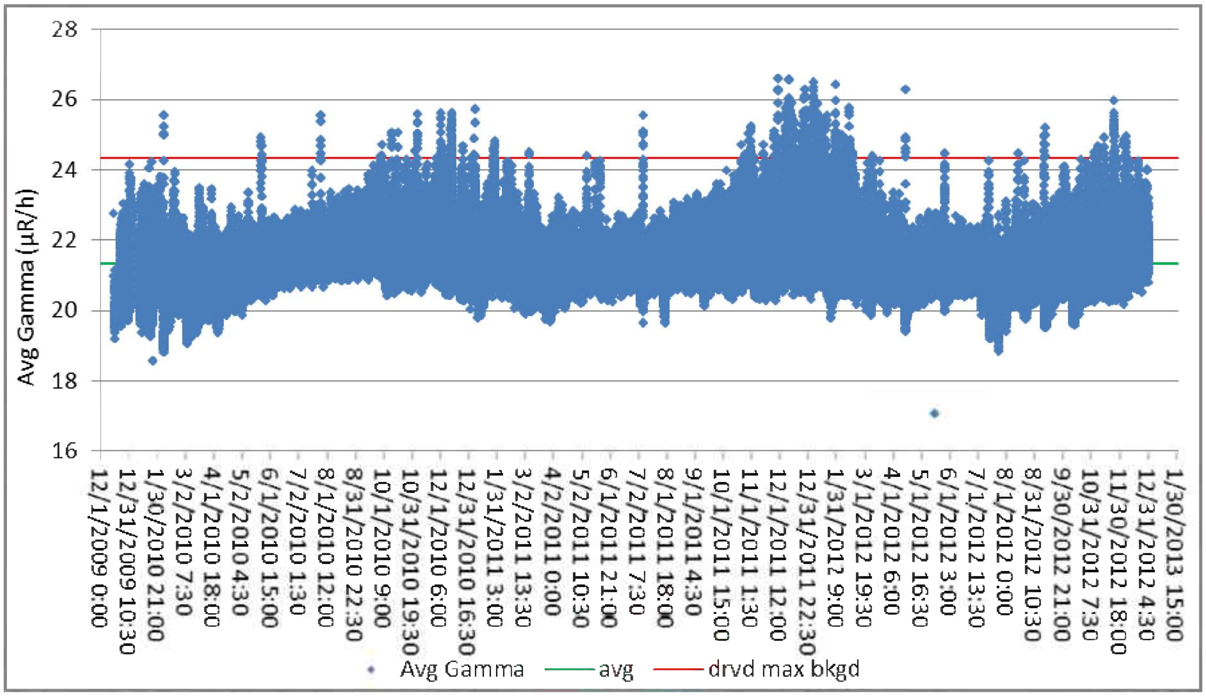

Figure 12. At Station 401 average 10-minute gamma values (blue dots) ranged between 17.07 and 26.59 µR/h over the period of record. The mean value (green line) and mean + 3 µR/h (red line) are also shown.

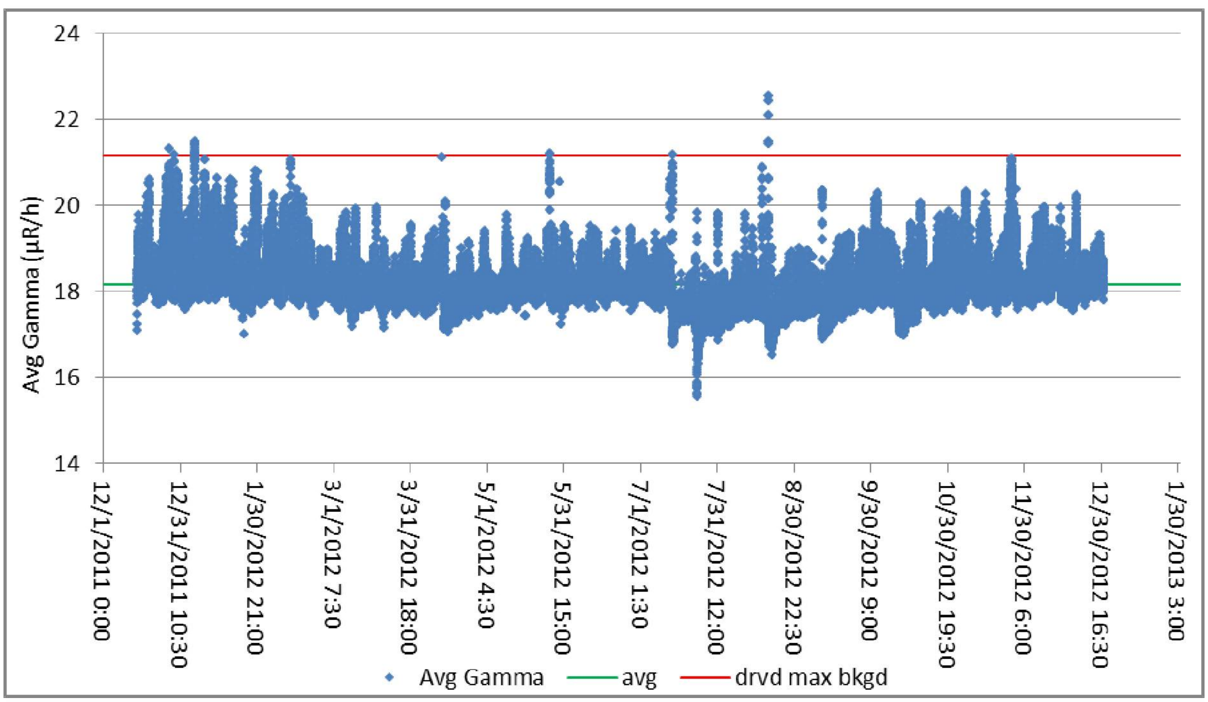

Figure 13. At Station 402 average 10-minute gamma values (blue dots) ranged between 15.55 and 22.54 µR/h over the period of record. The mean value (green line) and mean + 3 µR/h (red line) are also shown.

The gamma record from Station 400 (Figure 11) shows several step changes. The average 10-minute gamma values for each of the distinct intervals were calculated to determine the impact of using step-interval-based background values instead of period-of-record-based background values (Table 14). Using the step-interval background resulted in 17 occasions when the observed gamma exceeded background compared to 47 events when the period-of-record background was used. Because it is a more conservative assessment (more events in excess of background), the following discussion is based on the period of record determination of background at Station 400. Distinct step changes are not observed in the gamma record at Stations 401 and 402. Therefore, assessments of events when observed gamma exceeded the background gamma value are based on the period of record determination of background. The background gamma values were exceeded 47, 85, and 5 times during the period-of-record at Stations 400, 401, and 402, respectively (Table 13, Appendix E).

The largest number of occasions when the observed gamma values exceeded the individual station background value occurred at Station 401, which was 85 times in approximately three years of data collection (Table 13). However, the greatest difference between the observed gamma and the background gamma occurred at Station 400, which was a difference of 3.98 µR/h (Table 15). Station 402 has the fewest number of occasions when the background was exceeded and the smallest difference between the maximum observed gamma and the background gamma (Table 15). It is presumed that the background is exceeded less frequently and by a lesser amount at Station 402 because of the shorter PoR.

Table 14. Fewer observed gamma values exceeded the gamma background (period-of-record average + 3 µR/h) values when the background values were determined for time intervals defined by step changes in the observed values at Station 400.

Segment	Start date time	End date time	Average	Maximum	# of occasions observed gamma > maximum background gamma
PoR[1]	1/1/2009 (0000)	12/31/2012 (2350)	19.52	22.52	47
A	1/1/2009 (0000)	3/3/2009 (1030)	20.49	23.49	2
B	3/3/2009 (1050)	5/20/2009 (1110)	21.95	24.95	2
C	5/20/2009 (1120)	12/13/2009 (0430)	20.91	23.91	2
D	12/13/2009 (0440)	8/11/2010 (1310)	20.50	23.50	5
E	8/11/2010 (1320)	4/18/2012 (1030)	18.99	21.99	5
F	4/18/2012 (1030)	12/31/2012 (2350)	17.81	20.81	1

[1] PoR = period of record for data collection

Table 15. Summary statistics describing events when the observed gamma exceeded the background gamma value for the respective monitoring station.

	Gamma Observations (μR/h)	Deviation from Background (μR/h)
	Station 400	
Background	22.52	
Occurrences	47	47
Maximum Observed	26.50	3.98
Minimum Observed	22.54	0.02
Average Observed	23.27	0.75
Standard Deviation	0.77	0.77
	Station 401	
Background	24.32	
Occurrences	85	85
Maximum Observed	26.59	2.27
Minimum Observed	24.34	0.02
Average Observed	25.04	0.72
Standard Deviation	0.60	0.60
	Station 402	
Background	21.16	
Occurrences	5	5
Maximum Observed	22.54	1.38
Minimum Observed	21.18	0.02
Average Observed	21.55	0.39
Standard Deviation	0.57	0.57

Table 16 and Figures 14 and 15 describe the occurrence of events when the observed gamma values exceed the background gamma value at each station. Calendar year 2009 produced 35 events in excess of the background gamma at Station 400 (Table 16). Years 2011 and 2012 produced the most events (34 and 35, respectively) in excess of the local background at Station 401. The observed gamma values exceeded the local background for Station 402 on only a few occasions (Table 16) during the approximately 1.5 years of data collection. The background gamma was most commonly exceeded (83 percent of occurrences) in the spring and early summer at Station 400 (Figure 14), but at Station 401 88 percent of the greater-than-background events occurred in the fall and winter. Three of the five times when the background was exceeded at Station 402 occurred during the winter months (Figure 14). Of these high gamma events, only four occurred at approximately the same time at Stations 400 and 401. An additional four high gamma events occurred at approximately the same time at Stations 401 and 402. High gamma events were never observed at all three monitoring stations at approximately the same time. The occurrence and frequency of high gamma events is not consistent for Stations 400 and 401, which have the longest periods of record. Additionally, the seasonality of high gamma events is not consistent at the monitoring stations. These observations suggest that annual and seasonal patterns are not consistent across the TTR landscape but are unique to each monitoring station location.

Events when background is exceeded at Station 400 are distributed fairly evenly throughout the day, but they may be least likely in the late evening (Figure 15). At Station 401, most of the greater-than-background events (75 percent) occurred between 0600 and 0800 hours in the morning, but events were also common before 0600 and in the early afternoon (Figure 15). The background at Station 402 was exceeded more frequently in the early morning (Figure 15). During the day, the events that exceed background appear to be most common in the morning and early afternoon, even though they may occur at almost any time during the day.

Table 16. The number of events each year when the observed gamma exceeded the background gamma value for the respective monitoring station.

Year	Station 400	Station 401	Station 402
2008	NA	NA	NA
2009	35	NA	NA
2010	9	16	NA
2011	2	34	2
2012	1	35	3

NA = data not available; no data was analyzed for these years.

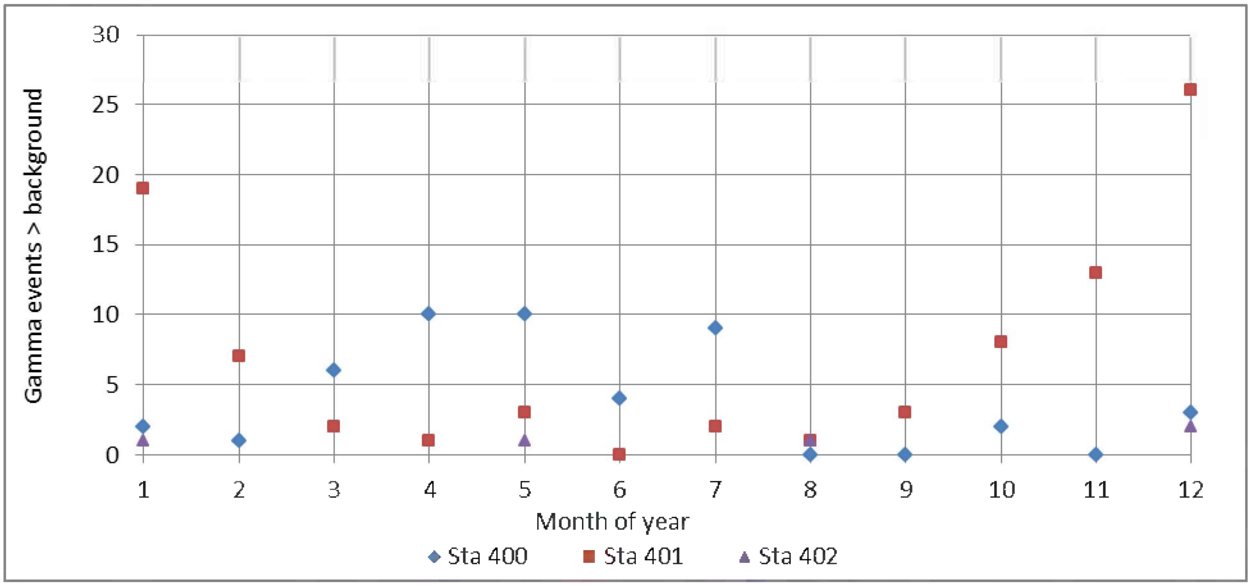

Figure 14. Occasions when observed gamma values exceeded the background gamma value were most common in the spring and summer at Station 400 and fall and winter at Station 401.

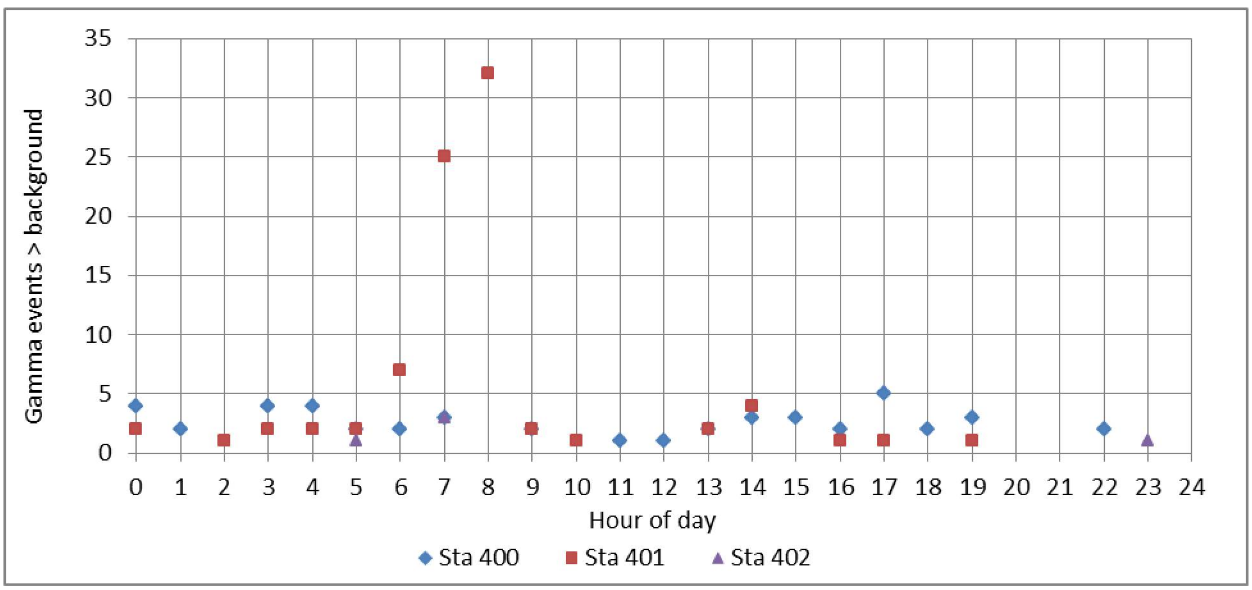

Figure 15. Occasions when the observed gamma values exceeded the background value were most common in the predawn morning and late afternoon at Station 400 and in the early morning at Station 401.

Three occasions when the observed gamma exceeded the background values—the July 26, 2010 event at Stations 400 and 401 and the January 6, 2012 and May 26, 2012 events at Stations 401 and 402—were selected for a preliminary assessment of the relationships between the gamma events and associated meteorological and environmental factors. The duration of these events is described in Table 17.

Table 17. On eight occasions the observed gamma values exceeded the station background value simultaneously at two stations. On no occasion did the observed gamma exceed the background gamma at all three stations simultaneously.

Date (mm/dd/yyyy)	Station 400			Station 401			Station 402		
	Start Time (hhmm)	Duration (hh:mm)	Gamma	Start Time (hhmm)	Duration (hh:mm)	Gamma	Start Time (hhmm)	Duration (hh:mm)	Gamma
5/23/2010	1400	0:30	22.68	1410	1:30	24.79	NCE	NCE	NCE
7/26/2010	0630	1:40	23.94	0640	1:30	25.54	NCE	NCE	NCE
7/7/2011	1920	0:10	22.54	1700	1:00	25.52	NCE	NCE	NCE
12/27/2011	NCE	NCE	NCE	0620	4:20	25.98	0500	0:10	21.33
12/29/2011	NCE	NCE	NCE	0740	1:50	26.26	0700	0:10	21.18
1/6/2012	NCE	NCE	NCE	0250	7:20	26.47	0730	1:40	21.49
1/21/2012	0910	1:20	24	1000	1:00	25.54	NCE	NCE	NCE
5/26/2012	NCE	NCE	NCE	0920	0:10	24.44	0720	0:20	21.21

NCE = no corresponding event was identified

Slight variations in gamma radiation at a single location may be the result of changes in local meteorological conditions (UNSCEAR, 2000) and environmental characteristics that are influenced by the weather. Rainfall and snowfall may cause increased gamma values because the dust washed from the atmosphere often contains gamma emitting materials. This effect is exacerbated when the precipitation accumulates on the PIC instrument. The measured ambient gamma energy level may also depend on barometric pressure. Increasing barometric pressure may suppress the release of gamma emitting gasses in the soil, such as radon, which may reduce the gamma energy observed at the detector. High soil moisture content fills the void space in the soil and impedes or prohibits the release of gamma emitting gasses as well. The impact of these environmental factors on the gamma signal can be conceptually understood when considered individually. However, in the natural environment, these factors interact in complicated ways that lead to variability in the gamma signal. For example, the rainfall that washes gamma emitting dust from the air, tending to increase the gamma signal, also increases the soil moisture content that tends to lower the gamma signal. The low barometric pressure that accompanies a rainfall event tends to increase the release of gamma-emitting soil gas, but the increase in soil moisture content due to the rainfall also tends to decrease the release of gamma-emitting soil gas. As a result of these complicated interactions, it has not been possible to quantitatively determine the relationships between meteorological and environmental conditions and the observed gamma signals. Therefore, the following review of the gamma signal variations identifies relatively unique variations and compares them to patterns in meteorological and environmental phenomena as a first-cut explanation of the gamma energy variations.

On July 26, 2010, the observed gamma values exceeded the station background values between the hours of 0520 and 0810 at Station 400 and the hours of 0620 and 0750 at Station 401. The maximum observed gamma values exceeded the background values by 1.42 and 1.22 µR/h at Stations 400 and 401, respectively. Data presented in Figures 16 and 17 show that precipitation, soil moisture, and humidity rose simultaneously with the gamma event. However, the changes in these parameters that occurred later in the day are not accompanied by changes in the gamma values. Small increases in wind speed may be associated with the elevated gamma levels, but the wind speed variations at other times of the day are not accompanied by changes in the gamma values. At Station 401, the wind appears to have been from the west and northwest during the initial moments of the gamma event. They tended to be more from the east and southeast later in the event. Winds at Station 400 were much more variable and came from all directions during the gamma event.

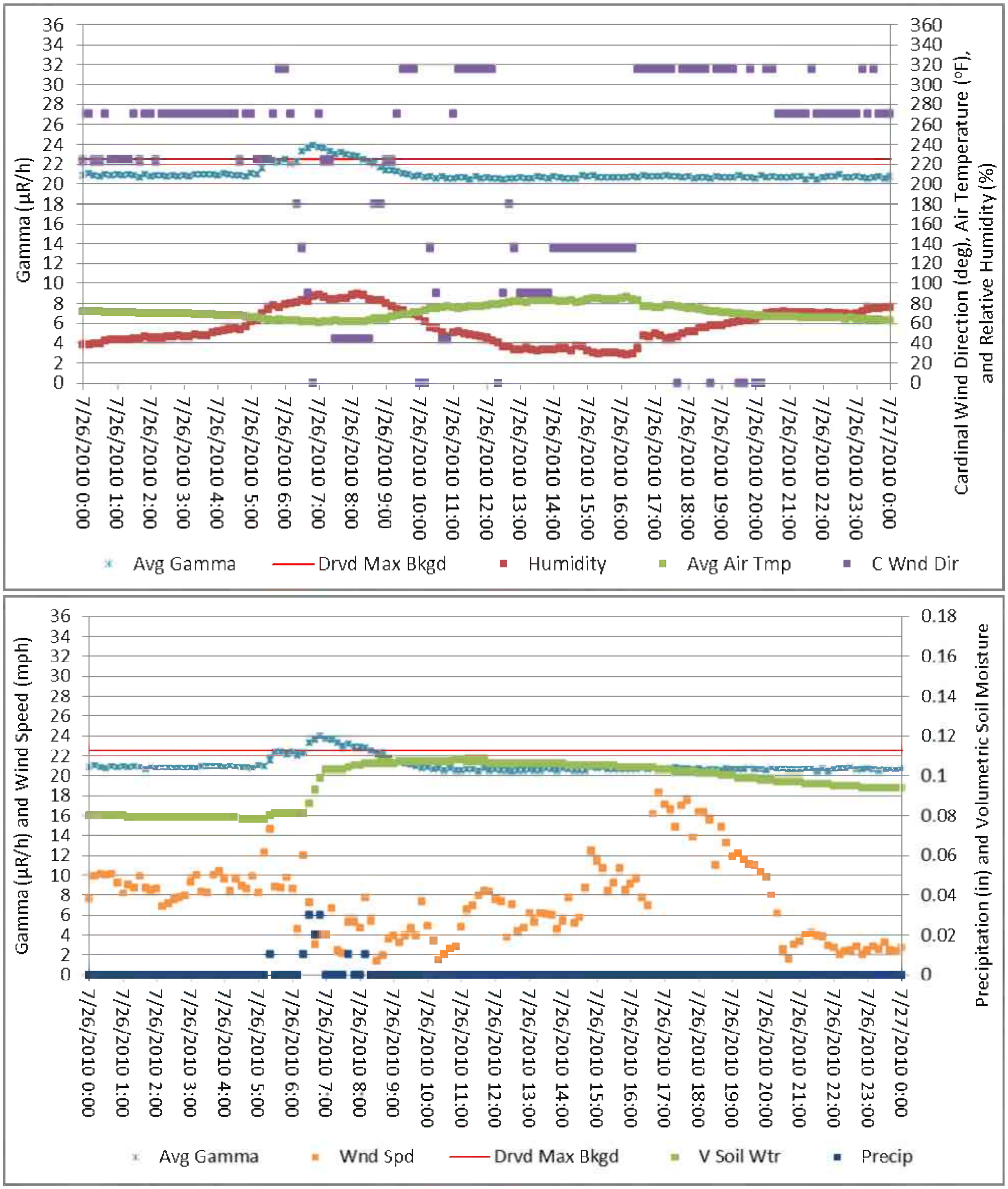

Figure 16. Various environmental parameters and observed gamma values for the occasion when observed gamma > background at Station 400 on July 26, 2010.

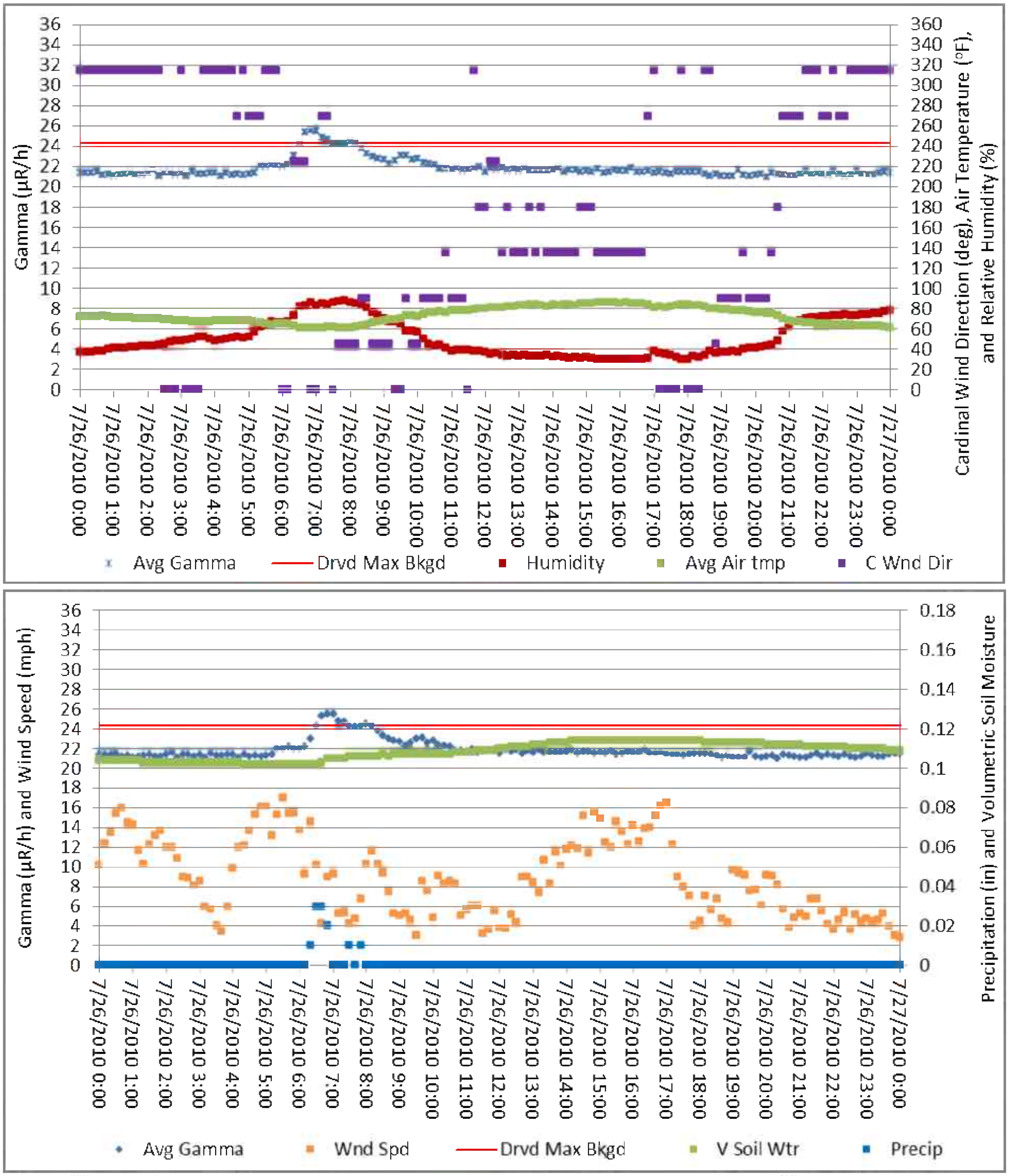

Figure 17. Various environmental parameters are plotted with the gamma values for the observed gamma > the background event on July 26, 2010, at Station 401.

On January 6, 2012, the observed gamma values exceeded the station background values between the hours of 0250 and 1010 at Station 401 and the hours of 0730 and 0910 at Station 402. The maximum observed gamma exceeded the background values by 2.15 μR/h and 0.33 μR/h at Stations 401 and 402, respectively. No precipitation was recorded at either Station 401 or 402 during this gamma event and even though there are fluctuations in the humidity and soil moisture data, there appears to be no correlation with the gamma data (Figure 18 and 19). Winds were light, (less than approximately 5 mph) and generally from the south during the gamma event. The wind direction switched to northwesterly and the gamma values were slightly depressed at both stations in the afternoon following the excess gamma event. Air temperatures during the day (January 6, 2012) appear to increase in a typical diurnal pattern. There does not appear to be a visually identifiable correlation between the gamma event and the monitored meteorological and environmental parameters.

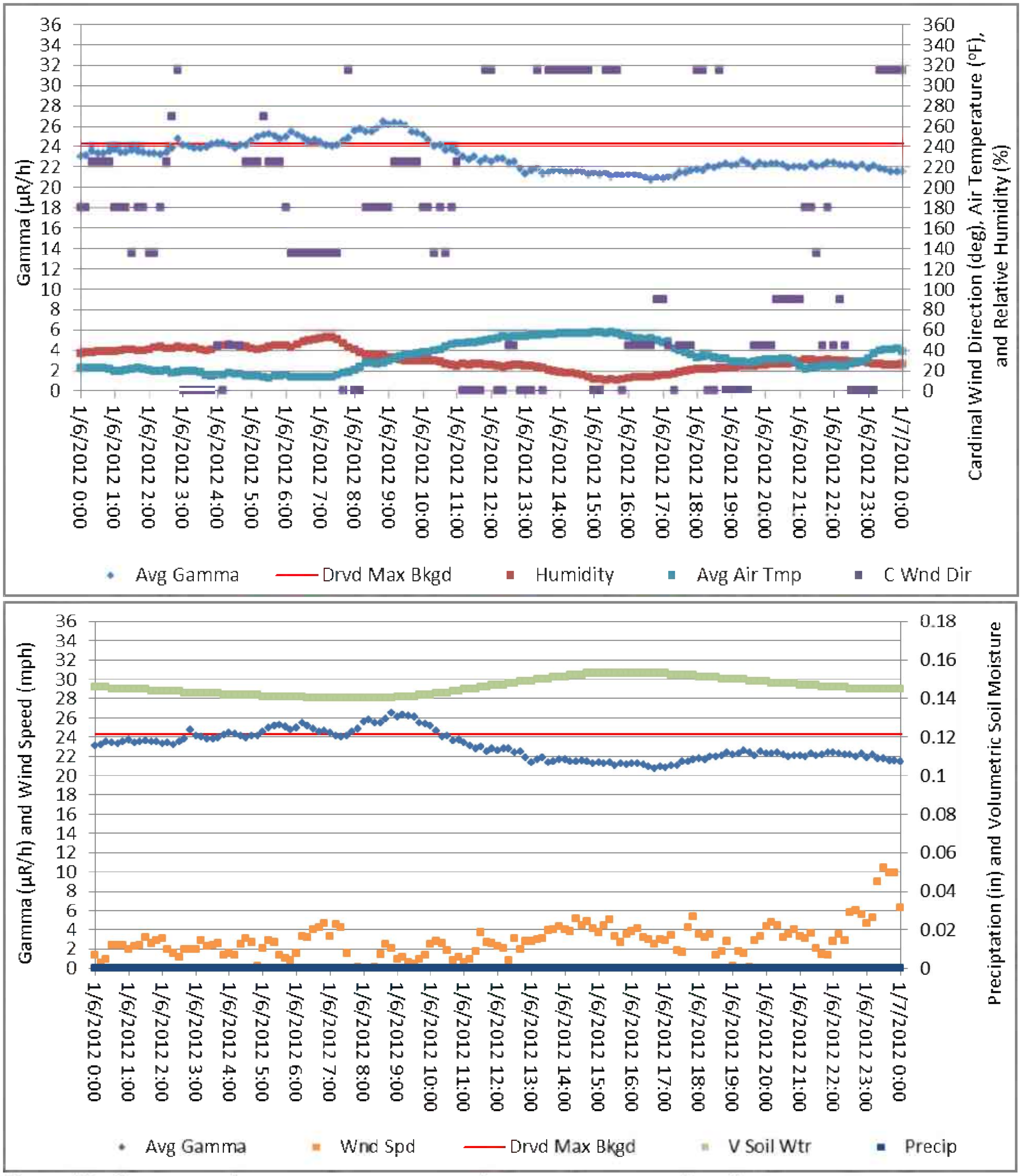

Figure 18. Various environmental parameters and observed gamma values for the occasion when observed gamma > background at Station 401 on January 6, 2012.

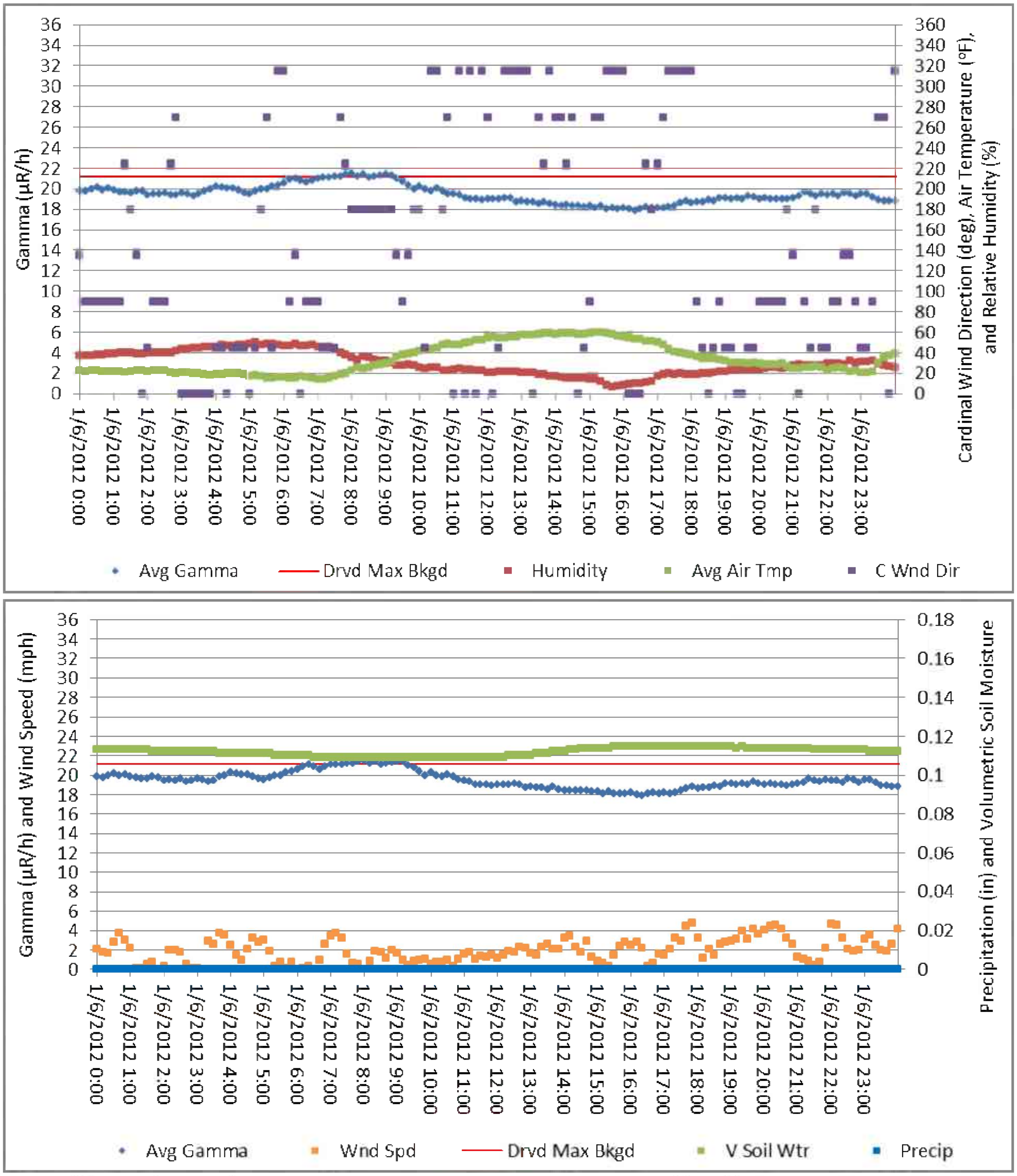

Figure 19. Various environmental parameters and observed gamma values for the occasion when observed gamma > background at Station 402 on January 6, 2012.

On May 26, 2012, the observed gamma values began to increase at approximately 0550 and continued to be elevated until approximately 1130 at Station 401 (Figure 20). However, they did not exceeded the station background value until approximately 0920, and then only for approximately 10 minutes. At Station 402, the increase began at approximately 0600 and gamma values remained elevated until approximately 1040 (Figure 21). The peak observed gamma during this event occurred approximately 0720 and lasted approximately 20 minutes. The maximum observed gamma values exceeded the background values by 0.12 μR/h and 0.05 μR/h at Stations 401 and 402, respectively. Humidity was high during the night and was just under 80 percent at both stations. As the rain began at approximately 0340 at Station 401, the humidity at both stations rose to almost 100 percent and remained there until the rain quit, and then it dropped quickly to approximately 55 percent. Soil moisture showed a slow rise during the rainfall. On this occasion, the increase in gamma and the rainfall events occurred at approximately the same time. Wind speed was generally less than 10 mph during the gamma event, but increased to approximately 25 mph as the gamma values decreased. The winds were from the south and southwest as the gamma values were increasing and continued from that direction during most of the time the gamma was elevated. Prior to and following the gamma event the winds were predominately from the west without any apparent impact on the gamma values. The air temperature followed a typical diurnal pattern, even though the warming trend was delayed until after the rainfall ended. There was no clear impact of air temperature on the gamma values.

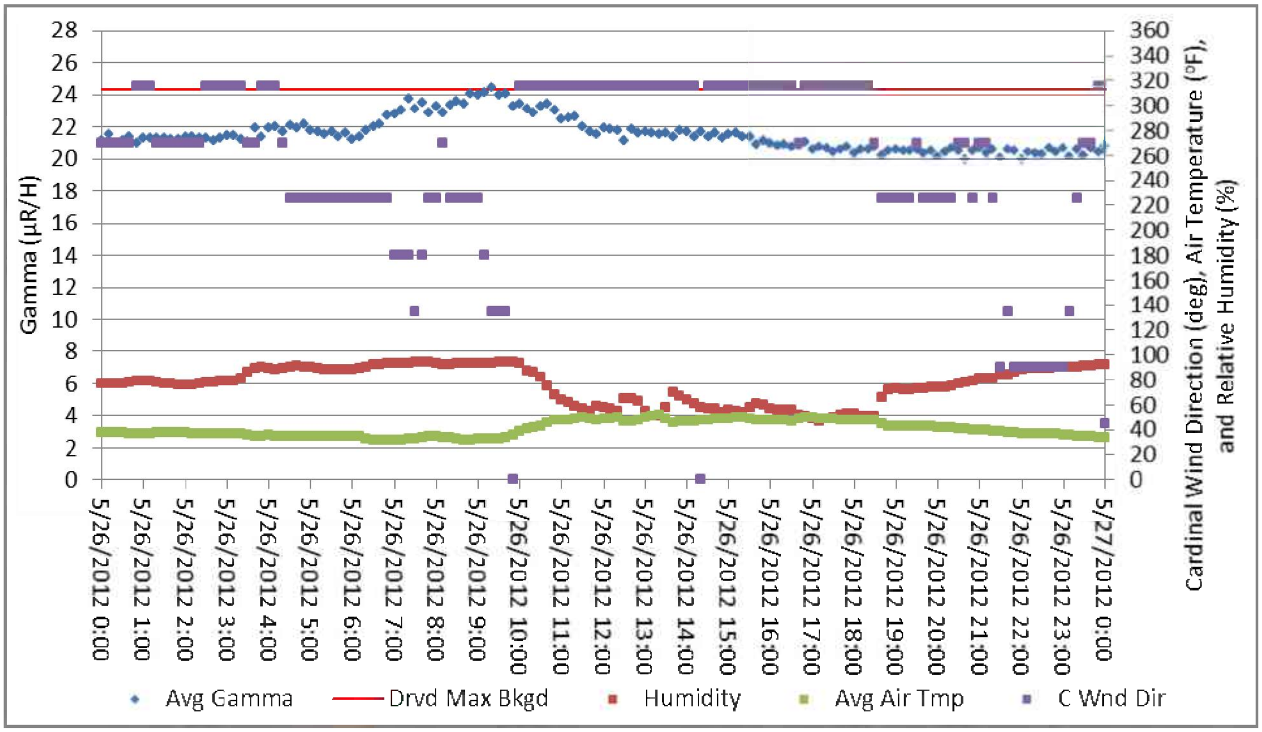

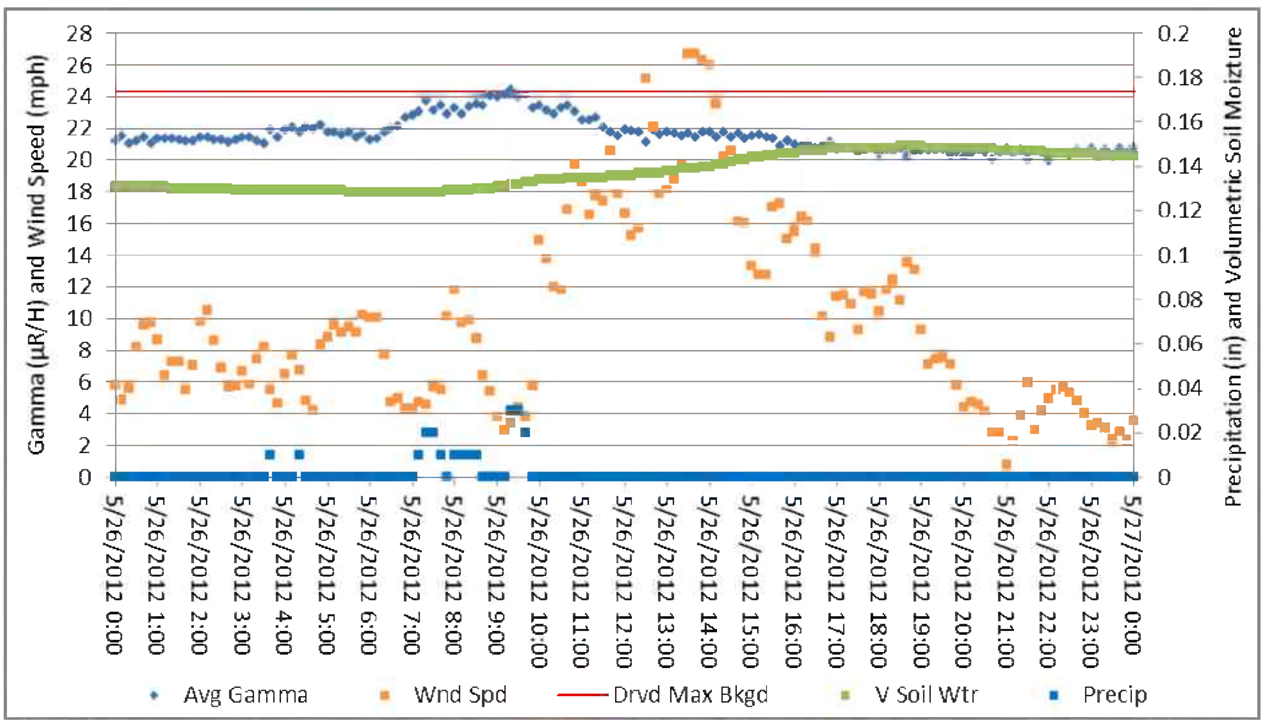

Figure 20. Various environmental parameters and observed gamma values for the occasion when observed gamma > background at Station 401 on May 26, 2012.

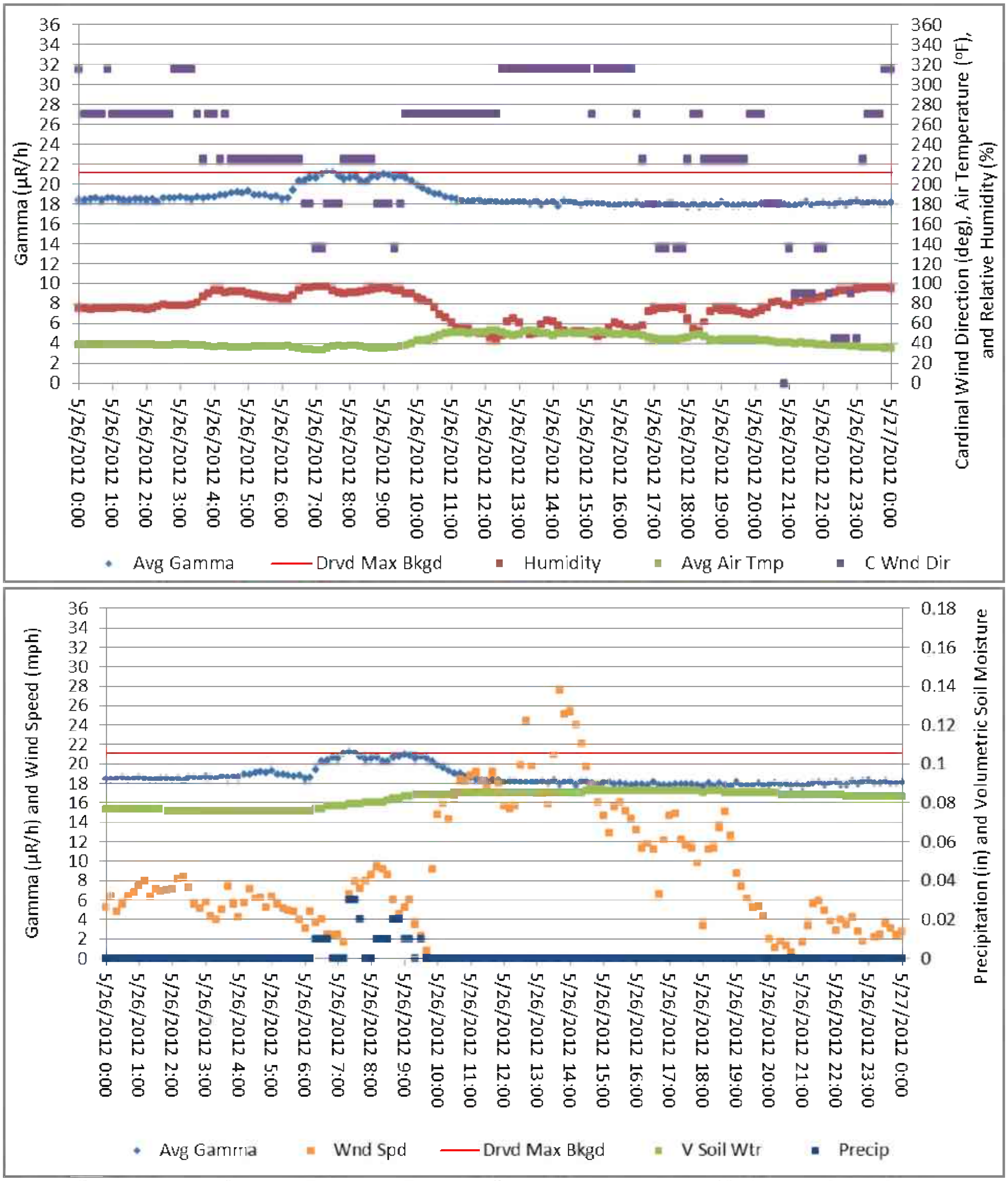

Figure 21. Various environmental parameters and observed gamma values for the occasion when observed gamma > background at Station 402 on May 26, 2012.

It has been suggested that low barometric pressure is associated with higher gamma values because the low pressure allows radon gas to be more readily passed through the ground. Figures 22 and 23 show the barometric pressure patterns associated with the elevated gamma events at Station 400 on July 26, 2010, and Station 402 on May 26, 2012. Barometric pressure measurements are not collected at Station 401, but they should be similar to the observations from the other stations. At Station 400 on July 26, 2010, the barometric pressure closely paralleled the gamma values during the elevated gamma event (Figure 22). However, later in the day the barometric pressure declined without any response in the gamma data. At Station 402 on May 26, 2012, the barometric pressure showed a steady increase that started before the elevated gamma event began and continued throughout the day (Figure 23). There appears to be no response in the gamma values to this increasing barometric pressure change.

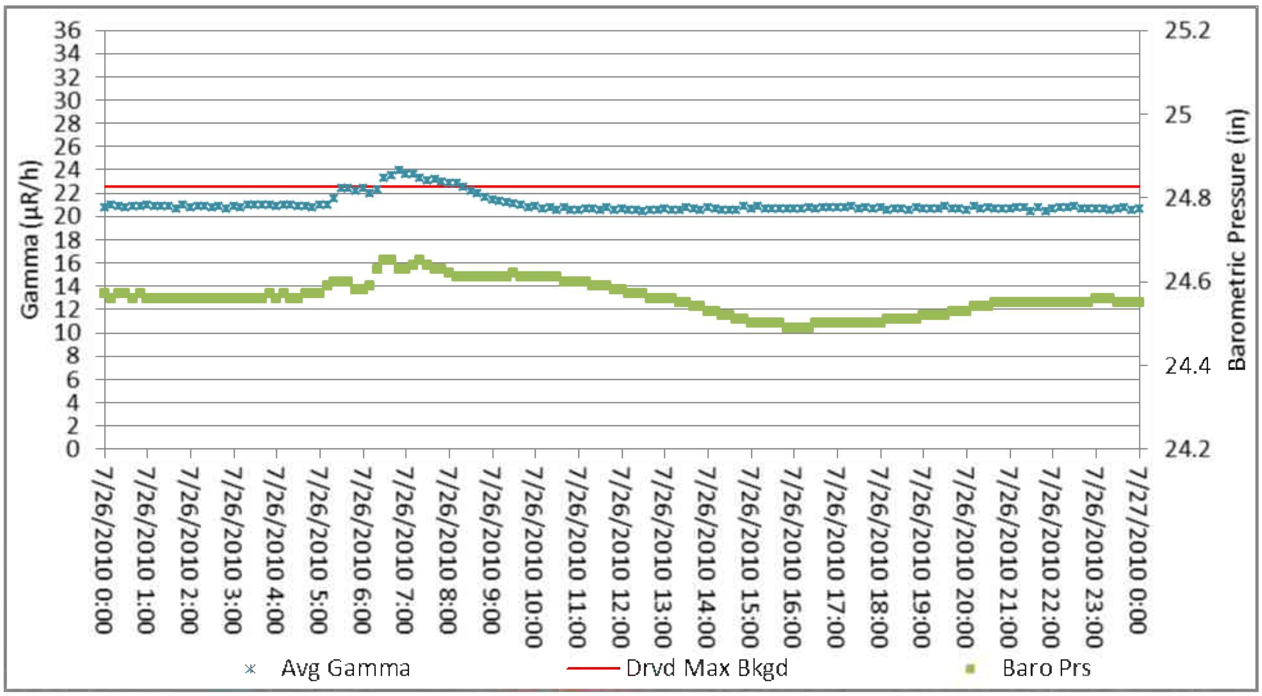

Figure 22. Barometric pressure tracked the gamma values closely during the elevated gamma event at Station 400 on July 26, 2010.

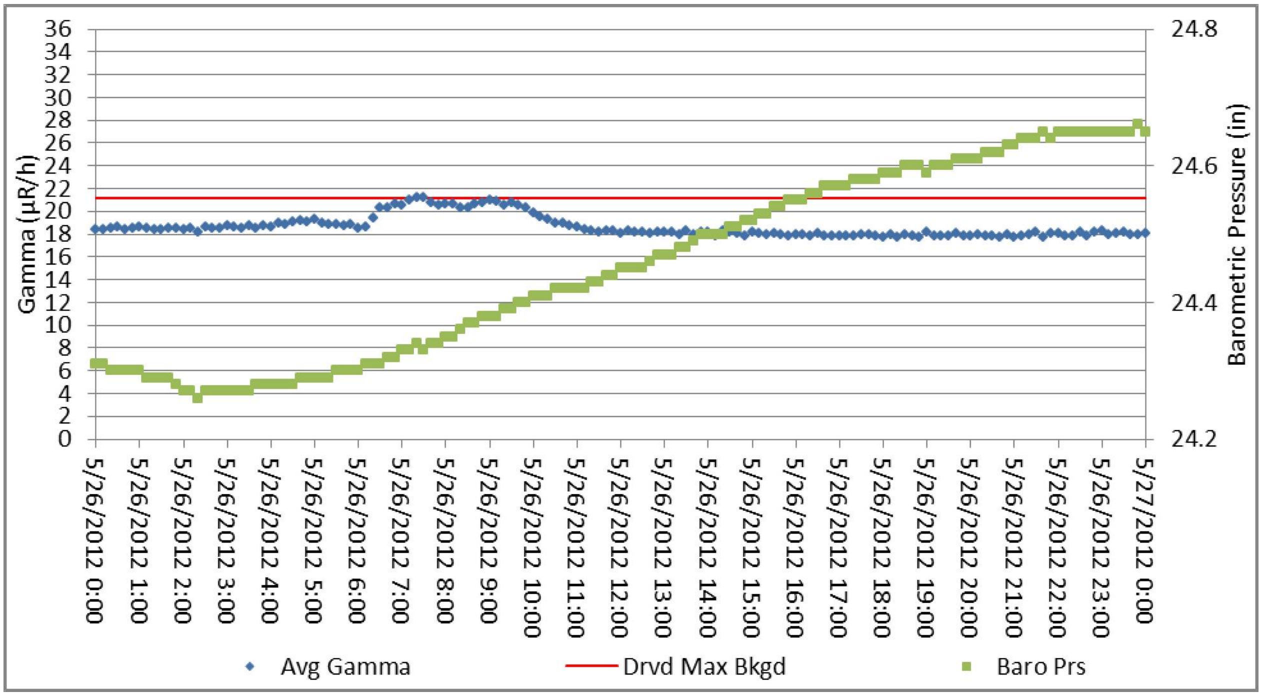

Figure 23. Gamma values showed no response to barometric pressure changes at Station 402 during the elevated gamma event on May 26, 2012.

Plotting observed gamma values against eight cardinal (north, northeast, south, etc.) wind directions (Figure 24) shows that although the background gamma value may be exceeded during winds coming from any direction, the highest gamma values at each monitoring station are associated with different wind directions. At Station 400, the highest gamma values are associated with winds from the southeast to the west. At Station 401, winds from the south and west are associated with the highest gamma values. At Station 402, the highest observed gamma values are associated with winds from the north and northeast. Station 402 gamma values associated with winds from the south and southwest are only slightly greater than gamma values associate with winds from other directions. The highest gamma values at each station (Figure 24) are associated with winds from the two dominant wind directions: southerly and northerly.

Stations 401 and 402 are located adjacent to and on the north side of Clean Slate III and I, respectively. Station 400 is located approximately 7 km northwest of the Clean Slate sites. The position on the north sides of the surface contamination sites suggests that higher gamma values would be associated with winds from the south. This expectation is substantiated at Station 401. The higher gamma values at Station 402 are associated with northerly winds. Additionally, differences between the largest gamma values for each cardinal wind direction is no more than 2.5 µR/h at Station 400 and only approximately 1.2 µR/h at Stations 401 and 402. These observations suggest that the Clean Slate contamination sites have little impact on the maximum gamma values observed at the monitoring station.

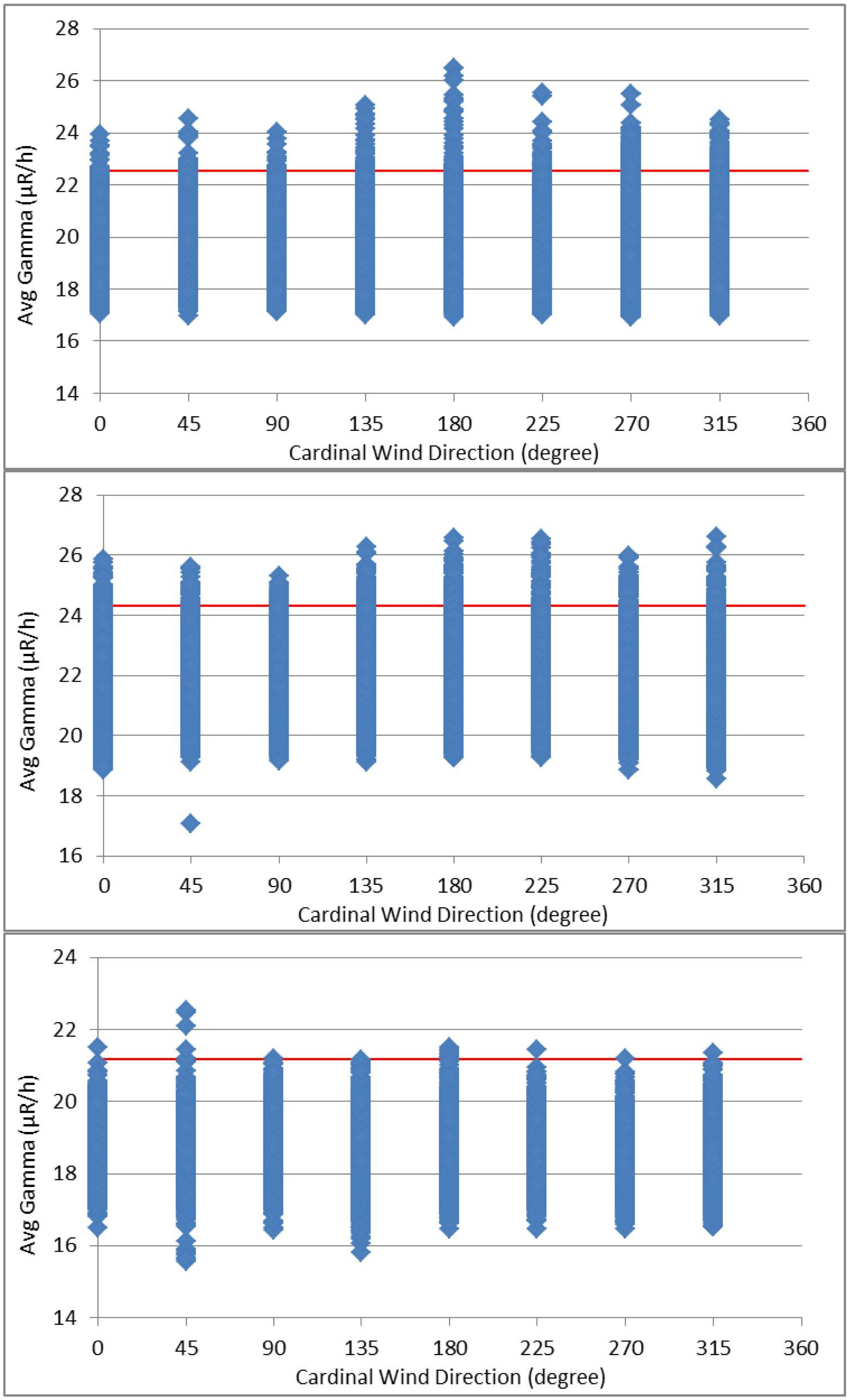

Figure 24. Observed gamma values show different relationship to cardinal wind direction at each of the TTR monitoring stations (top: Station 400; center: Station 401; bottom: Station 402). The red lines show the background value for each station.

The daily average gamma exposure for each year of record at the three TTR monitoring stations range from 18.13 µR/h to 21.39 µR/h. These values consistently exceed the values for all, or all but one, of the CEMP stations that surround the TTR (Table 18). Geology and geography characteristics for the TTR and surrounding CEMP monitoring stations are presented in Table 19. The CEMP station at Sarcobatus is situated in a geological environment that is most similar to the TTR stations, which likely explains why the Sarcobatus and TTR gamma values generally exceed those reported at the other CEMP stations. Additionally, the elevation at the TTR stations is 1,400 ft to 1,500 ft higher than the elevation at the Sarcobatus station. This may explain why the gamma values at TTR are typically higher than values at Sarcobatus. However, because the average gamma values at Sarcobatus and TTR stations are approximately equivalent, it seems unlikely that the gamma observations at the TTR stations are the result of wind transport of contaminated soil material.

Table 18. Daily average gamma exposure (µR/h) (PIC observations) for CEMP stations surrounding the TTR during the period of data collection. (Sources: DOE, 2010, 2011, 2012, 2013)

Station Location	2009	2010	2011	2012
TTR Station 400	21.02[1]	19.99[1]	18.97	18.15
TTR Station 401	20.86[2]	21.33[2]	21.39	21.25
TTR Station 402	ND	ND	18.68[3]	18.13
Goldfield	15.20	15.15	14.90	15.10
Nyala Ranch	14.25	13.65	14.35	15.20
Rachel	15.45	15.05	14.95	15.30
Sarcobatus Valley	19.50	16.90	16.40	16.55
Stone Cabin Ranch	17.25	16.50	16.95	13.75
Tonopah	16.35	16.10	16.20	16.15
Twin Springs Ranch	19.50	19.40	19.90	19.50

[1]Station 400 data was collected for 363 days in 2009; 358 days in 2010.
[2] Station 401 data was collected for only 11 days in 2009; 359 days in 2010;
[3] Station 402 data for 2011 was collected for only 18 days.
ND = no data collected, station not established.

Table 19. Comparison of geology and geography of TTR and surrounding CEMP monitoring stations.

Station	Location: Latitude Longitude (° ' ")	Elevation (ft)	Geological Environment	Geological Source Material	Reference
TTR Station 400	37 47 10 -116 45 21	5534	Quaternary alluvium	Tertiary volcanics: tuff, rhyolite, andesite	Cornwall, 1972
TTR Station 401	37 45 39 -116 40 58	5392	Quaternary alluvium	Tertiary volcanics: tuff, rhyolite, andesite	Cornwall, 1972
TTR Station 402	37 42 33 -116 39 32	5387	Quaternary alluvium	Tertiary volcanics: tuff, rhyolite, andesite	Cornwall, 1972
Goldfield	37 42 38 -117 14 25	5590	Bedrock	Tuff, basalt	Albers and Stewart, 1972
Nyala Ranch	38 14 54 -115 43 44	4842	Quaternary alluvium	Tuff, quartzite, limestone, dolomite	Kleinhampl and Ziony, 1985
Rachel	37 38 36 -115 44 21	4854	Quaternary alluvium	Tertiary volcanics, sandstone	Tschanz and Pampeyan, 1970
Sarcobatus	37 16 46 -117 01 58	4014	Quaternary alluvium	Tertiary volcanics: tuff, basalt, rhyolite,	Cornwall, 1972
Stone Cabin	38 12 25 -116 37 58	5806	Quaternary alluvium	Tertiary volcanics: tuff	Kleinhampl and Ziony, 1985
Tonopah	38 03 37 -117 13 14	6180	Bedrock	Dacite and Latite	Kleinhampl and Ziony, 1985
Twin Spring	38 12 14 -116 10 26	5146	Quaternary alluvium	Tuff, Basalt	Kleinhampl and Ziony, 1985

As shown in Table 18 and discussed above, average gamma radiation values observed at the TTR monitoring stations are higher than at surrounding CEMP stations. The higher gamma values observed at the TTR stations may be due differences in the geological environment surrounding the stations and in the elevation of the stations. The geological environment surrounding the TTR stations is most like the area surrounding the CEMP station in Sarcobatus Flat, which reports the highest gamma values for CEMP stations surrounding the NTTR. The TTR gamma observations may exceed the Sarcobatus Flat observations because the TTR stations are 1,400 ft to 1,500 ft higher in elevation. Jones (1961) describes decreasing gamma counts with decreasing altitude. Therefore, gamma radiation exposure in the vicinity of the TTR monitoring stations is somewhat higher than the exposures reported at the surrounding CEMP stations. However, the observed gamma exposures at the TTR stations are less than the 26.99 μR/h (converted from 2.27 mSv/yr assuming a 1:1 rad:roentgen approximation) estimated by Moeller (2006) to be the average natural background dose rate to residents of Nevada. The TTR gamma observations are approximately equivalent to or slightly higher than the background gamma exposure levels (15 μR/h to 20 μR/h [Anonymous, 2002; Stegen *et al.*, 2006]) reported for Denver, Colorado, which is at an elevation of approximately 5,200 ft. This elevation is within a few hundred feet of the elevations at the TTR stations, so these numbers suggest that gamma exposure in the vicinity of the TTR stations is similar to the exposure experienced in Denver.

ANALYSIS OF SOIL TRANSPORT BY SUSPENSION AND SALTATION

Particulate mass larger than 10 microns in aerodynamic diameter (PM_{10}) is a criteria pollutant that is regulated by the National Ambient Air Quality Standards (NAAQS) that are specified in the Clean Air Act (40 CFR part 50), which was last amended in 1990. The NAAQS limit for PM_{10} is 150 μg/m^3 and the standard states that this limit should not be exceeded more than once per year, on average, over three years. These standards are appropriate for application to a populous metropolitan area. In contrast, exposure limit standards in occupational settings as specified by the Occupational Safety and Health Agency (OSHA) can be orders of magnitude greater—for example, in the shipyard industry—with limits as high as 5,000 μg/m^3 over an eight-hour work shift (29 CFR). In both cases, the substance that the particles consist of is not specified and certain inhalable aerosols that have comparatively high concentrations of toxins can be hazardous at much lower concentrations than are reflected in the standards.

Neither the NAAQS standard for PM_{10} nor the OSHA standards are pertinent to the present study. First, the primary concern at TTR is not the typical sources of PM_{10} that are encountered in populated areas or in specific occupational settings, such as mines or shipyards. The specific concern at TTR is with the potential resuspension of radionuclide-contaminated soil material under high-wind conditions. In this context, there is no specific level of PM_{10} that can be construed to be a limit. Instead, the PM_{10} measurements at TTR are intended to identify periods and conditions when the resuspension of soil dust occurs and to determine what conditions result in comparatively high rates of resuspension. The assessment reported here is conducted with regard to resuspension of soil material without concern for the presence or absence of radionuclide contamination on the suspended soil particles.

Second, the measurement of PM_{10} for regulatory and occupational health purposes (e.g., 40 CFR Part 53 Subpart D, 1987) requires using very specific techniques that are intended to ensure comparability among measurements regardless of where they are conducted. At TTR, these specific techniques, referred to as Federal Reference Methods (FRM) or Federal Equivalent Methods (FEM), are not employed because they require a substantial amount of infrastructure that is not available. Moreover, FRM and FEM monitors generally provide lower time resolution measurements than the near real-time particle profilers that are in use at TTR. The data here are presented in terms of reconstructed PM_{10}, a quantity that is derived from the number concentrations (i.e., # particles/unit volume of air) of particles in the different size bins that the particle profiler is able to differentiate. The intent is to translate particle counts to a quantity that is more easily compared with PM_{10}. However, it is erroneous to try to use reconstructed PM_{10} to determine compliance or lack of compliance with a mass-based PM_{10} standard. The reconstructed PM_{10} quantity is useful for examining data from the same measurement location over time, comparisons between stations that use the same particle profiler instrument, and for gross comparison with standards that are specified in terms of a PM_{10} limit.

Reconstructed PM_{10} is a quantity that is more easily understood than the raw particle counts reported from the particle profiler. It can be calculated using the equation:

$$Reconstructed\ PM10\ \left(\frac{\mu g}{m^3}\right) = \sum_{n=1}^{8} C_n * M_n = \sum_{n=1}^{8} C_n * \rho * \frac{4\pi * {r_n}^3}{3} * BF_n \qquad (1)$$

where C_n is the number concentrations of particles in bin n in #/m^3 and M_n is the mass of an average particle in bin n (μg), which is calculated as the volume of such a particle (m^3) multiplied by the density ρ (μg/m^3), which is assumed to equal that of silica (2.6 X 10^9 μg/m^3). The volume of the average particle is calculated using the volume equation for a sphere with radius r_n. The radius of an average particle in bin n is determined as the logarithmic mean of the minimum and maximum radii of that bin. For example, if the manufacturer has stated that a specific particle size bin has particles with radii that span a range from 0.5 μm to 1.0 μm, then the representative radius for that size bin would be 0.707 μm. The parameter BF_n is the fraction of the bin that is included in the PM_{10} size fraction. For bins in which the upper bound for the particle size is below 10 μm, the parameter has a value of unity. For bins in which the lower bound is above the 10 μm limit, the parameter is zero. For the bin in which the upper limit is above 10 μm, but the lower limit is below this value, BF is equal to the fraction of the bin that is below 10 μm.

Annual summaries for reconstructed PM_{10} concentrations are shown for Station 400 for the years 2008 through 2012 in Figures 25 through 29. Figures 30 through 34 show comparable data for Station 401 for the years 2008 through 2012, whereas Figures 35 and 36 show data for Station 402 for the years 2011 and 2012. The y-axis scale for all figures is logarithmic so that it is possible to view the wide range of concentrations that are encountered over the course of a year at any one station. With the caveat that the reconstructed PM_{10} is suitable only for gross comparison with the mass-based PM_{10} that is used to set standards, it is noteworthy that all data shown are well below the eight-hour OSHA standard of 5,000 μg/m^3. It is also true that when averaged over 24 hours (data not shown), the reconstructed PM_{10} exceeds the NAAQS standard of 150 μg/m^3 six times at Station 401 and one time at Station 400. These exceedances may be of concern if they occur in a populated area, but they are not of regulatory interest in the context of the present study because they are in remote areas and because the instrument used to measure reconstructed PM_{10} is not accepted as a federal standard method. Therefore, the ensuing discussion has no implications in the context of a federal or health-based standard for air quality. Instead, the focus is on understanding what environmental conditions lead to the resuspension of soil dust that is measurable as elevated reconstructed PM_{10} with respect to relatively clean background air.

At all sites, despite substantial day to day variation, it is generally true that PM_{10} concentrations are higher in the spring (March through May) and the late summer (the middle of July to the end of August) than they are during the winter months (December through February) and early summer months (June through the middle of July). The late fall period (October through the end of November) sometimes exhibits elevated PM_{10} concentrations. Although these are broad generalizations and the time frames used should be considered only rough guidelines, the above-noted trend can be explained as follows: In central Nevada, as in most of the southwestern United States, synoptic-scale frontal systems are most prevalent during the spring and windblown dust is associated with these windy periods. Similarly, the late summer can herald the occurrence of thunderstorms, especially in the afternoons of hot and humid days. Although these events do not always result in rain, they are usually associated with high winds and have the potential to cause elevated PM_{10}. During winter, the soil is sometimes frozen and often wet for prolonged periods. Consequently, winter frontal systems tend not to result in as much suspended dust. The late fall period is often associated with wildfire season. These types of events would certainly elevate the PM_{10} concentration, but they are not directly relevant to the wind erosion of soils at TTR. In some locales, agricultural activities such as harvesting and seasonal road construction and maintenance can be a significant source of fugitive dust. However, these activities are largely absent from the TTR.

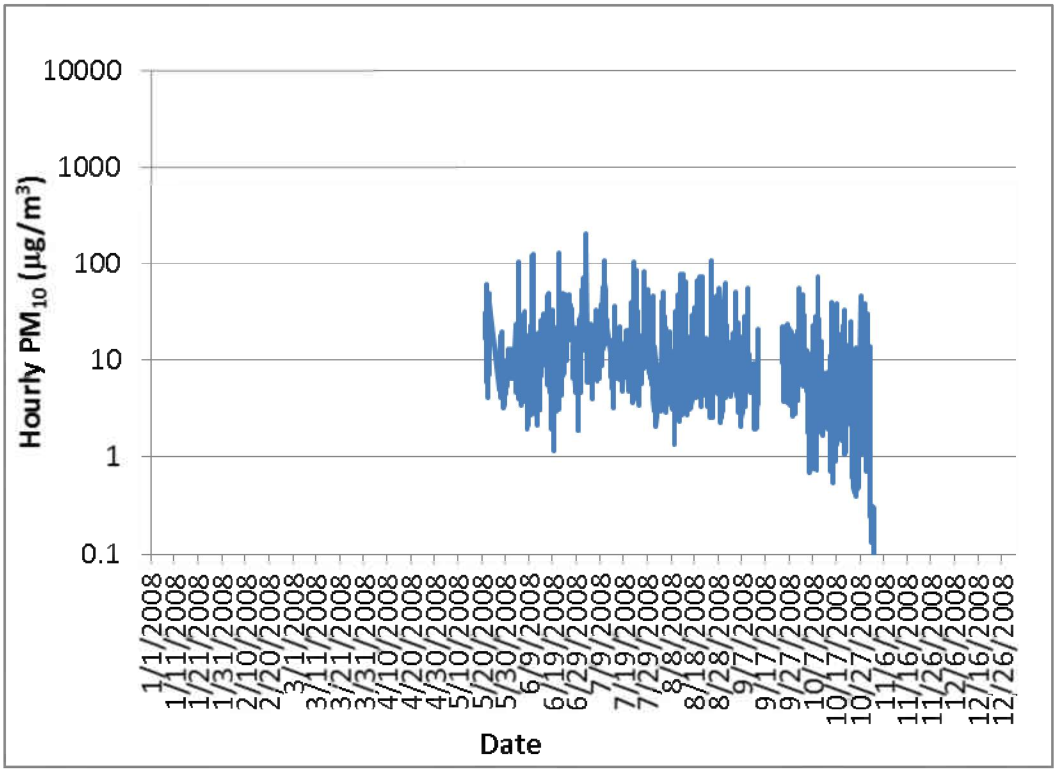

Figure 25. Station 400 reconstructed hourly PM_{10} concentrations (µg/m^3) for 2008.

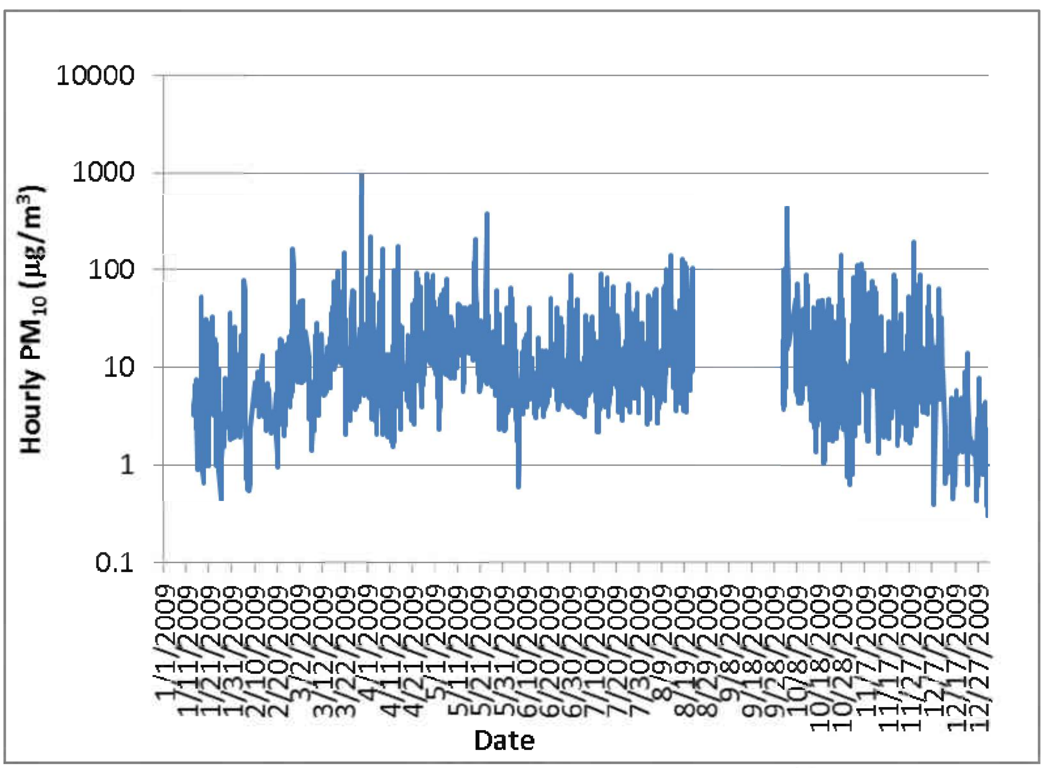

Figure 26. Station 400 reconstructed hourly PM_{10} concentrations (µg/m^3) for 2009.

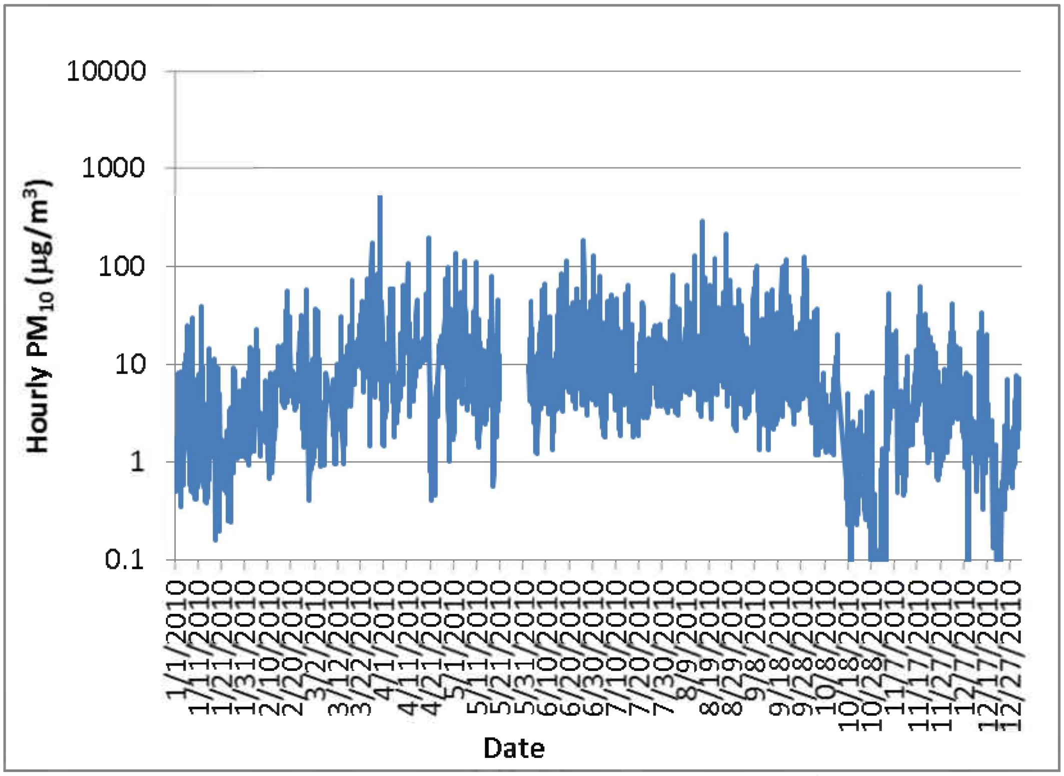

Figure 27. Station 400 reconstructed hourly PM_{10} concentrations ($\mu g/m^3$) for 2010.

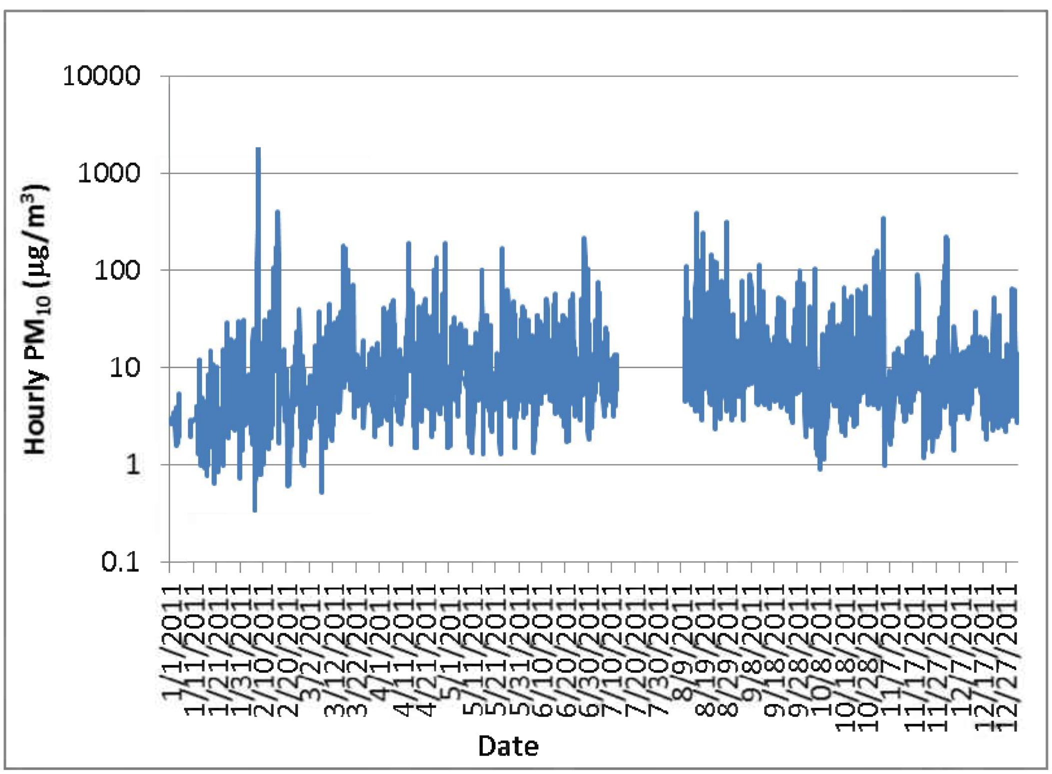

Figure 28. Station 400 reconstructed hourly PM_{10} concentrations ($\mu g/m^3$) for 2011.

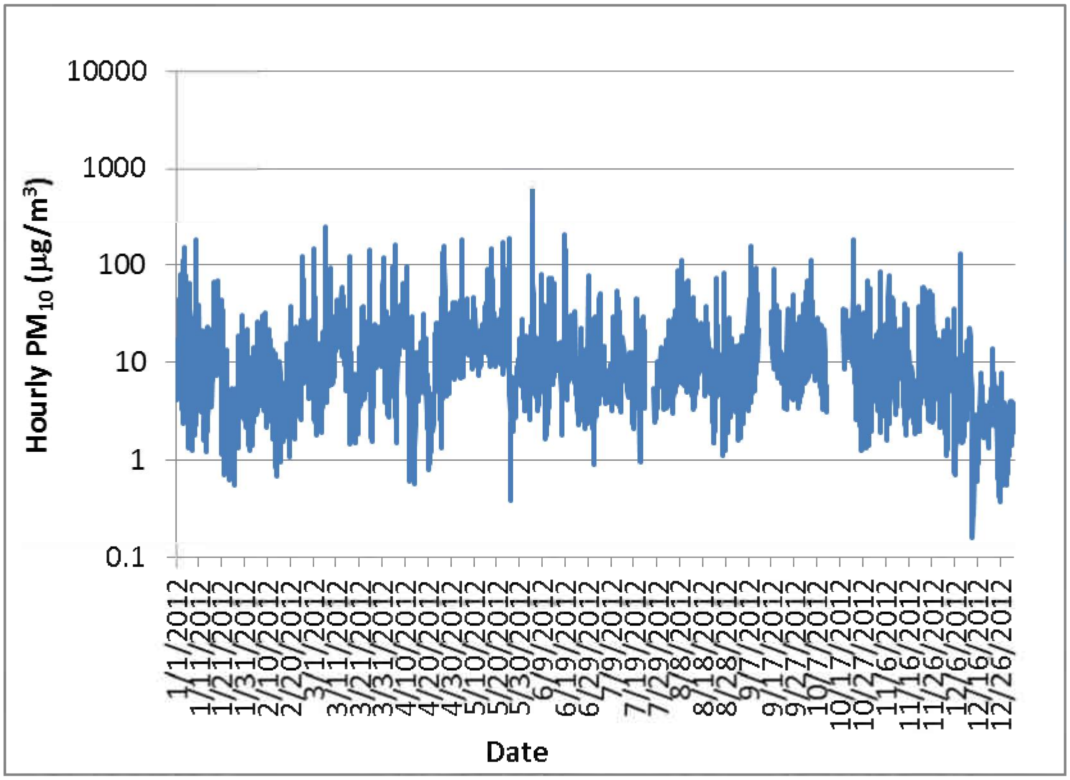

Figure 29. Station 400 reconstructed hourly PM_{10} concentrations ($\mu g/m^3$) for 2012.

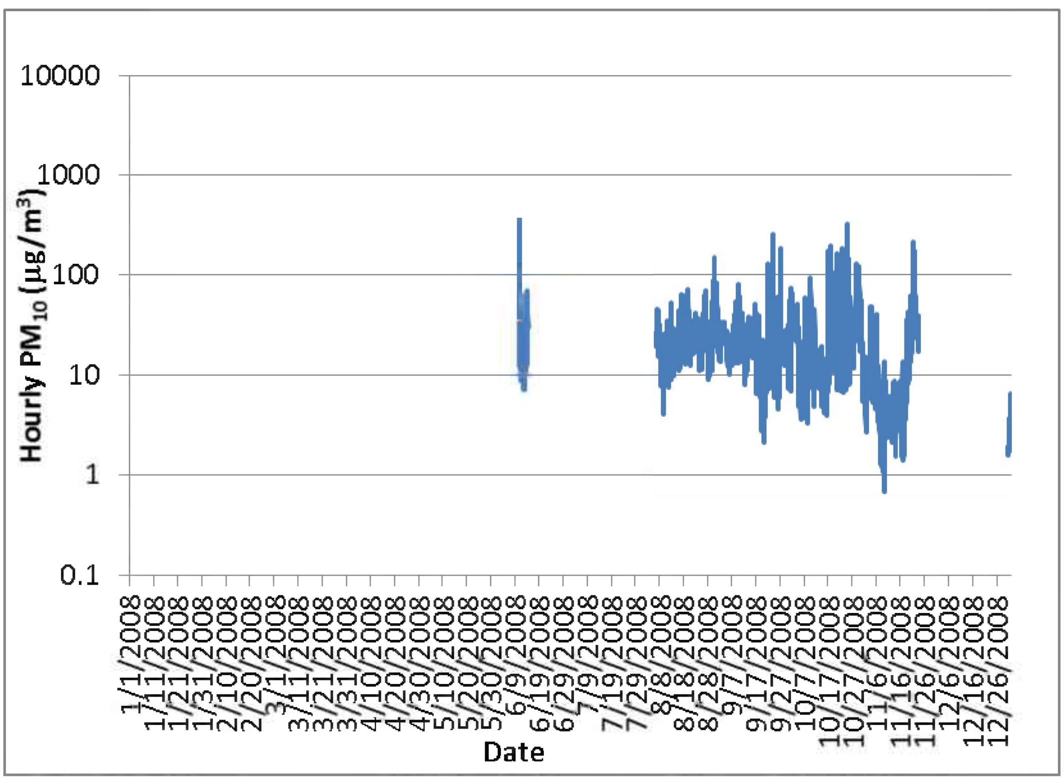

Figure 30. Station 401 reconstructed hourly PM_{10} concentrations ($\mu g/m^3$) for 2008.

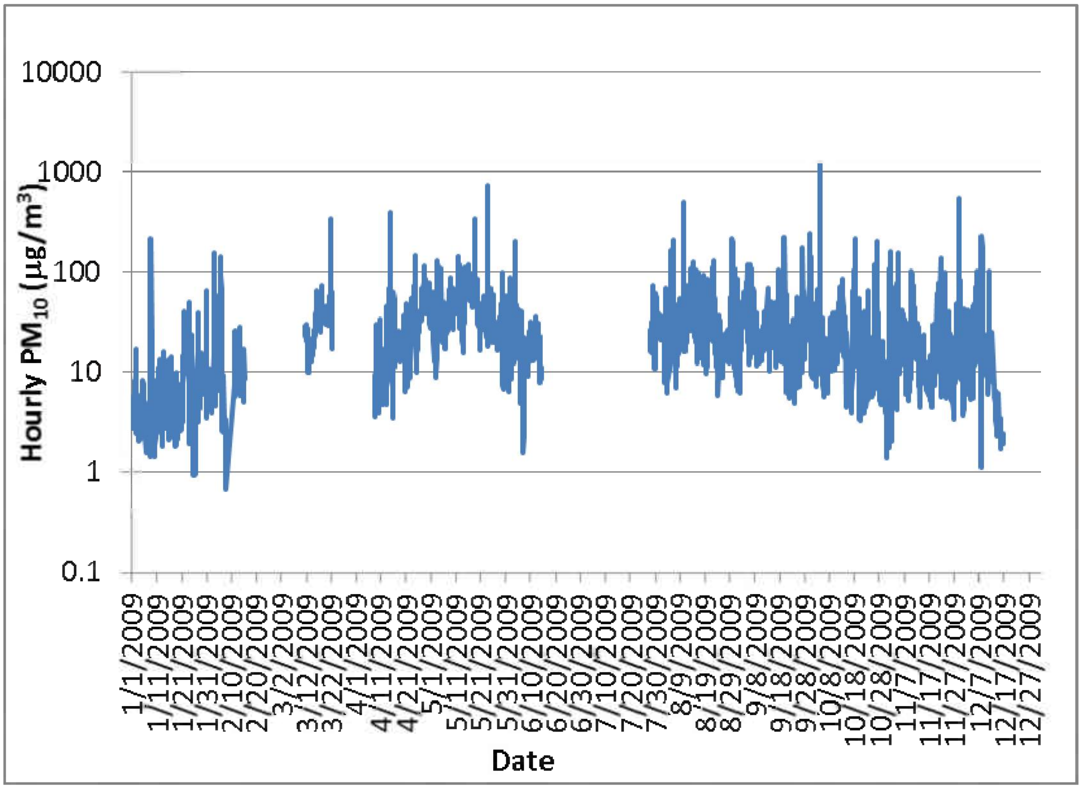

Figure 31. Station 401 reconstructed hourly PM_{10} concentrations ($\mu g/m^3$) for 2009.

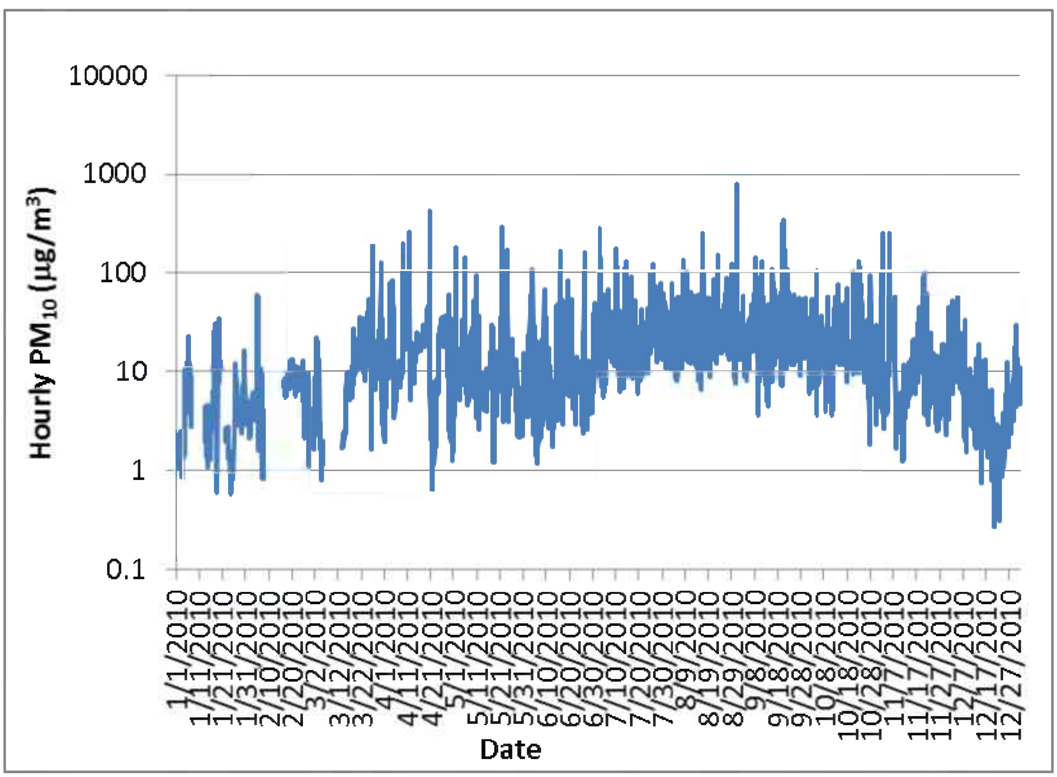

Figure 32. Station 401 reconstructed hourly PM_{10} concentrations ($\mu g/m^3$) for 2010.

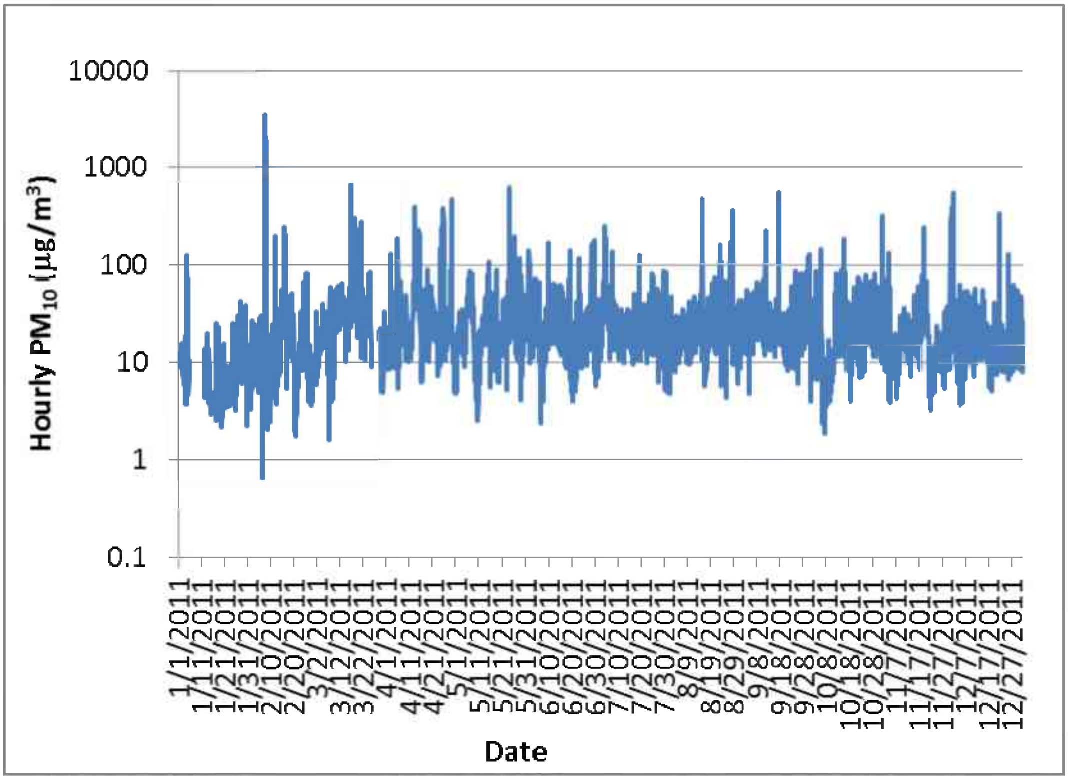

Figure 33. Station 401 reconstructed hourly PM_{10} concentrations (µg/m^3) for 2011.

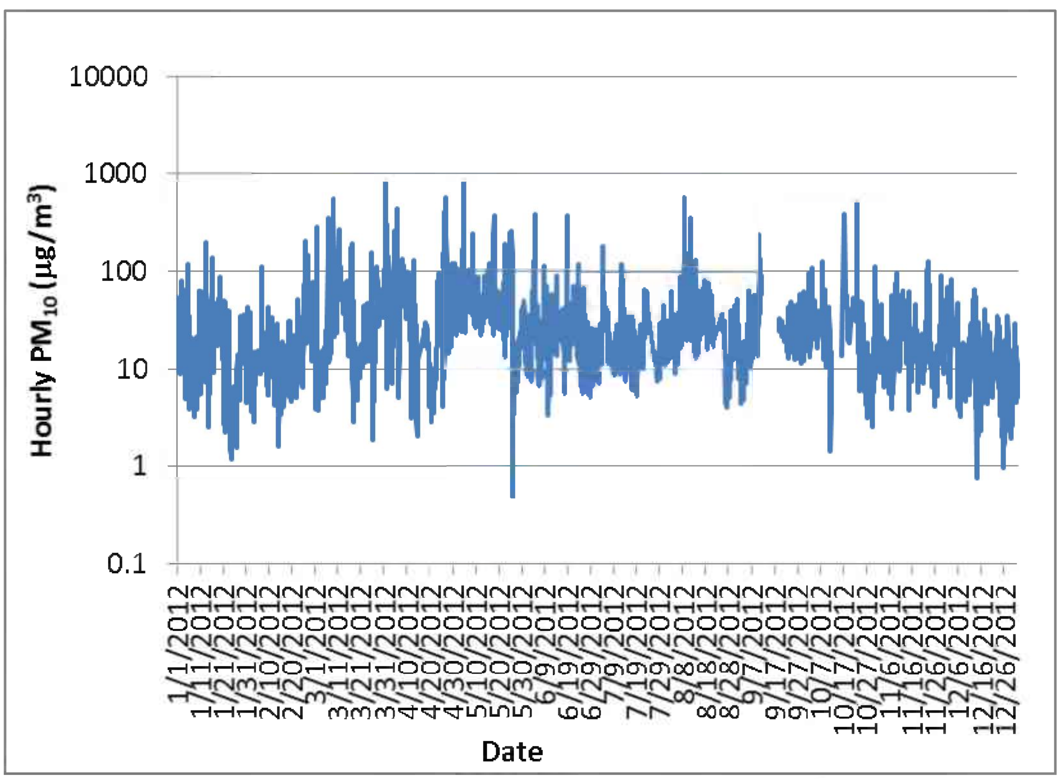

Figure 34. Station 401 reconstructed hourly PM_{10} concentrations (µg/m^3) for 2012.

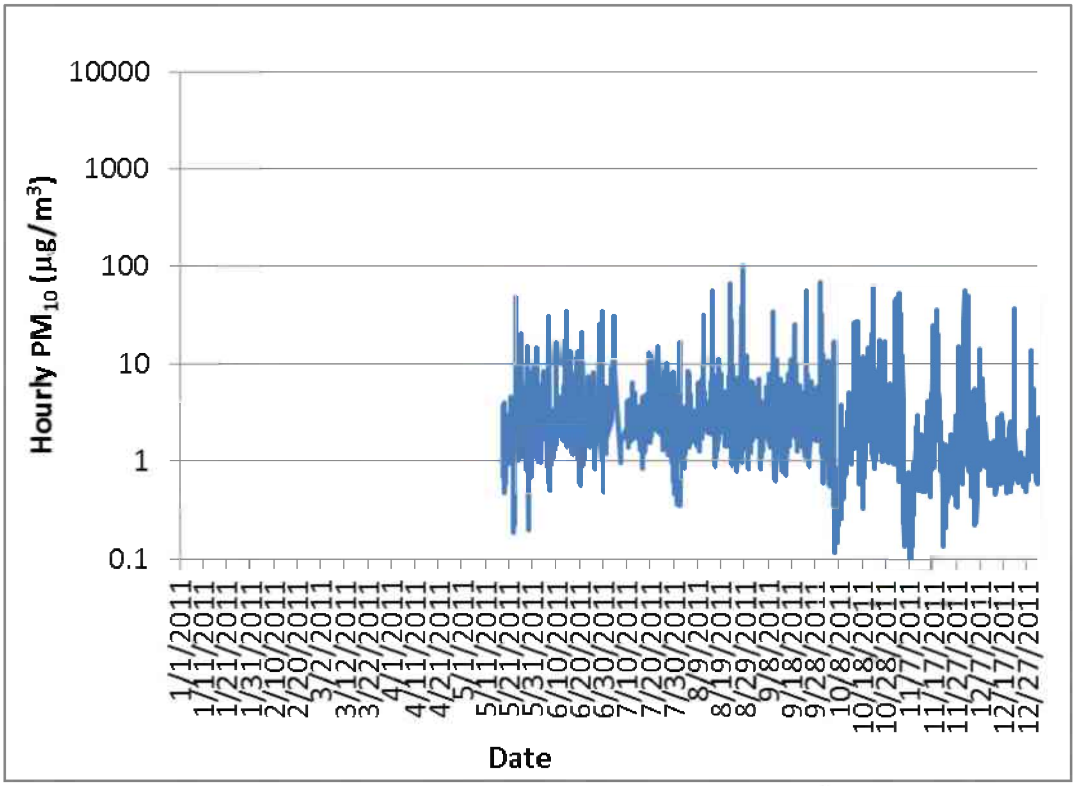

Figure 35. Station 402 reconstructed hourly PM_{10} concentrations (µg/m^3) for 2011.

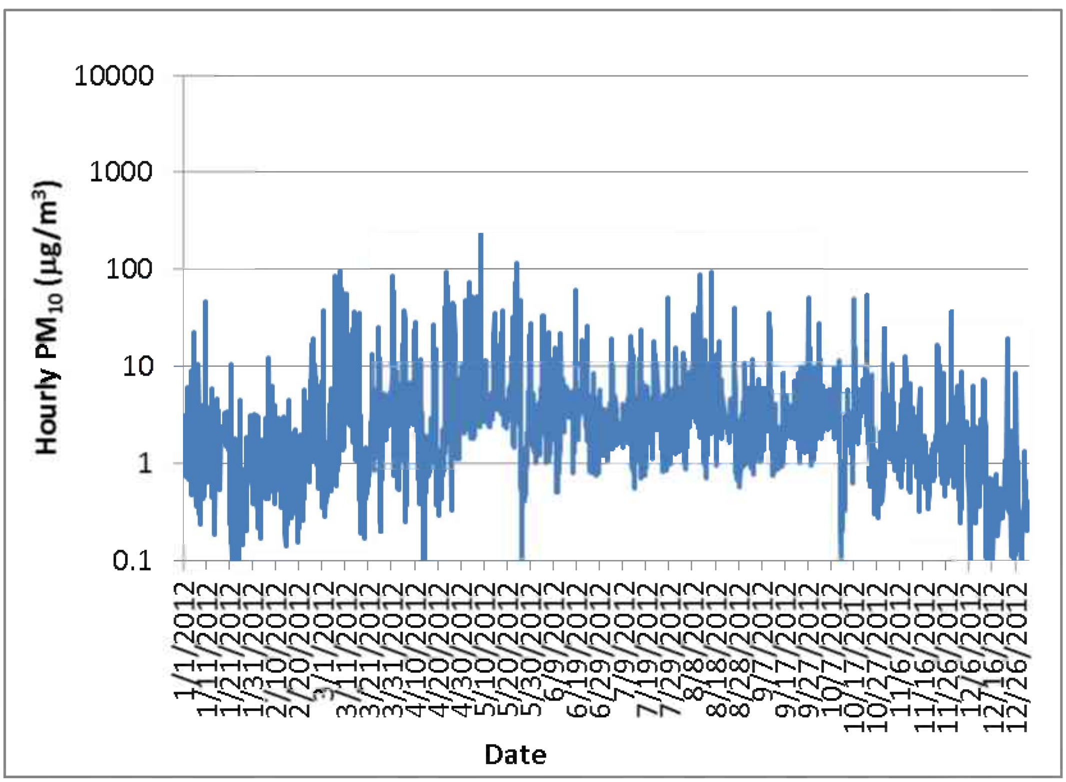

Figure 36. Station 402 reconstructed hourly PM_{10} concentrations (µg/m^3) for 2012.

DISTRIBUTION OF WIND

It is useful to examine only winds that are greater than 15 mph (Figures 37 through 39) because that value of wind speed can be considered an approximate lower-limit threshold for the wind suspension of dust in general (e.g., Pelletier [2006]). Earlier summaries of annual data from the TTR stations (Hartwell *et al.*, 2012; Mizell *et al.*, 2013) corroborate the choice of 15 mph as a lower limit for when the effect of wind on dust concentrations becomes evident. At Station 400, this nominal threshold wind speed is exceeded 7.2 percent of the time, whereas at Stations 401 and 402 it is exceeded 10.9 percent and 9.6 percent of the time, respectively. This suggests that Station 400 may be more sheltered from wind effects than the other two sites. As a fraction of all winds above 15 mph, the occurrence of winds in the 25 mph to 30 mph and greater than 30 mph ranges at Station 400 is also less frequent than at the other two sites. Perhaps this can also be attributed to a sheltering effect imposed by the buildings and other structures that are part of the ROC at the SNL compound or the proximity of topographic relief to the northwest of the Station 400 site (Figure 2). For example, there is a building that is approximately 20 m to the west of the original location of Station 400 (2008-2012) that would account for the observed lower wind speeds. At its newer location (late 2012), Station 400 is relatively unobstructed from the west, but it is within approximately 10 m of a building on the north. It is difficult to avoid such obstructions when placing a monitoring station within a facility that consists of buildings, but the measured parameters (e.g., wind speed) reflect the conditions at the measurement location. They are also useful when conducting the detailed analysis of relationships between wind (measured at a location under the local conditions) and dust (measured at the same location) that is done in the subsequent sections.

The seasonal distribution of winds exceeding 15 mph and associated wind directions was also examined. Data are shown in Figures 40 through 43 for the four nominal seasons (defined in the figure captions) for Station 401. Because similar qualitative conclusions can be drawn for the Station 400 and Station 402 data, we omit showing those additional figures here. The most striking feature of the seasonal distribution of winds at Station 401 is that winds in excess of 15 mph are the most frequent in the spring and are also the most likely to be associated with the highest wind speed category (greater than 30 mph). This is indicated by the larger percentages (as represented by the concentric circle scale) associated with the pink bands (and dark red bands for wind speeds greater than 30 mph) in Figure 41 compared to Figures 40, Figure 42, and 43. The spring period is also the only one of the four where the frequency of occurrence of winds from the two main prevailing direction lobes is approximately the same. This is in keeping with what is expected during wind events that are brought about by the passage of a frontal system. High winds in one direction at the beginning of the wind storm are often accompanied by comparably high winds in nearly the opposite direction at the end of the wind storm (e.g., Bluestein [1993]). An example of such an event at Station 401 is provided in Figure 44.

In contrast, in the summer (Figure 42) and fall (Figure 43), winds tend to occur more often from the southerly lobe of the prevailing wind direction. Perhaps this is a result of monsoonal flows and associated outflow from thunderstorms to the south of the TTR. Most high-wind events in winter (Figure 40) are associated with flow from the northwesterly lobe of the prevailing wind. With these observations in mind, in the context of windblown dust, it would be ideal to consider the effect of winds from the northwesterly lobe separately from winds approaching from the southwesterly lobe. The difference in PM_{10} response to these two prevailing wind directions, but not separated by season, is examined in a following section. It would also be ideal to separate the effect on dust emission of winds occurring during different times of the year. This latter analysis is at this time somewhat difficult to complete with the relatively small amount of data that would be available. Analysis of dust and wind interaction on a seasonal basis is postponed until sufficient data is available to more adequately represent the average seasonal conditions at those sites. Instead, specific parameters—such as soil temperature, relative humidity, and soil moisture—are examined for their effect on PM_{10} dust emission and resultant concentrations because the effect of these parameters is more readily seen.

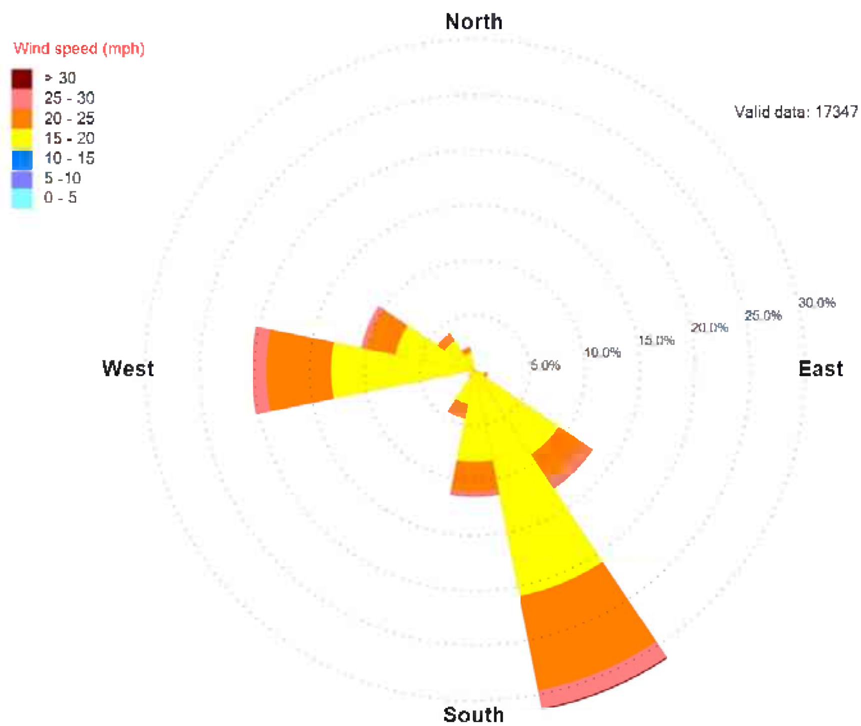

Figure 37. Wind rose for Station 400. Data are for periods when 10-minute average wind speed exceeds 15 mph.

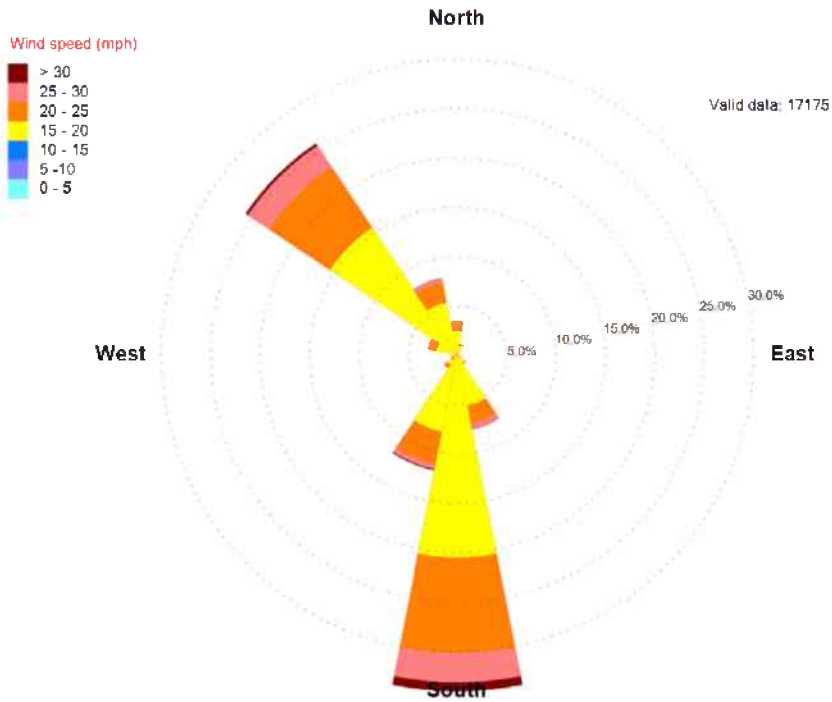

Figure 38. Wind rose for Station 401. Data are for periods when 10-minute average wind speed exceeds 15 mph.

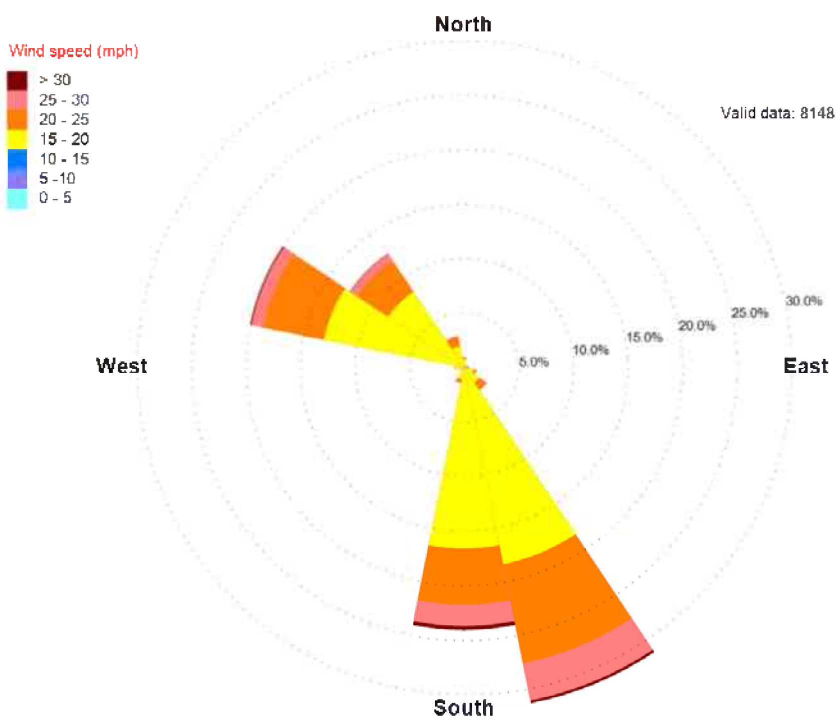

Figure 39. Wind rose for Station 402. Data are for periods when 10-minute average wind speed exceeds 15 mph.

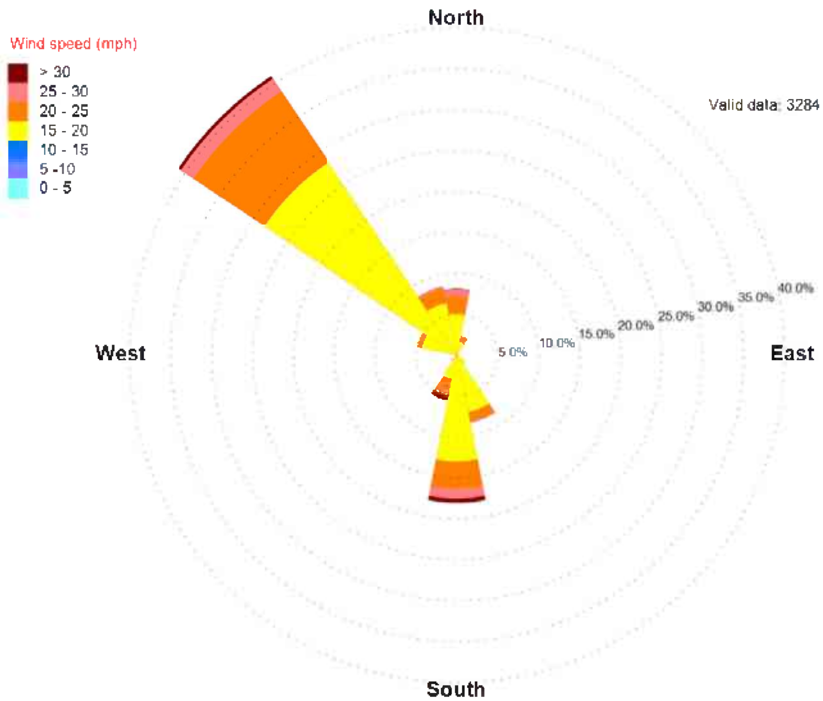

Figure 40. Wind rose for Station 401. Data are for periods in the winter (December 1-February 29) when 10-minute average wind speed exceeds 15 mph.

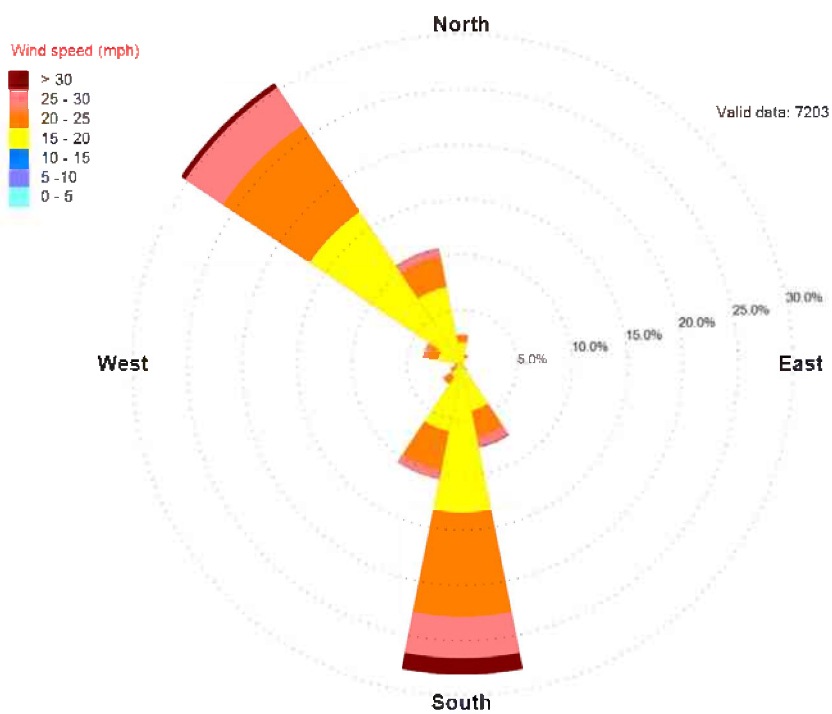

Figure 41. Wind rose for Station 401. Data are for periods in the spring (March 1-May 30) when 10-minute average wind speed exceeds 15 mph.

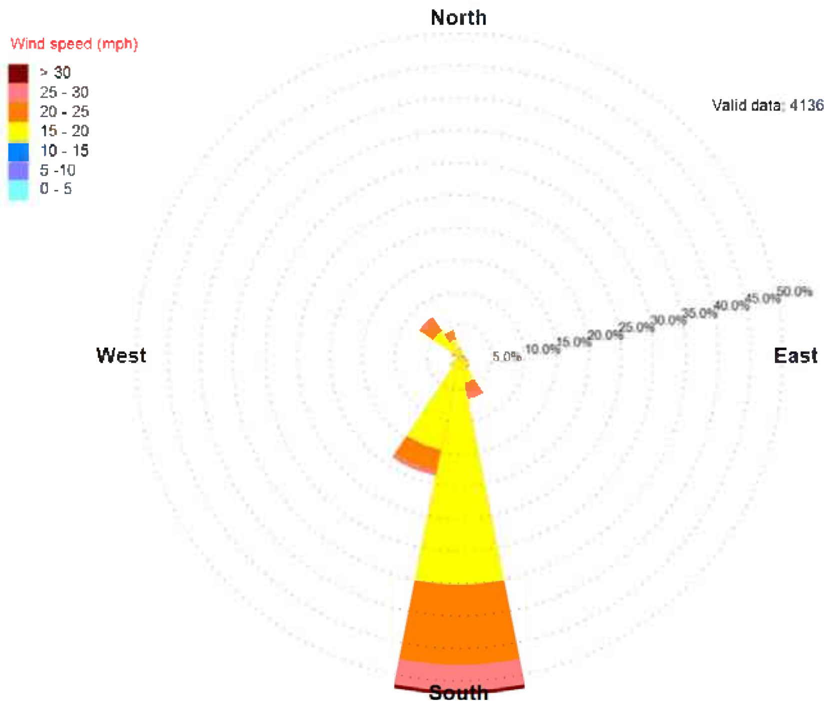

Figure 42. Wind rose for Station 401. Data are for periods in the summer (June 1-August 31) when 10-minute average wind speed exceeds 15 mph.

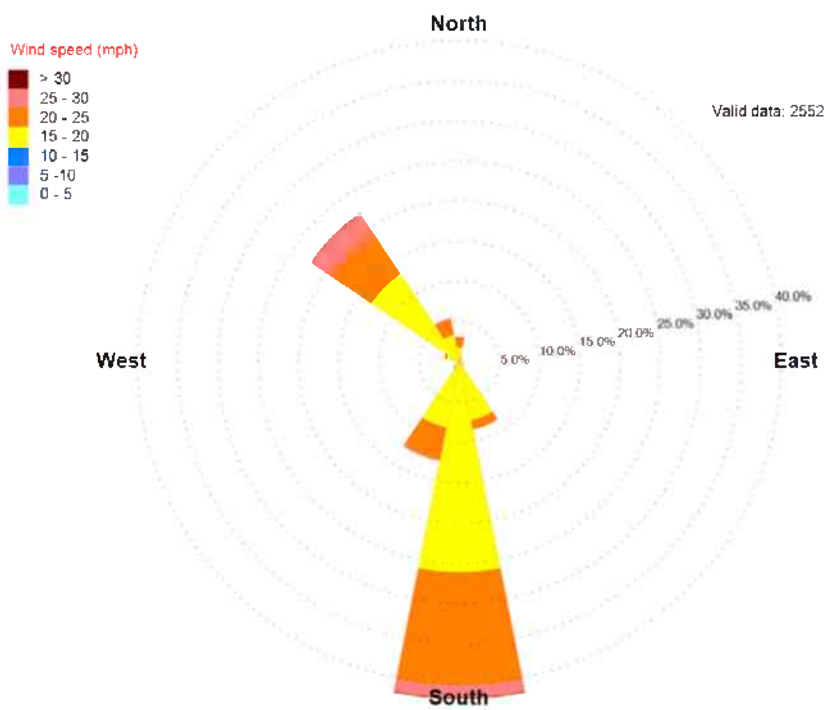

Figure 43. Wind rose for Station 401. Data are for periods in the fall (September 1-November 30) when 10-minute average wind speed exceeds 15 mph.

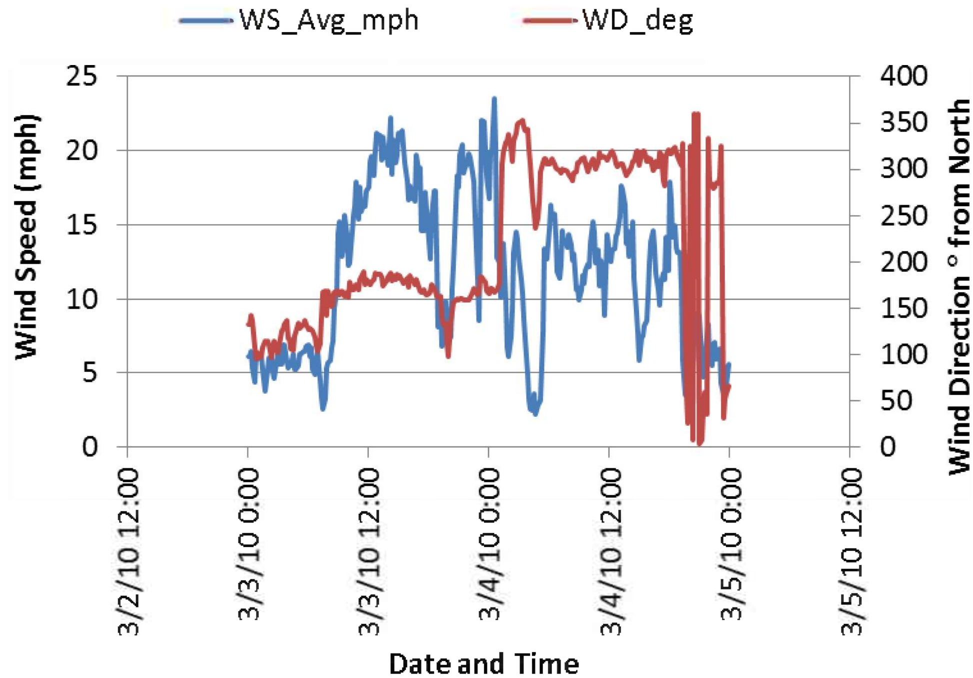

Figure 44. Example of springtime frontal passage at Station 401.

INFLUENCE OF ENVIRONMENTAL PARAMETERS ON SOIL RESPONSE TO WIND SPEED

There are numerous parameters that impact whether or not a specific set of wind conditions result in dust emissions at a given site. Three parameters that impact soil wind erodibility are the soil temperature, the soil water content, and the ambient relative humidity. These parameters are directly measured at Stations 400, 401, and 402 and can be used to determine if there are clear threshold effects above or below which potential soil wind erosion can be considered negligible. The analysis presented here is necessarily empirical and relies on a few subjective assumptions, but the data strongly indicate that such threshold effects do exist. Note that due to data gaps during March and April of 2009 and because soil temperature data were not available until 2010, the analysis at Station 401 has been limited to the years 2010 to 2012.

It is reasonable to expect that in the presence of even a small amount of water, soil temperatures approximately below the freezing point of water would freeze the soil and effectively cease wind erosion. Figure 45 shows 10-minute PM_{10} concentrations that are reconstructed from the particle profiler at Station 400 plotted against the soil temperature under four different wind conditions. Here and in ensuing discussions, 50 $\mu g/m^3$ is used as a cutoff level for 10-minute PM_{10} concentrations for Station 400 and 401. The 50 $\mu g/m^3$ level was chosen as a cutoff because regional concentrations of PM_{10} can routinely exceed this level, even in the absence of windblown dust. The 95th percentile PM_{10} concentration in the absence of wind (i.e., less than 15 mph) at Station 400 is 29.7 $\mu g/m^3$, whereas it is 50.2 $\mu g/m^3$ at Station 401. Choosing the higher value as a threshold indicator for windblown dust for both stations is the approach that was adopted for this report. In subsequent reports, it may be determined that separate thresholds should be used for each of the three sites. Currently, PM_{10} exceeding the 50 μg/m^3 level when winds are higher than 15 mph has been operationally defined as an indicator of likely windblown dust activity. Because the amount of data available from Station 402 is much less than the other two sites, estimates of thresholds for the three parameters of interest are based on those found for Stations 400 and 401 rather than using the 50 μg/m^3 level. As additional data become available for Station 402, thresholds for parameters can be estimated directly from the reconstructed PM_{10} at that site.

A threshold for a parameter that has the potential to shut down the windblown dust system can be inferred as follows: If PM_{10} concentrations routinely exceed the 50 μg/m^3 level under high-wind conditions, then the parameter in question has not crossed the threshold beyond which dust emission is rendered negligible. If PM_{10} levels do not exceed or only rarely exceed the 50 μg/m^3, then it is assumed that PM_{10} emissions are effectively mitigated. Figure 45 shows that the PM_{10} response to wind at soil temperatures above freezing is quite different than the response at soil temperatures below freezing, with the former exhibiting the potential for much higher PM_{10} under comparable wind conditions. At temperatures less than approximately 30 °F, PM_{10} concentrations remain generally below this level except for a few data points that all correspond to measurements during the early morning hours of December 8, 2009. Therefore, 30 °F appears to be the temperature at which there is a change in the dust emissions regime. Using similar arguments, the same temperature threshold is identified for Station 401 (see Figure 46) and simply adopted for Station 402 (Figure 47). Note that there are far fewer data at Station 402. Consequently, until additional measurements are available, in certain cases it is simply assumed that the same thresholds that hold for Stations 400 and 401 also hold for Station 402.

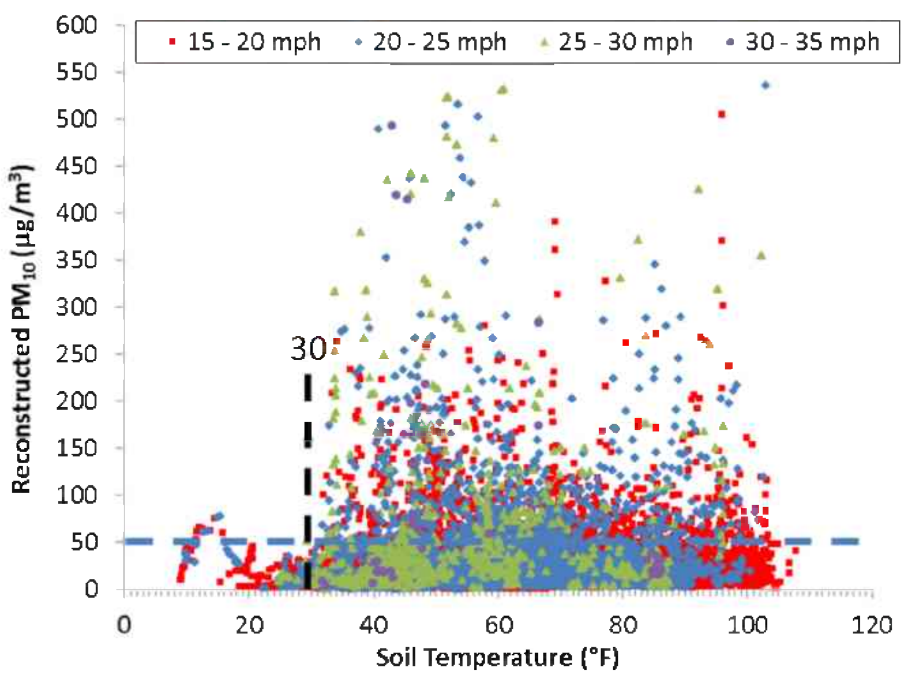

Figure 45. Station 400 10-minute reconstructed PM_{10} versus soil temperature for periods with wind speed greater than 15 mph.

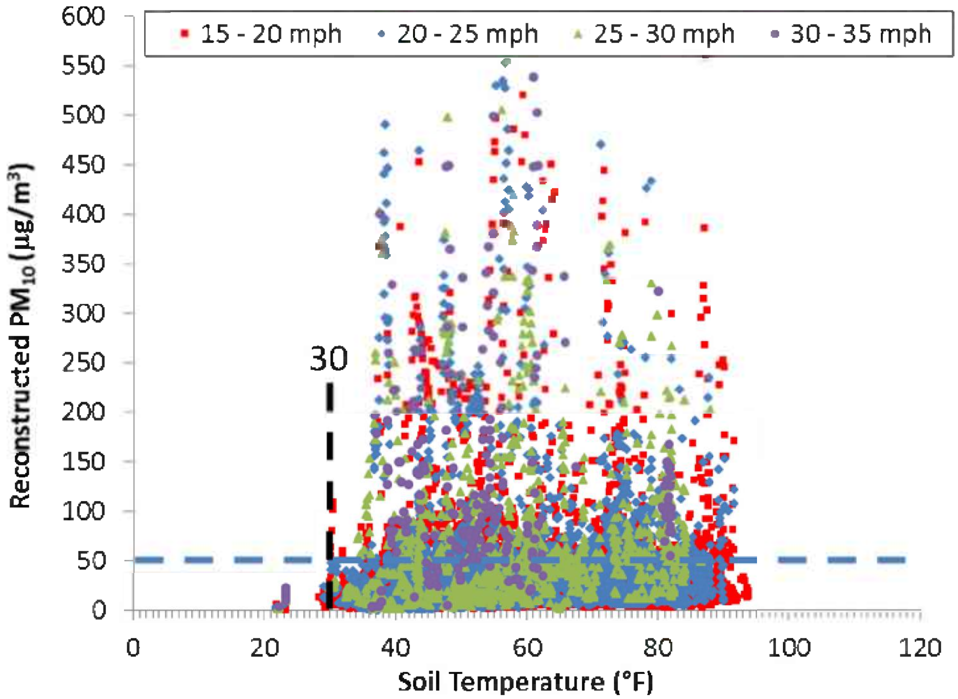

Figure 46. Station 401 reconstructed PM_{10} versus soil temperature for periods with wind speed greater than 15 mph.

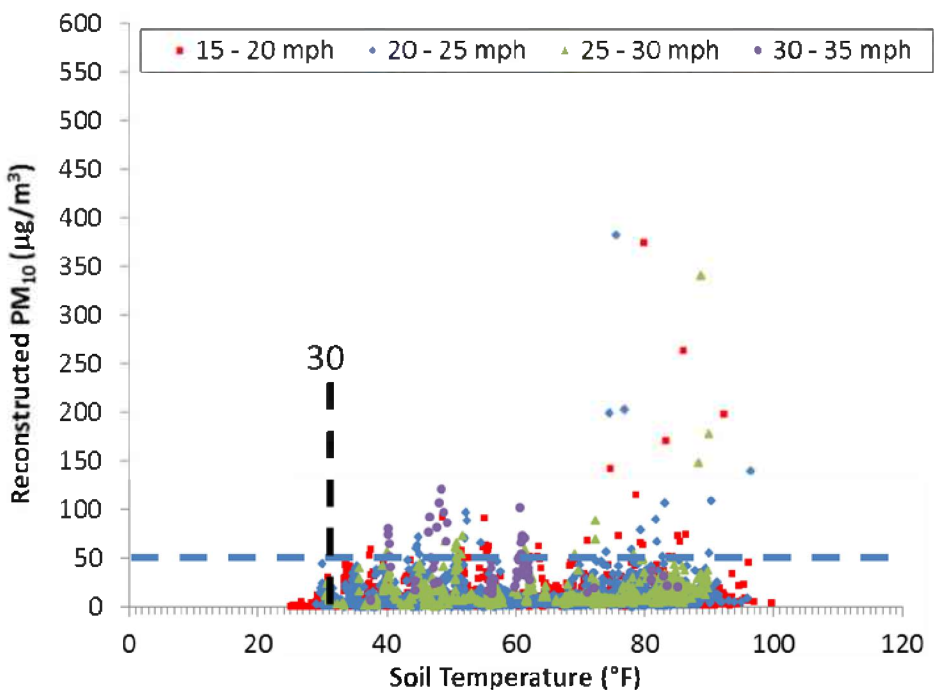

Figure 47. Station 402 reconstructed PM_{10} versus soil temperature for periods with wind speed greater than 15 mph.

Figures 48 through 50 display the same type of information for relative humidity versus PM_{10}. Note that relative humidity is a useful proxy for precipitation. Although precipitation is measured at all three stations, the precipitation metric only provides information about how much rainfall occurred over a specific measurement period, in this case a 10-minute interval. This information does not provide insight into the effect of precipitation on the landscape. For example, two hundredths of an inch of precipitation in the hot month of July probably impacts a soil's potential for dust emissions for a few hours at most. In contrast, the same amount of rain in December could be enough to suppress dust emissions for days. Relative humidity (RH) is a useful proxy for the influence of rain on soil erodibility because RH increases during rainfall events and remains elevated when the top layers of the soil surface are wet. Moreover, RH is a good indicator for fog, mist, and sprinkling rain events that do not register on precipitation gauges. In examining Figures 48 through 50, a case can be made that dust emissions are at least partially mitigated at RH greater than 70 percent. It may be possible to more confidently use the 70 percent value as a threshold with the addition of more years of data. At this time, the more conservative value of 90 percent is adopted for all three stations. This is supported by the observation that during active precipitation at all three sites, the average RH is 85 percent or greater and the median value is 90 percent or greater.

The soil volumetric water content is also a useful metric for determining whether or not a soil may be too wet to be emissive. Unfortunately, most soil moisture measurements, including the time domain reflectometry (TDR) device used at the TTR monitoring stations provide an integrated measurement of soil moisture over the top several inches of soil. Because the top hundredths of an inch of soil can be dry and wind erodible while the soil is visibly wet at a depth of only a few inches, the TDR device does not provide a direct measurement of the soil moisture in the region of greatest interest for dust emission. Nevertheless, it is clear from Figures 51 through 53 that there is a TDR-measured soil moisture, expressed as volumetric water fraction, above which dust emissions are effectively mitigated. The threshold soil volumetric water content at each site likely varies as a result of local differences in soil properties. Table 20 includes a summary of the threshold values for RH, soil moisture, and soil temperature for all three sites at TTR.

There are two parameters that are not measured at any of the sites, but that also exert enormous influence on whether or not dust emissions occur under given wind conditions. The degree to which a soil forms a surface crust (biotic or abiotic) directly affects its susceptibility to wind erosion. Generally, a crust that is formed through the growth of microorganisms or the cementation of soil particles after a rainfall event has the capacity to completely mitigate dust emissions (Belnap and Gillette, 1998). Predicting whether or not such a crust is present is not straightforward and we are not aware of any reliable techniques to do so remotely. Vegetative growth—beyond the formation of a biotic crust—can profoundly change the way a soil responds to wind stress. In general, even small amounts of vegetative cover from short grasses can be sufficient to protect the soil from the erosive effects of wind stress (Raupach *et al.*, 1993). Changes in vegetative cover over the course of the seasons are not routinely monitored at any of the three sites at TTR.

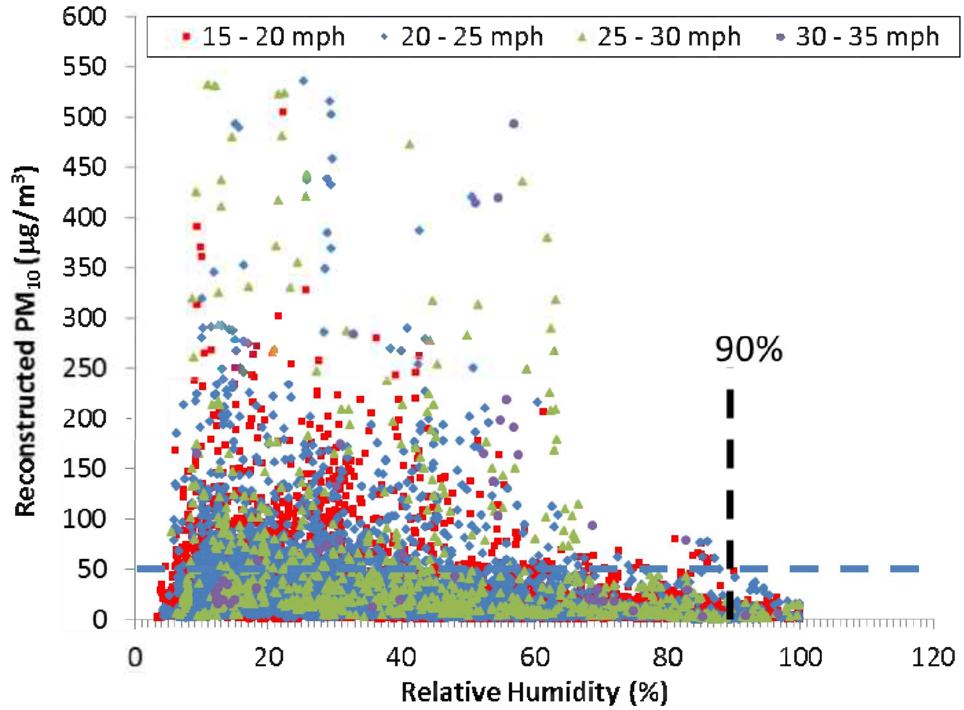

Figure 48. Station 400 reconstructed PM_{10} versus relative humidity for periods with wind speed greater than 15 mph.

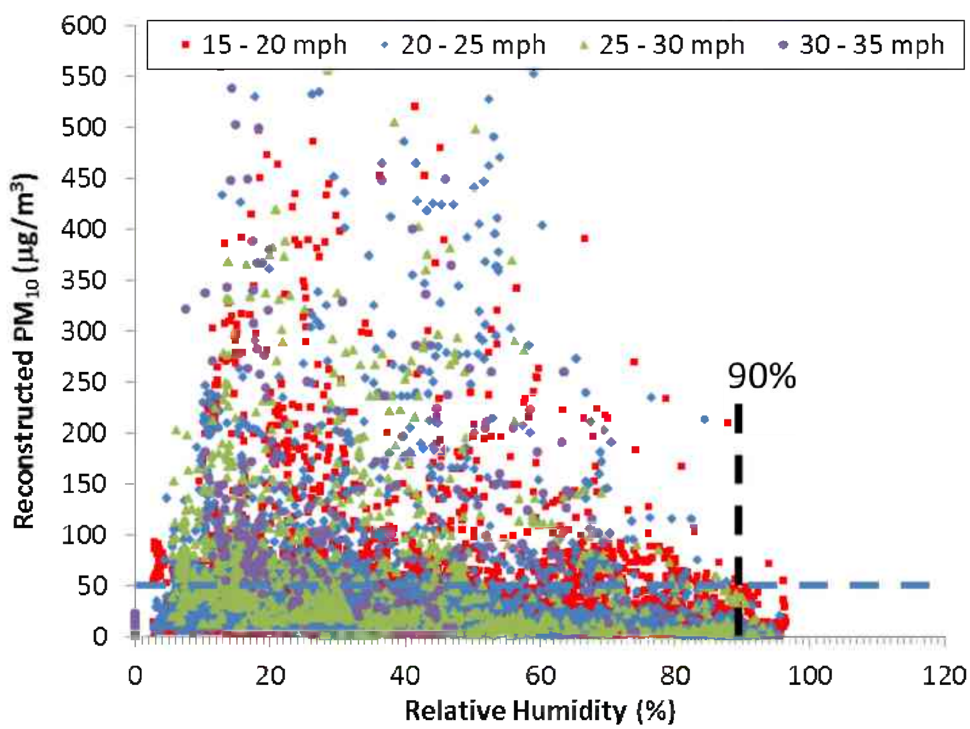

Figure 49. Station 401 reconstructed PM_{10} versus relative humidity for periods with wind speed greater than 15 mph.

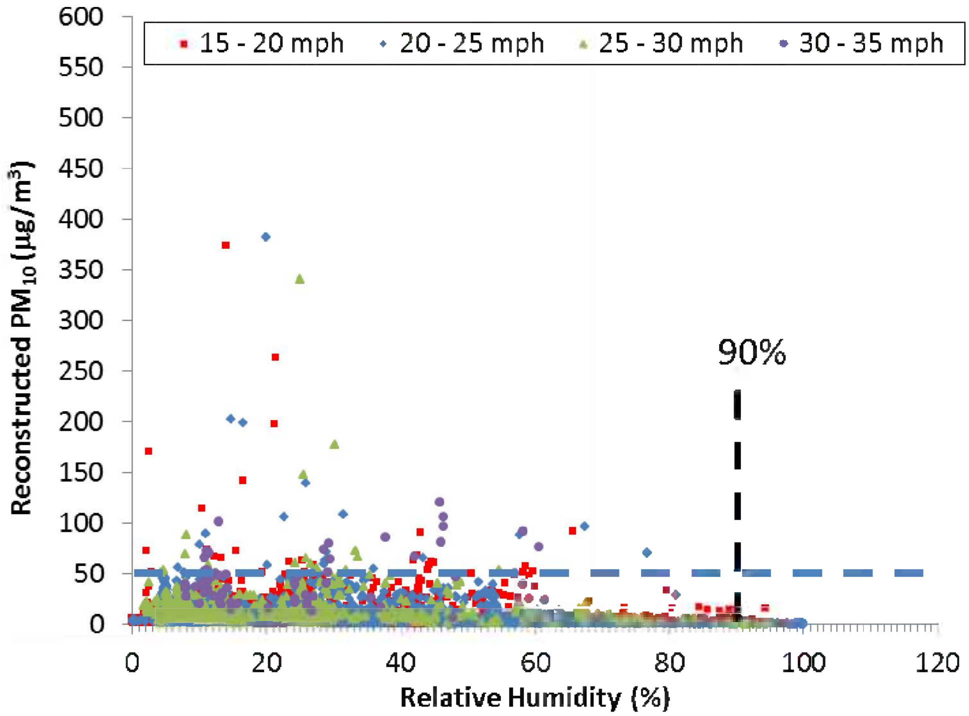

Figure 50. Station 402 reconstructed PM_{10} versus relative humidity for periods with wind speed greater than 15 mph.

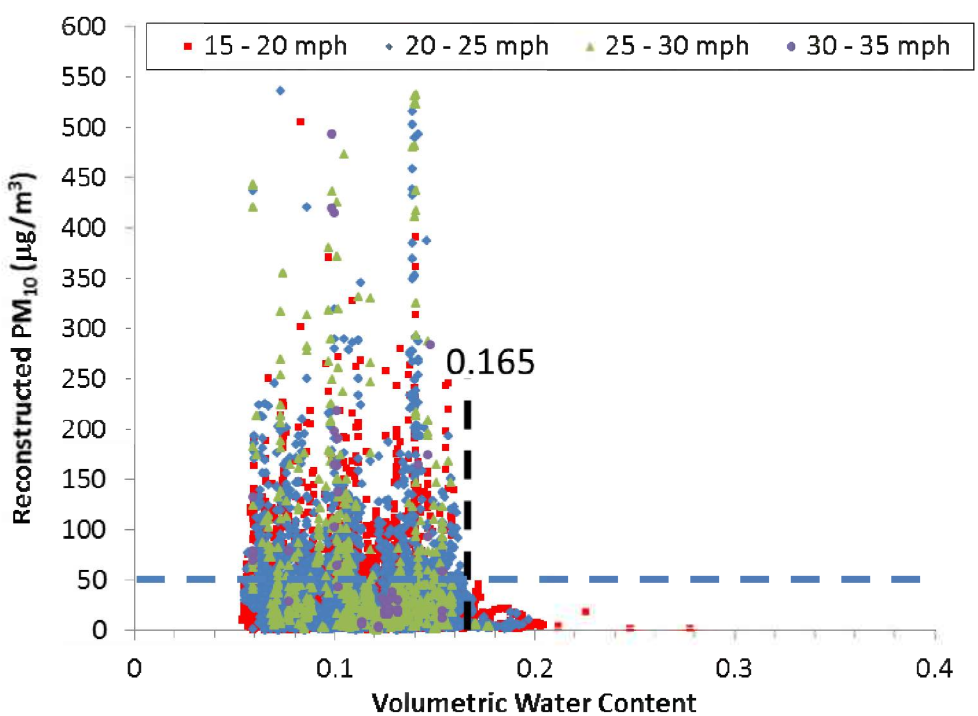

Figure 51. Station 400 reconstructed PM_{10} versus soil water content for periods with wind speed greater than 15 mph.

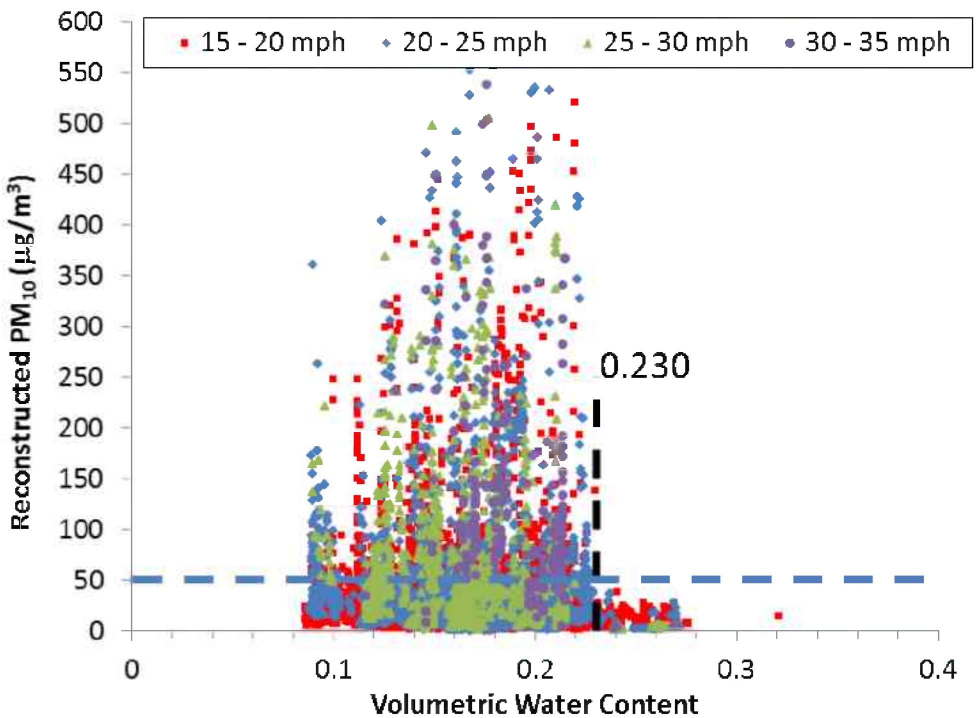

Figure 52. Station 401 reconstructed PM_{10} versus soil water content for periods with wind speed greater than 15 mph.

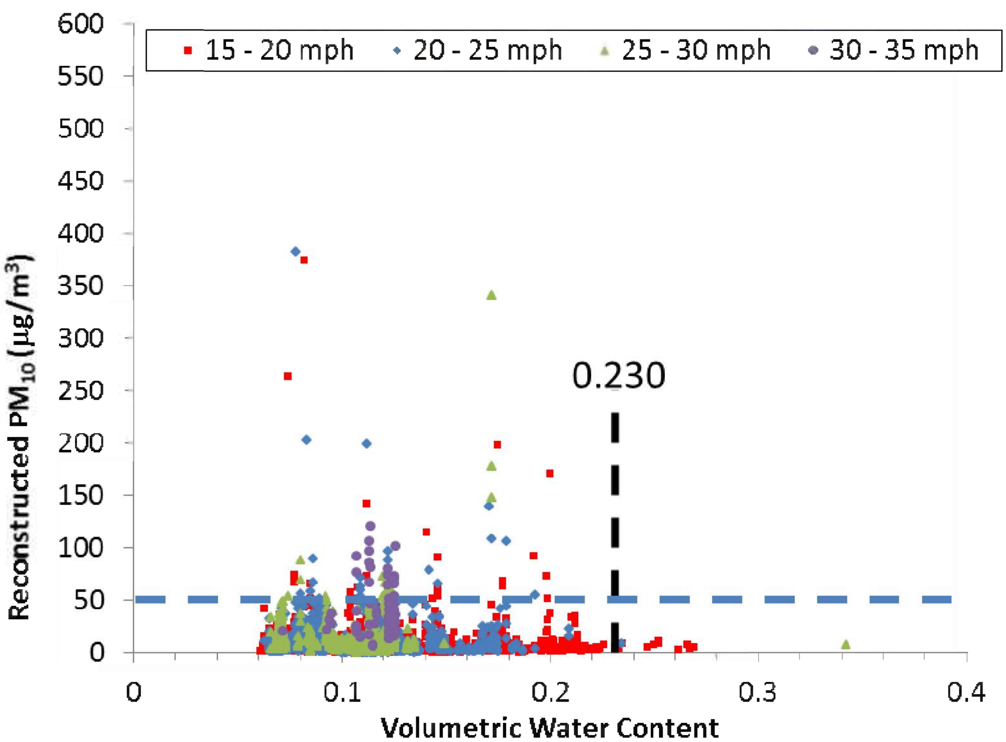

Figure 53. Station 402 reconstructed PM_{10} versus soil water content for periods with wind speed greater than 15 mph.

Table 20. Summary of threshold values for dust emission suppression.

Site	Temperature cutoff (degrees Fahrenheit)	Relative humidity cutoff (%)	Soil moisture cutoff (water content by volume)
Station 400	30	90	0.165
Station 401	30	90	0.230
Station 402	30	90	0.230

SAND MOVEMENT AND DUST CONCENTRATIONS UNDER THE INFLUENCE OF WIND SPEED AND DIRECTION

Forecasting the wind induced movement of dust remains an uncertain science. Although it is sometimes useful to express the relationship between wind and dust in terms of averages of a large number of measurements, it is important to understand that at the current state of the science, the consequence of a particular set of wind conditions cannot be known a priori with a high degree of certainty. Dust emissions are largely attributed to a sandblasting process, termed "saltation," which is the result of the initiation and transport of sand-sized particles (62 µm to 2,000 µm) that subsequently impact and abrade the soil (Shao *et al.*, 1993). If that soil surface contains silt or clay material, a percentage of the fine materials can also be entrained and transported as individual or aggregates of particles (Alfaro *et al.*, 1997; Alfaro *et al.*, 2004). These smaller particles contribute to the suspended dust load that is measured in the form of PM_{10}. Direct entrainment of silt- and clay-sized materials is uncommon because of their tendency to form aerodynamically smooth surfaces (requiring higher wind speed to entrain small particles) or be incorporated into soils as aggregates held together by interparticle bonds (formed by biotic or abiotic crusts).

The importance of saltation to the initiation of dust emission cannot be overstated. However, techniques for measuring saltation are less accurate than those available for measuring suspended particulate matter. Because saltation is a phenomenon that happens close to the ground, sand-movement measurements are inherently more susceptible to local conditions and the instrument's surroundings. For example, the specific location of a nearby boulder, shrub, or fence can have a large impact on the saltation measured by an electronic instrument, such as the Sensit (used at Stations 400 and 401), or even a simple sand trap. Despite the importance of saltation as an initiator of dust emissions, it is generally much more difficult to quantify as an aggregate over an appreciable area (on the order of hundreds of meters) than suspended PM_{10} concentration. For this reason, we focus our attention on wind-speed and wind-direction effects on reconstructed PM_{10} from ambient particle counters. We do note that the Sensit instruments used at Station 401 and 402 do indicate that sand movement does accompany elevated PM_{10} during high-wind events. However, because these instruments are known to have directionally sensitive response, a threshold for registering sand movement and nonlinear responses to sand movement, quantitative comparisons of sand movement are not included.

The distribution of PM_{10} concentrations when winds are from the west northwest (WNW, defined as approach angles ranging from 247.5° to 360°) and from the south southwest (SSW, defined as approach angles ranging from 112.5° to 247.5°) for Station 400 and wind speeds between 15 mph and 20 mph are shown in Figure 54. Station 400 results for wind speeds between 20 mph and 25 mph, 25 mph and 30 mph, and 30 mph and 35 mph are shown in Figures 55, 56, and 60, respectively. Also shown in the figures are the mean PM_{10} values. Because PM_{10} concentrations are frequently log-normally distributed, the mean PM_{10} concentrations are generally higher than the median (50 percent) values. In examining this information for Station 400, it appears that when winds are from the WNW direction, the mean PM_{10} concentration is slightly higher than when winds are from the SSW. Median values of PM_{10} concentrations for 15 mph to 20 mph winds and 20 mph to 25 mph winds also tend to be higher when winds are from the WNW. However, both median and mean values of PM_{10} for winds from the WNW and SSW directions are within a factor of two of one another regardless of wind speed category.

Similar information is provided for Stations 401 and 402 in Figures 58 through 61 and Figures 62 through 65, respectively. There are some differences between Stations 401 and 400. In contrast to Station 400 (Figure 54), at Station 401 the median PM_{10} concentrations when winds are between 15 mph and 20 mph (Figure 58) are higher when winds are from the SSW compared to when they are from the WNW. However, the mean PM_{10} concentrations for the same wind speed category are slightly higher when winds are from the WNW compared to the SSW. Although there are small differences between the two stations, an overarching observation is that the values of mean PM_{10} and median PM_{10} (and most percentile values between 10 percent and 90 percent) associated with the two wind approach angles are generally within a factor of two of one another at Station 401 as they are at Station 400. The same can be said of Station 402. Although it would be interesting to identify the reason for this difference in PM_{10} concentration between wind from the two different directions (WNW and SSW), considering the range of PM_{10} concentrations that are observed under the same wind-speed and wind-direction conditions (one to two orders of magnitude), this factor of two difference is comparatively small.

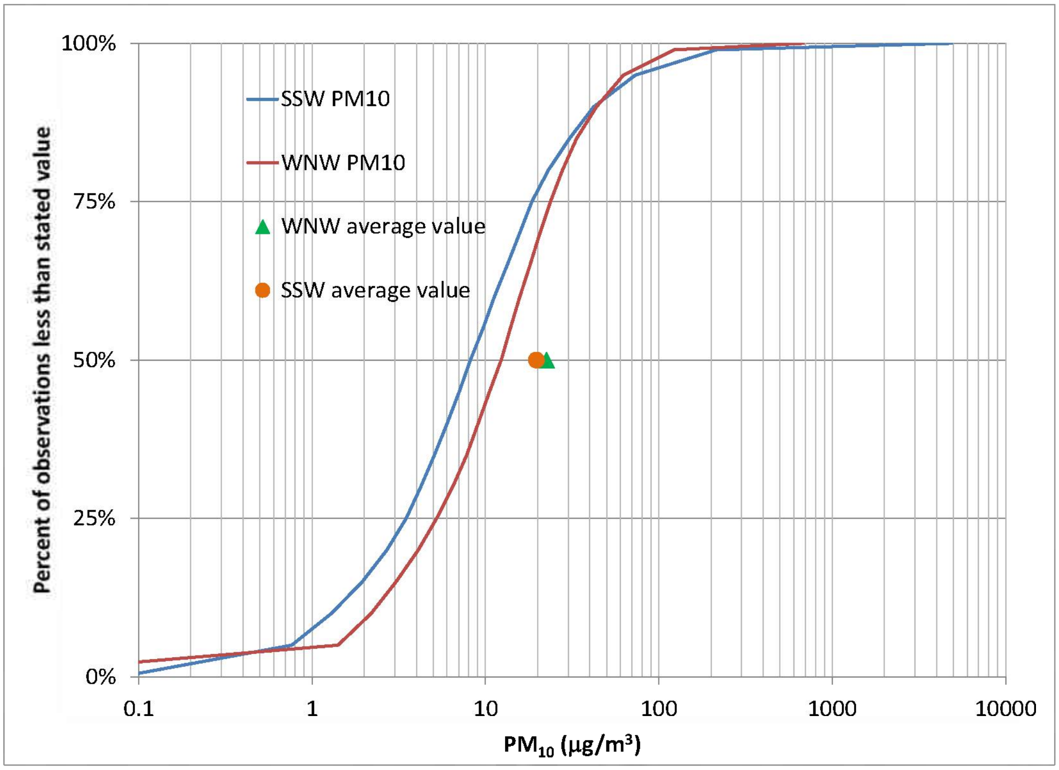

Figure 54. Station 400 distribution of PM_{10} concentration for wind speeds 15-20 mph. # points: WNW - 10545, SSW - 17387.

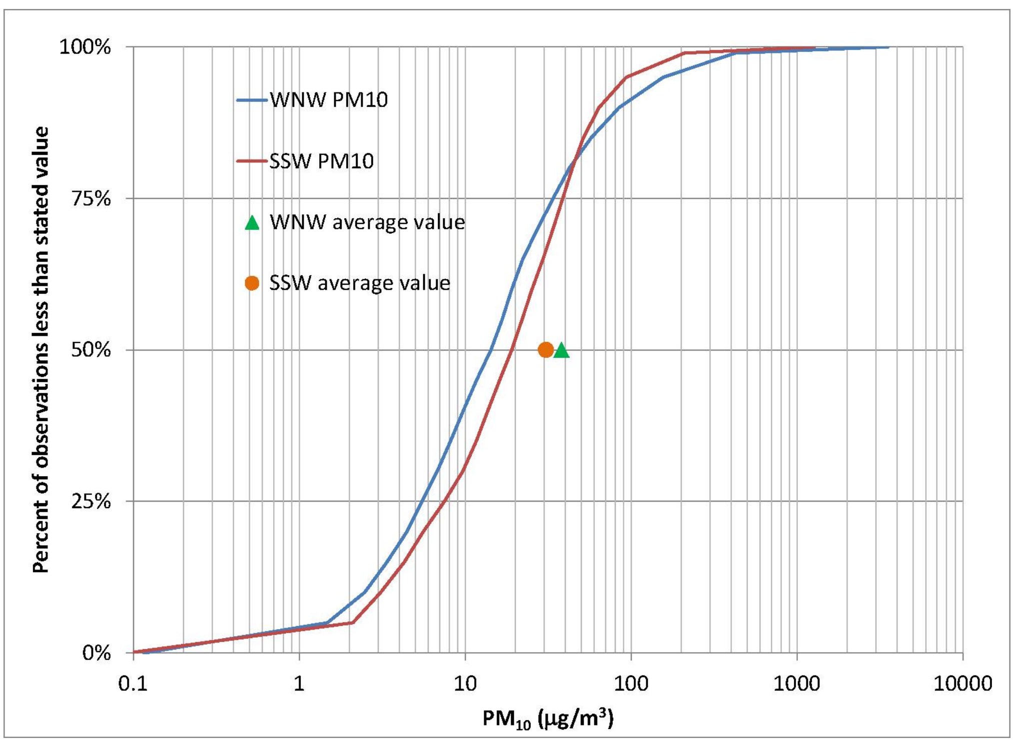

Figure 55. Station 400 distribution of PM_{10} concentration for wind speeds 20-25 mph. # points: WNW - 3947, SSW - 6330.

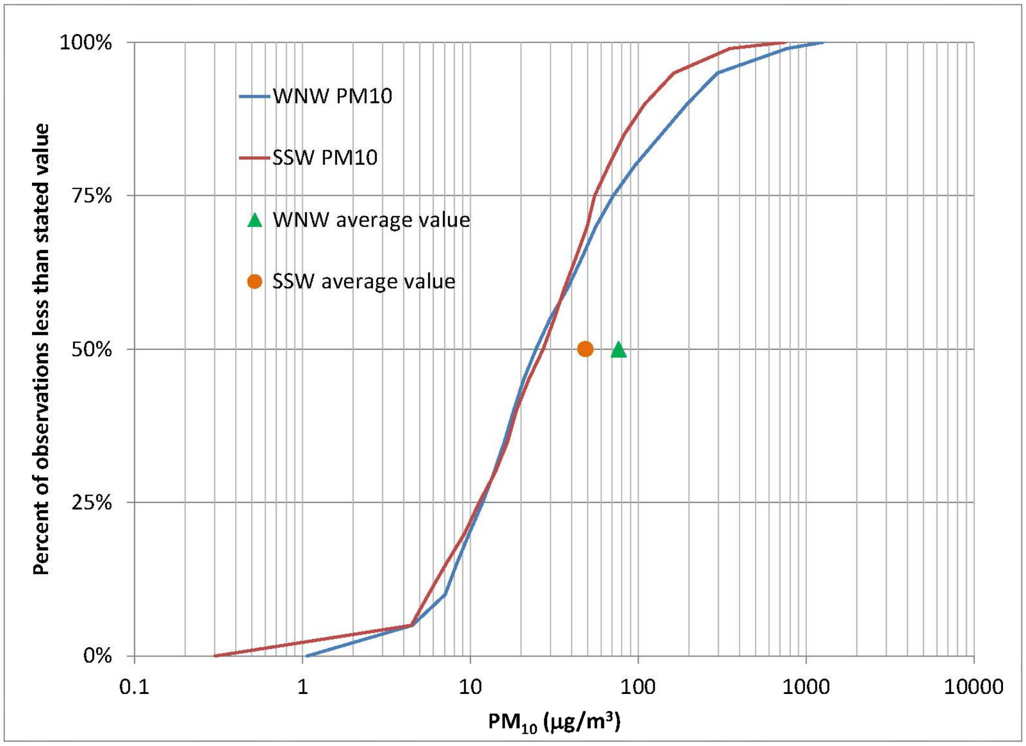

Figure 56. Station 400 distribution of PM_{10} concentration for wind speeds 25-30 mph. # points: WNW - 945, SSW - 1625.

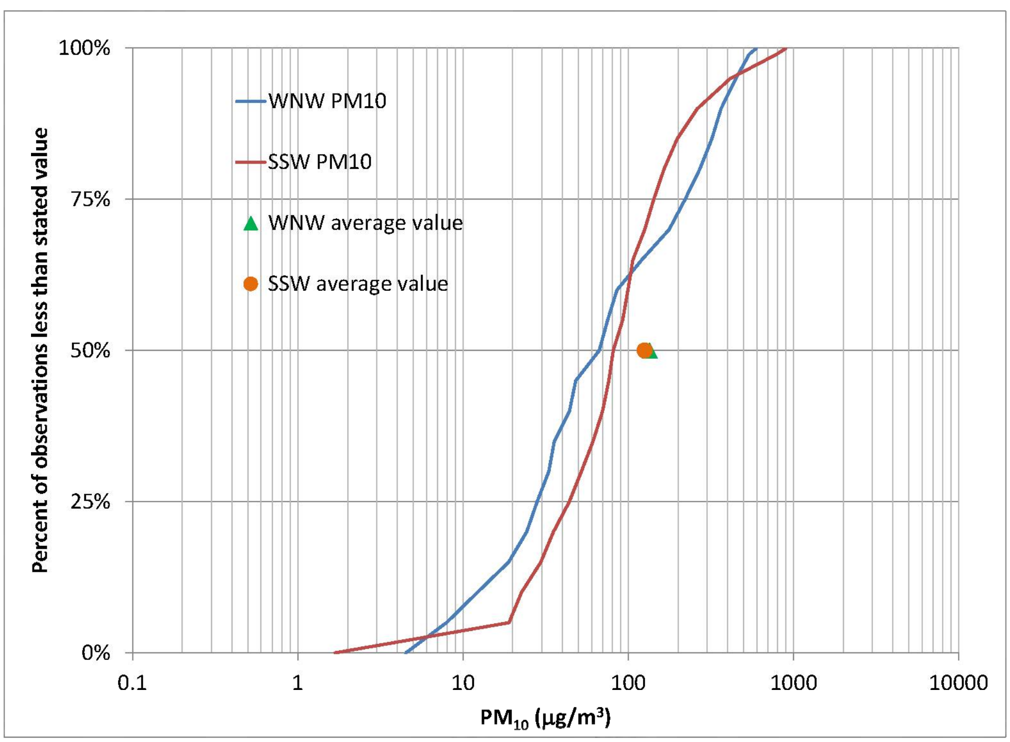

Figure 57. Station 400 distribution of PM_{10} concentration for wind speeds 30-35 mph. # points: WNW - 61, SSW - 281.

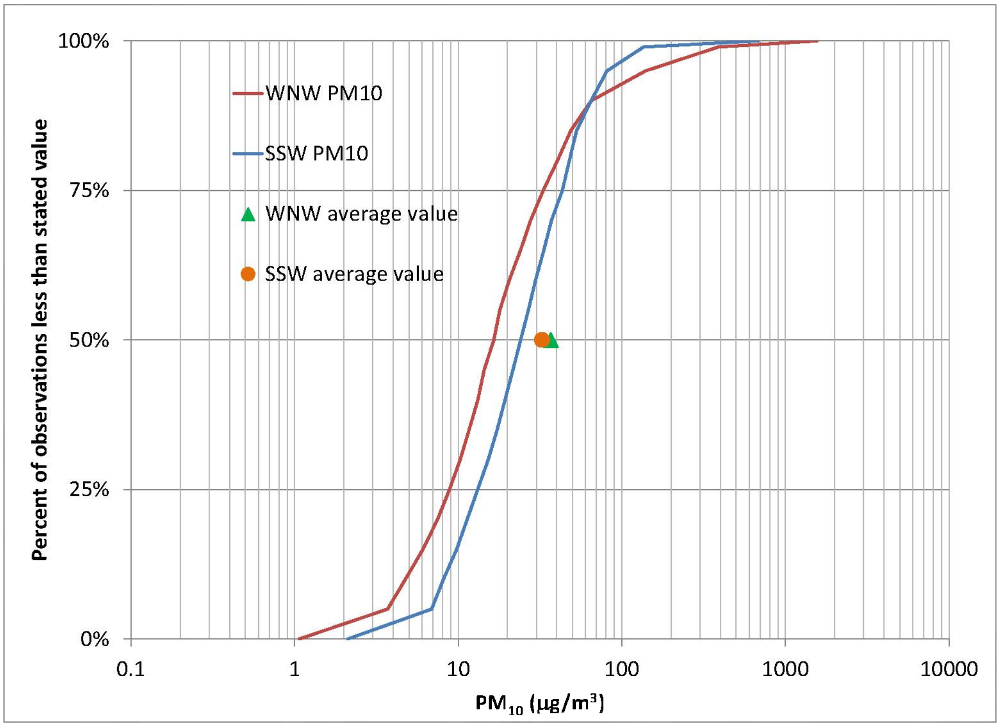

Figure 58. Station 401 distribution of PM_{10} concentration for wind speeds 15-20 mph. # points: WNW - 1706, SSW - 2683.

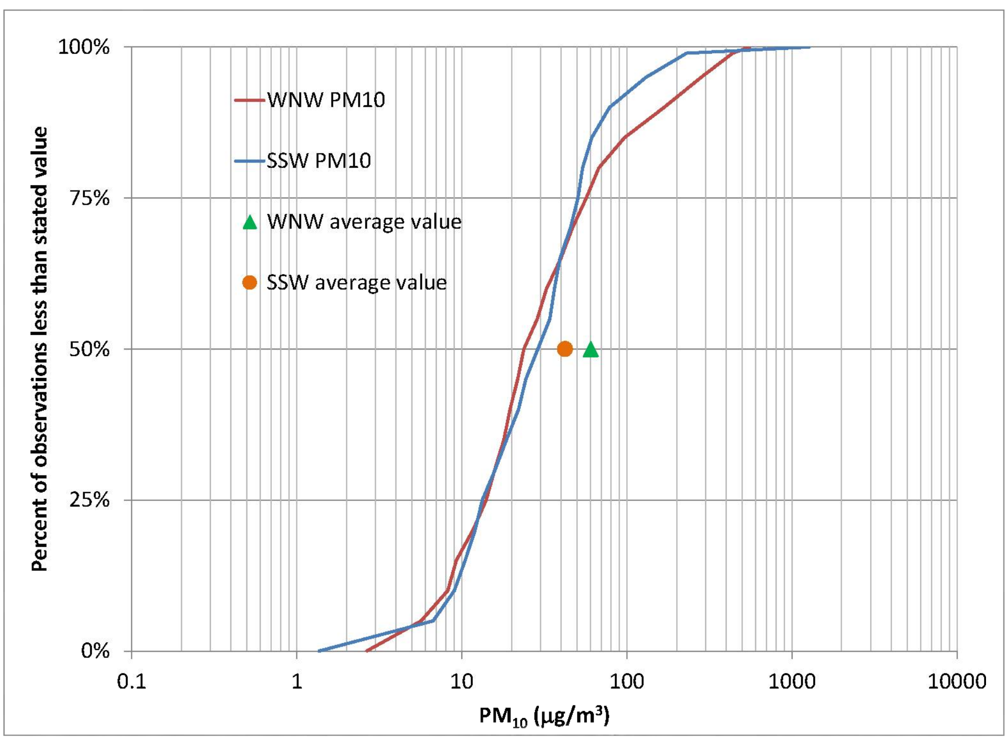

Figure 59. Station 401 distribution of PM_{10} concentration for wind speeds 20-25 mph. # points: WNW - 666, SSW - 1122.

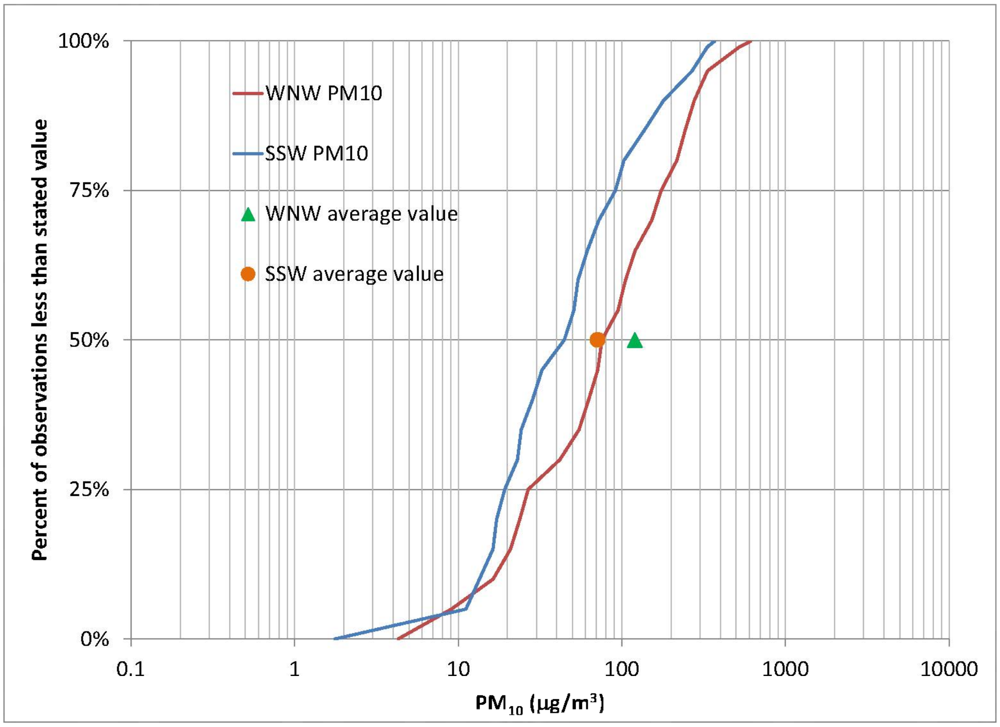

Figure 60. Station 401 distribution of PM_{10} concentration for wind speeds 25-30 mph. # points: WNW - 171, SSW - 291.

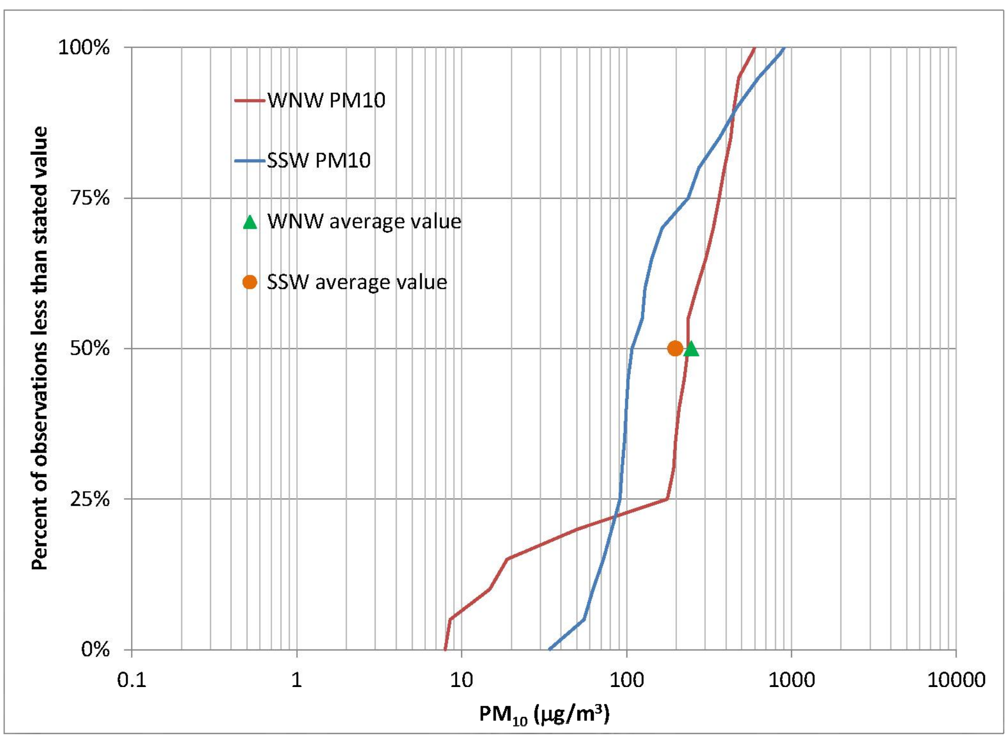

Figure 61. Station 401 distribution of PM_{10} concentration for wind speeds 30-35 mph. # points: WNW - 17, SSW - 68.

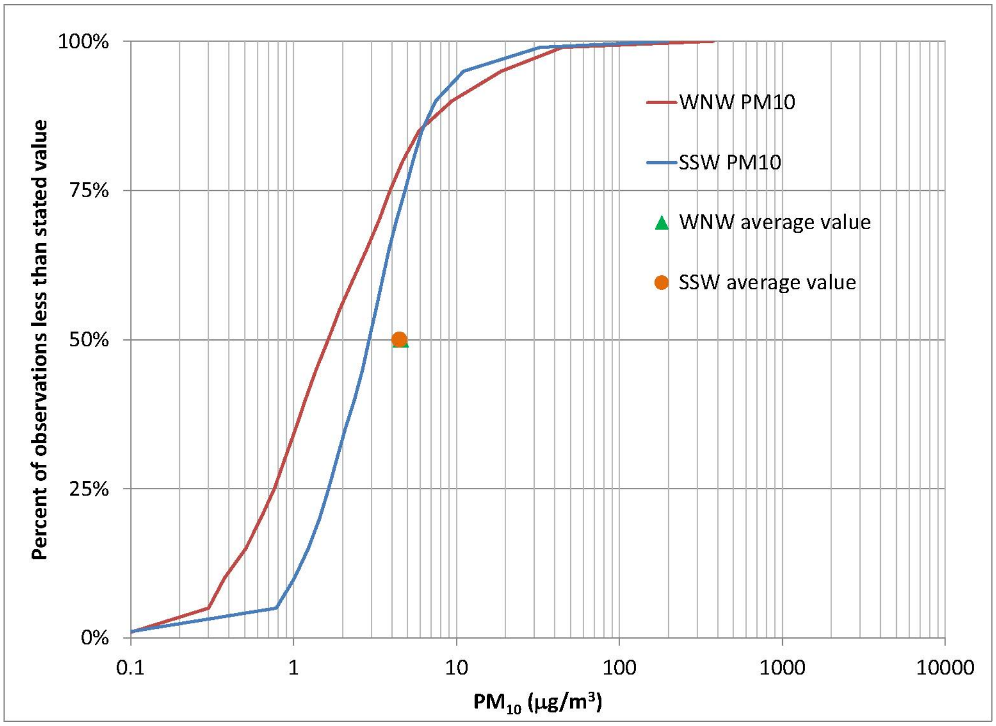

Figure 62. Station 402 distribution of PM_{10} concentration for wind speeds 15-20 mph. # points: WNW - 1723, SSW - 2611.

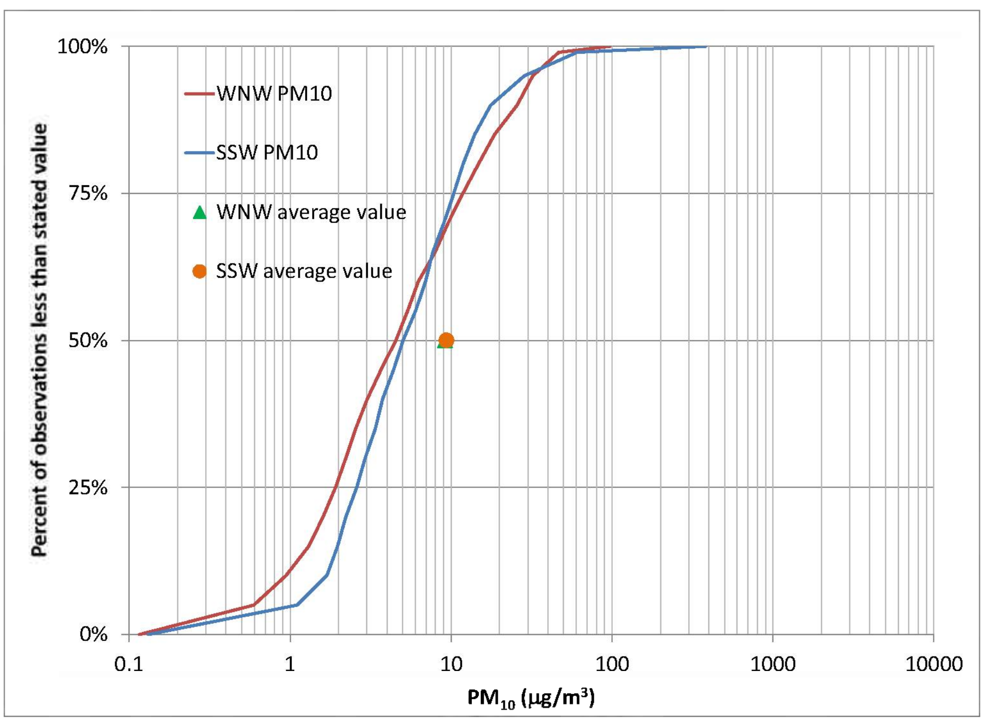

Figure 63. Station 402 distribution of PM_{10} concentration for wind speeds 20-25 mph. # points: WNW - 656, SSW - 956.

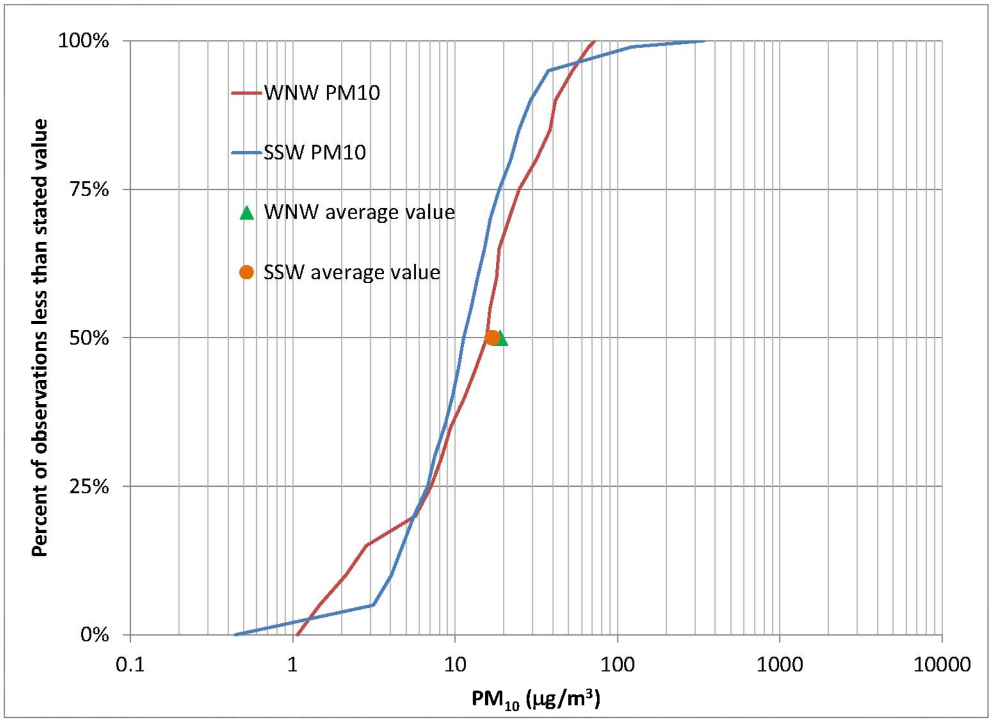

Figure 64. Station 402 distribution of PM_{10} concentration for wind speeds 25-30 mph. # points: WNW - 129, SSW - 241.

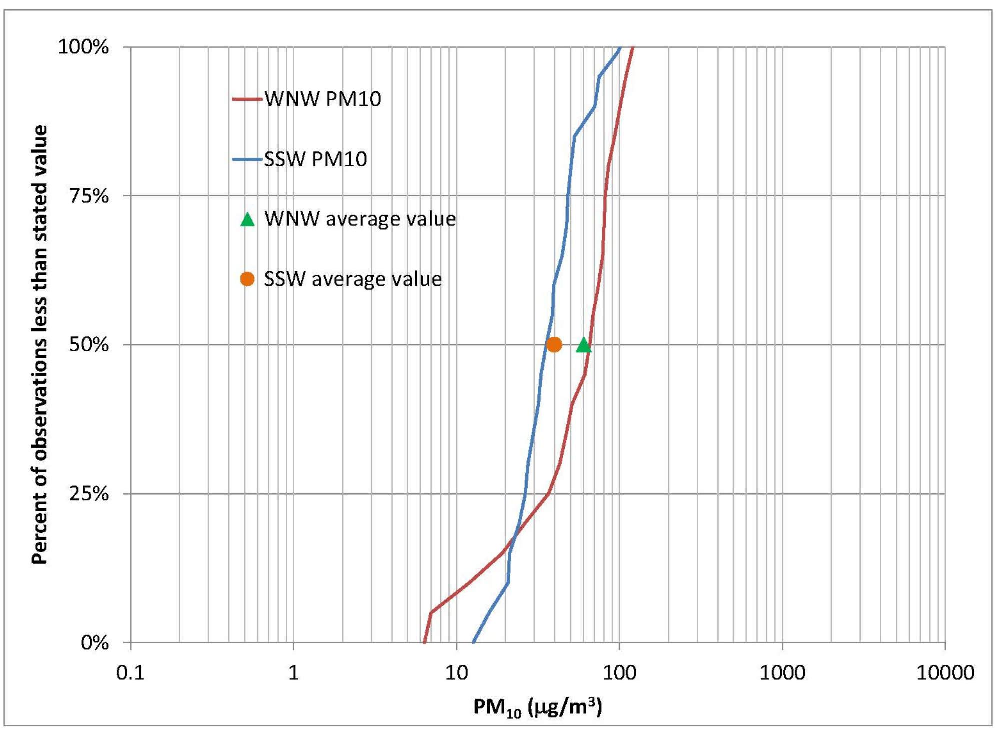

Figure 65. Station 402 distribution of PM_{10} concentration for wind speeds 30-35 mph. # points: WNW - 16, SSW - 48.

RELATIONSHIP BETWEEN PM_{10} DUST AND WIND SPEED

The median and 95th percentile PM_{10} concentration within a given wind speed class is plotted against the average wind speed in that class for Station 400 in Figure 66 and for Station 401 and 402 in Figures 67 and 68, respectively. In all cases, a power law fits the data quite well with all R^2 values above 0.9 (see Table 21). For each site, one set of equations provides an estimate of the 50th percentile value and the other set provides a conservative 95th percentile concentration. The 95th percentile concentration value is of interest in the context of exposure assessments because it can be substituted as a conservative, but not maximum, estimate for the concentration in the absence of actual measurements. This series of curve fits can be very useful for bounding the PM_{10} concentration in any 10-minute interval when the average wind speed exceeds 15 mph. These empirical fits were obtained with available data that satisfied the threshold criteria in Table 20 and for periods when 10-minute wind speed exceeds 15 mph.

The empirical fits described above can be used to assess exposure to a pollutant that is associated with PM_{10}. For example, if an individual was exposed to toxic substance x for n 10-minute intervals during a high-wind event, then the exposure to substance x can be estimated as:

$$\chi_y = \sum_{i=1}^{n} 10 \times PM10_{y,WS_i} \times \eta_{y,x} = \sum_{i=1}^{n} 10 \times a_y \times (WS_i)^{b_y} \times \eta_{y,x} \qquad (2)$$

where χ_y is the exposure to substance x at site y in units of $\mu g/m^3 \cdot$ minutes, WS_i refers to the average wind speed (mph) during 10-minute interval i, the values of a and b are obtained from Table 21, and η_x is the fraction of PM_{10} that is composed of substance x. The multiplier of 10 is used in Equation 2 because the concentration of PM_{10} that is calculated using the parameters in Table 21 is for a 10-minute interval. To estimate the median exposure level (i.e., the level at which there is an equal chance of actual exposure being higher or lower), the median values of a and b from Table 21 would be used. The 95th percentile values would be used if the intent is to obtain a more conservative estimate of exposure. This formulation is useful for chemical toxins as well as assessing radioactivity exposure provided that data or model derived estimates for η_x exist. The parameters of Table 21 and the formulation of Equation 2 are intended for illustration only. Changes are incorporated each time new information is available and the next set of changes is expected at the time of the next installment of this multiyear report.

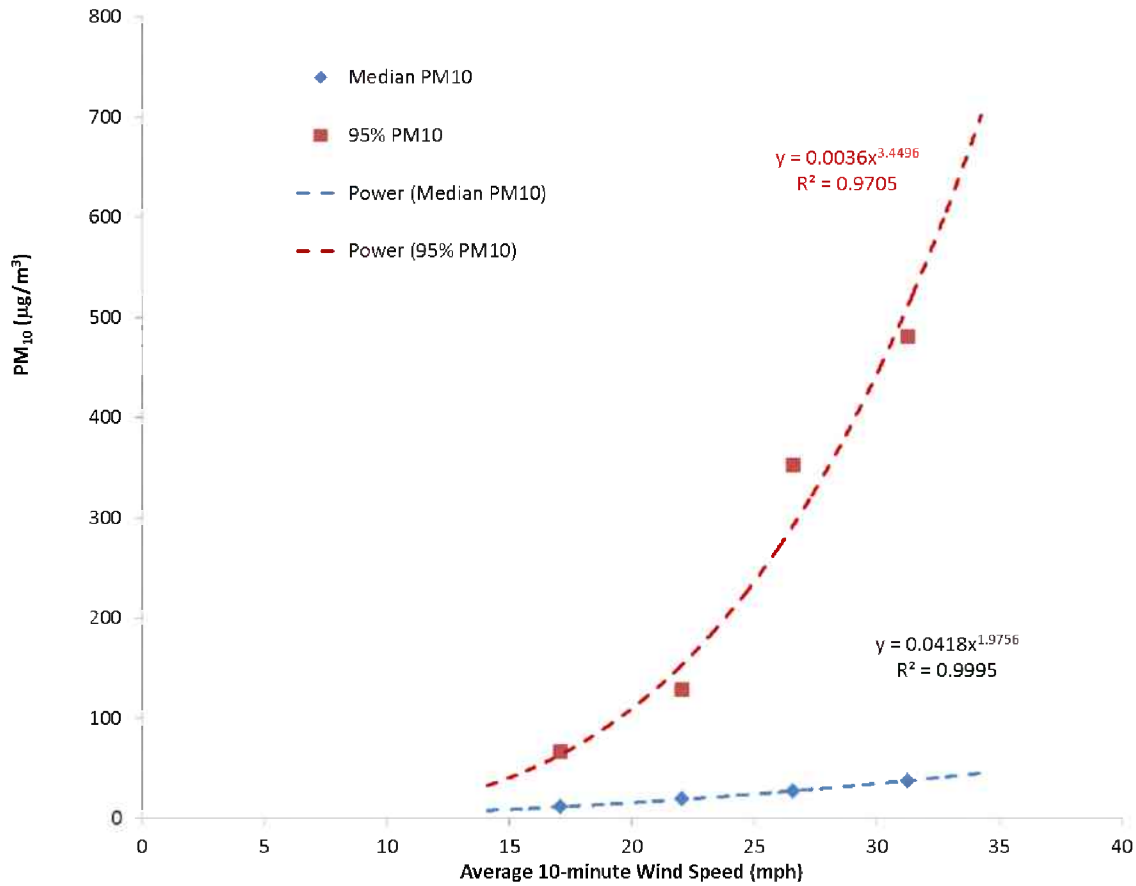

Figure 66. Station 400 PM_{10} median (50th percentile) and 95th percentile concentrations within a 5 mph wind speed bin among all available concentration data for 10-minute intervals that satisfied the threshold criteria in Table 20 versus the average wind speed within that bin. The dotted lines represent the best power law fits to the data.

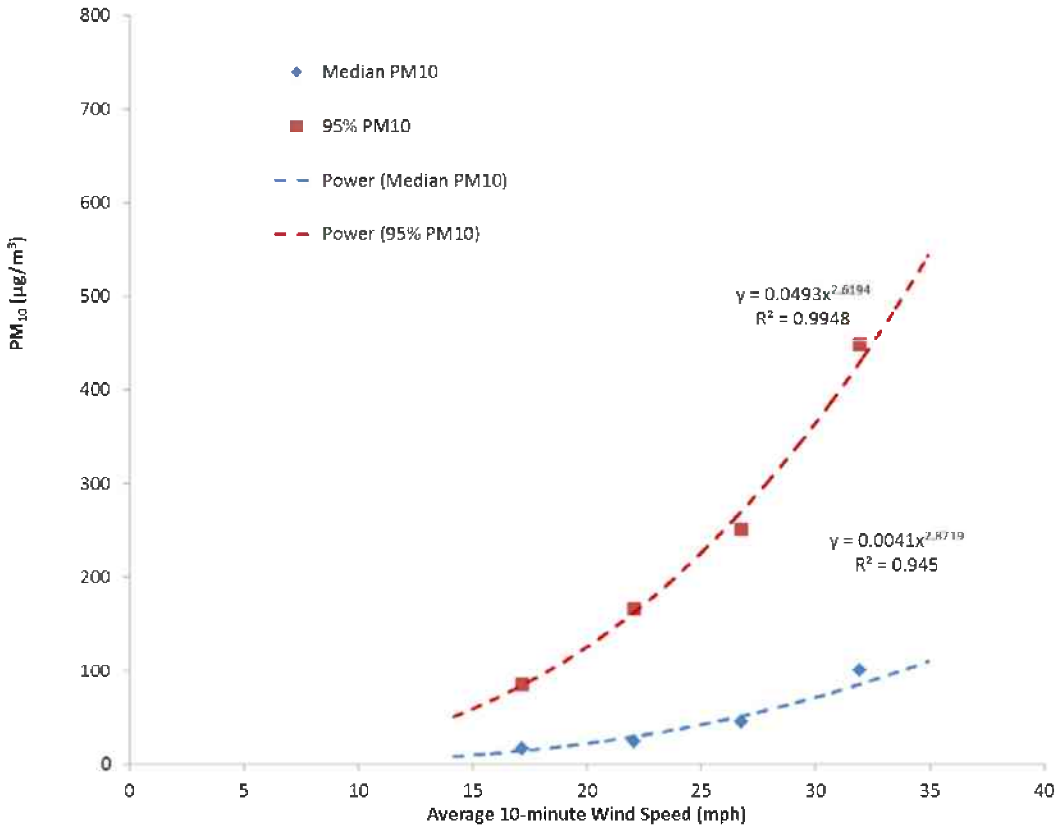

Figure 67. Station 401 PM_{10} median (50th percentile) and 95th percentile concentrations within a 5 mph wind speed bin among all available concentration data for 10-minute intervals that satisfied the threshold criteria in Table 20 versus the average wind speed within that bin. The dotted lines represent the best power law fits to the data.

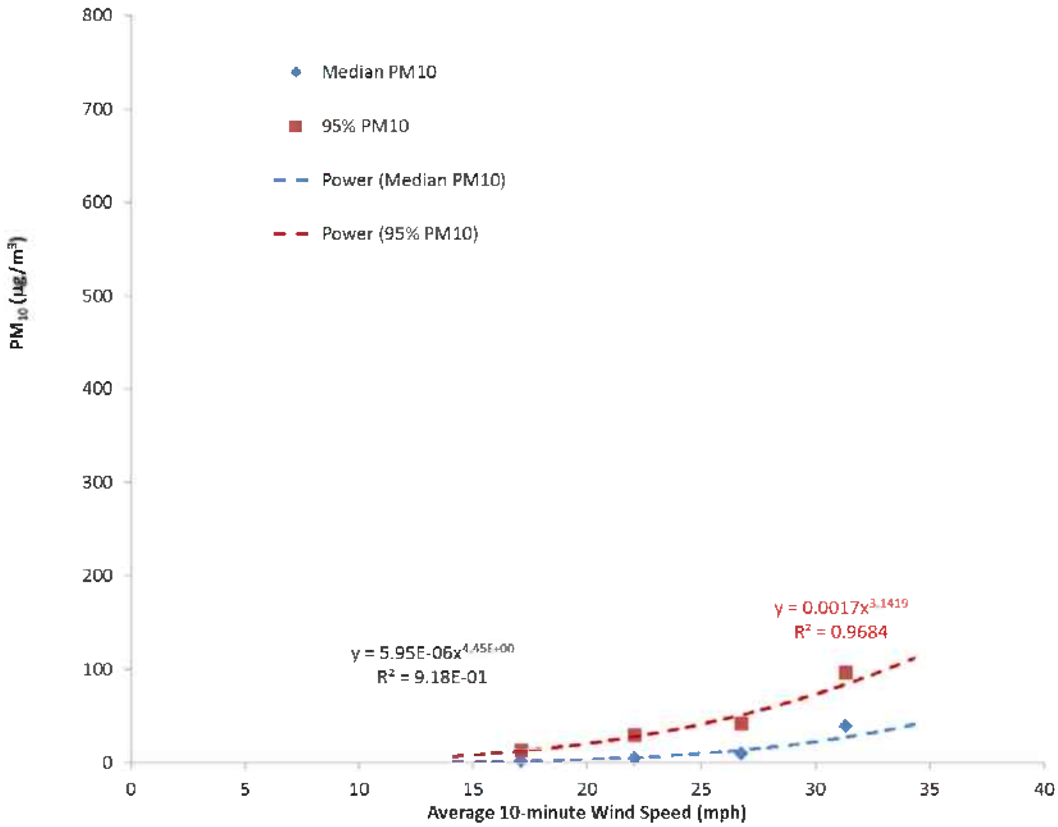

Figure 68. Station 402 PM_{10} median (50th percentile) and 95th percentile concentrations within a 5 mph wind speed bin among all available concentration data for 10-minute intervals that satisfied the threshold criteria in Table 20 versus the average wind speed within that bin. The dotted lines represent the best power law fits to the data.

Table 21. Summary of power law fitting coefficients for the equation $PM10\left(\frac{\mu g}{m^3}\right) = a.(WS(mph))^b$.

Site	Median coefficient (a)	Median exponent (b)	Median R^2	95% coefficient (a)	95% exponent (b)	95% R^2
Station 400	4.2 X 10^{-2}	1.98	1.00	3.6 X 10^{-3}	3.45	0.97
Station 401	4.1 X 10^{-3}	2.87	0.95	4.9 X 10^{-2}	2.62	0.99
Station 402	5.9 X 10^{-6}	4.45	0.92	1.7 X 10^{-3}	3.14	0.97

CONCLUSIONS

Gross alpha and gross beta values for airborne particulates collected at Station 400, adjacent to the ROC at the SNL compound are 10 percent to 45 percent higher than the values determined for samples collected from Stations 401 and 402, which are adjacent to Clean Slate III and Clean Slate I, respectively. The TTR and surrounding CEMP gross beta and gamma spectroscopy observations are of similar magnitude. Although gross alpha values for the TTR stations are higher than values reported for the surrounding CEMP stations, the failure to detect ^{241}Am in the gamma spectroscopy analysis suggests that plutonium is not the likely source of the alpha emissions. Therefore, there is no evidence of transport of radionuclide-contaminated soil particulates from the Clean Slate I or Clean Slate III sites.

Observed gamma values never exceeded the background by more than 4 μR/h. Inefficiencies in the PIC instrumentation at these low gamma levels suggest that exceeding the background by these amounts is probably insignificant. The occasions when observed gamma levels exceed the derived maximum background indicate neither transport from the Clean Slate sites nor a significant increase in gamma radiation exposure. It is likely that the annual average daily gamma radiation exposure values at the TTR stations are higher than at the surrounding CEMP stations as a result of differences in elevation and the geological environment surrounding the stations. The geological environment at the CEMP station at Sarcobatus Flat is most similar to the geological environment surrounding the TTR stations, but the TTR stations are between 1,400 ft and 1,500 ft higher than the Sarcobatus Flat station. The average gamma values at the TTR stations are approximately equivalent to or just slightly higher than the background estimates for Denver, which is at approximately the same altitude as the TTR stations. Comparisons of gamma observations and major meteorological parameters revealed no significant correlations.

High gamma values may be somewhat more likely when winds are from the south, but observed gamma values exceeded the derived maximum background gamma value during winds from any direction. Therefore, wind direction does not appear to be a predictor of gamma levels and there is no indication that wind is transporting gamma-emitting radionuclides form the Clean Slate sites. Dust levels and saltation counts generally increase as wind speed increases. The highest wind speed class (in excess of 35 mph) seldom occurs. Therefore, the greater mass of suspended dust is associated with moderate wind speeds.

RECOMMENDATIONS

Although it is likely that the TTR gross alpha values are the result natural conditions, it is recommended that a selection of air particulate samples be submitted for alpha spectroscopy analysis. Because the TTR gross alpha values are slightly higher than the surrounding CEMP station values and the NCRP national average values and because plutonium was the principal radionuclide dispersed into the environment as a result of the Clean Slate tests, alpha spectroscopy should be performed to identify the specific radionuclides producing the gross alpha results.

Saltation observations indicate that coarse-sized material is transported over the ground surface. To determine the significance of saltation as a potential mechanism for moving contaminated soil particles beyond the administrative boundaries of the Clean Slate sites, it is recommended that saltation collectors be installed at the monitoring stations.

Samples from these collectors should be retrieved periodically and submitted to the radiological laboratory for gross alpha, gross beta, gamma spectroscopy, and alpha spectroscopy analyses. An additional monitoring station located in Cactus Flat on the TTR is recommended to establish background conditions for the radiological parameters observed at Stations 400, 401, and 402. Separating observations of background conditions from observations influenced or potentially influenced by the Clean Slate soil contamination areas is difficult. Locating a monitoring station in an area known to be clear of radionuclide-contaminated soils would provide a definitive background level for the radionuclides evaluated as indicators of contaminated soil transport at the Clean Slate sites.

REFERENCES

Albers, J.P., and J.H. Stewart, 1972. Geology and mineral deposits of Esmeralda County, Nevada. Bulletin 78, Nevada Bureau of Mines and Geology, University of Nevada, Reno.

Alfaro, S.C., A. Gaudichet, L. Gomes, and M. Maille, 1997. Modeling the size distribution of a soil aerosol produced by sandblasting. *Journal of Geophysical Research* 102, 11239-11249.

Alfaro, S.C., J.L. Rajot, and W. Nickling, 2004. Estimation of PM20 emissions by wind erosion: main sources of uncertainties. *Geomorphology* 59, 63-74.

Anonymous, 2002. Oak Ridge Tennessee: A citizen's guide to the environment. Oak Ridge, TN, p. 28.

Barnett, W.D., H.L. Rarrick, and G.E. Tucker, Jr., 1964. Health physics aspects of Operation Roller Coaster. SC-4973 (RR), Sandia Corporation, Albuquerque, N.M., p. 38.

Belnap, J. and D.A. Gillette, 1998. Vulnerability of desert biological soil crusts to wind erosion: The influences of crust development, soil texture, and disturbance. *Journal of Arid Environments*, 39:133-142.

Bluestein, H.B., 1993. *Synoptic-Dynamic Meteorology in Midlatitudes: Vol. 2. Observations and Theory of Weather Systems*. Oxford University Press, p. 594.

Cornwall, H.R., 1972. Geology and mineral deposits of southern Nye County, Nevada. Bulletin 77, Nevada Bureau of Mines and Geology, University of Nevada, Reno.

Culp, T., W. Forston, D. Duncan, and R. Sanchez, 1997. 1996 Site Environmental Report Tonopah Test Range, Tonopah, Nevada, SAND97-2049, prepared by Sandia National Laboratories, Albuquerque, NM, for the U.S. Department of Energy.

Dick, J.L., J.D. Shreve, and J.S. Iveson, 1963. Operation Roller Coaster: Interim Summary Report, POIR-2500 (volume 1), U.S. Department of Defense.

DOE, 2009. Nevada Test Site Environmental Report 2008, DOE/NV/25964-790, C. Wills editor, prepared by National Security Technologies, Las Vegas, NV.

DOE, 2010. Nevada National Security Site Environmental Report 2009, DOE/NV/25964-1067, C. Wills editor, prepared by National Security Technologies, Las Vegas, NV.

DOE, 2011. Nevada National Security Site Environmental Report 2010, DOE/NV/25964-1305, C. Wills editor, prepared by National Security Technologies, Las Vegas, NV.

DOE, 2012. Nevada National Security Site Environmental Report 2011, DOE/NV/25946-1604, C. Wills editor, prepared by National Security Technologies, Las Vegas, NV.

DOE, 2013. Nevada National Security Site Environmental Report 2012, DOE/NV/25946-1856, C. Wills editor, prepared by National Security Technologies, Las Vegas, NV.

Duncan, D., W. Forston, and R. Sanchez, 2000. 1999 Annual Site Environmental Report Tonopah Test Range, Nevada, SAND2000-2229, prepared by Sandia National Laboratories, Albuquerque, NM, for the U.S. Department of Energy.

EG&G, 1979. An Aerial Radiological Survey of Clean Slates 1, 2, and 3, and Double Track, Test Range, EGG-1183-2387. Energy Measurement Group, EG&G, Las Vegas, NV.

Engelbrecht, J.P., I.G. Kavouras, D. Campbell, S.A. Campbell, S. Kohl, D. Shafer, 2008. Yucca Mountain Environmental Monitoring System Initiative, Air Quality Scoping Study for Tonopah Airport, Nye County, Nevada, DOE/NV/26383-LTR 2008-04.

Gertz, C.P., 2001. Overview of low-level waste transportation and disposal. U.S. Department of Energy, Nevada Operations Office, Las Vegas, p. 32.

Hartwell, T.W., J. Daniels, G. Nikolich, C. Shadel, K. Giles, L. Karr, and T. Kluesner, 2012. Air Monitoring Network at Tonopah Test Range: Network Description, Capabilities, and Analytical Results. DRI Report No. 45243. Prepared for the U.S. Department of Energy, National Nuclear Security Administration, Nevada Site Office. January, 2012.

Johnson, W.G. and S.R. Edwards, 1996. A historic evaluation of Operation Roller Coaster, Stonewall and Cactus Flats, Nellis Air Force Range and Tonopah Test Range, Nye County, Nevada, Desert Research Institute Historical Evaluation Short Report #SR090996-1, NTS Project #9649MA, prepared for the U.S. Department of Energy, Nevada Operations Office.

Jones, F.C., 1961. Cosmic-ray production of low-energy gamma rays. Journal of Geophysical Research, 66(7).

Kathren, R.L., 1984. Radioactivity in the Environment: Sources, Distribution, and Surveillance. Hardwood Academic Publishers, New York.

Miller, J.J., D.S. Shafer, K.J. Gray, B.W. Church, S.A. Campbell, and B.A. Holtz, 2005. Assessing potential exposure from truck transport of low-level radioactive waste to the Nevada Test Site, DOE/NV/13609-37, prepared for the U.S. Department of Energy, Nevada Site Office, Las Vegas.

Mizell., S.A., G. Nikolich, C. Shadel, G. McCurdy, and J.J. Miller, 2013. Tonopah Test Range Air Monitoring: CY2012 Meteorological, Radiological, and Airborne Particulate Observations. DRI Report No. 45250. Prepared for the U.S. Department of Energy, National Nuclear Security Administration, Nevada Site Office. July, 2013.

Moeller, D.W., L.S.C. Sun, 2006. Comparison of natural background dose rates for residents of the Amargosa Valley, NV, to those in Leadville, CO, and the states of Colorado and Nevada. *Health Physics Society*, 91(4), pp. 338-353.

NARP, 2005. Radiation detection and measurement, NARP internet supplement_Rev 1.122211, accessed August 23, 2013 through U.S. Department of Defense, Nuclear Weapons Accident Response Procedures website: http://www.acq.osd.mil/ncbdp/narp/Radiation_Data/Radiation_Detection_and_Measurement.htm.

NCRP, 1975. Natural background radiation in the United States, National Council on Radiation Protection and Measurements Report 45.

NCRP, 1987. Ionizing radiation exposure of the population of the United States, National Council on Radiation Protection and Measurements Report 93.

NRC, 2011. Biological effects of radiation, fact sheet, U.S. Nuclear Regulatory Commission, p. 4.

NSTec. 2010. Radiological worker training study guide. National Securities Technologies, Las Vegas, Nevada, 107pp.

NSTec, 2012. Nevada National Security Site Environmental Report 2011, DOE/NV/25946-1604, prepared by National Security Technologies, LLC, for the

U.S. Department of Energy, National Nuclear Security Administration, Nevada Site Office.
Pelletier, J.D., 2006. Sensitivity of playa windblown-dust emissions to climatic and anthropogenic change. *Journal of Arid Environments*, 66:62-75.
Raupach, M.R., D.A. Gillette, and J.F. Leys, 1993. The effect of roughness elements on wind erosion threshold. *Journal of Geophysical Research*, 98(D2): 3023-3029.
Rowlett, R. 2012. How Many? A dictionary of units of measurement. http://www.unc.edu/~rowlett/units/index.html accessed, accessed December 18, 2013.
Schaeffer, J.R., 1970. Climatology of Tonopah Test Range, Nevada 1961-1969, SC-TM-70-0215, Sandia National laboratories, Albuquerque, NM.
Shao, Y., M. R. Raupach, and P.A. Findlater (1993). Effect of saltation bombardment on the entrainment of dust by wind. *Journal of Geophysical Research* 98, 719-712.
SNL, 2013. CY2012 Annual Site Environmental Report for Tonopah Test Range, Nevada and Kauai Test Facility, Hawaii, SAND2013-6179P, Sandia National Laboratories, Albuquerque, NM.
Stegen, R.L., T.R. Wood, J.R. Hackett, and A. Sogue, 2006. Cleaning up the streets of Denver. Proceedings of Waste Management '06, Tucson, AZ, February 6-March 2, 2006.
Tamura, T., 1974. The Dynamics of Plutonium in Desert Environments. In: Distribution and Characterization of Plutonium in Soils from Nevada Test Site, Report NVO-142, Oak Ridge National Laboratory, Environmental Sciences Division, Oak Ridge, TN.
Tamura, T., 1975. Characterization of Plutonium in Surface Soils from Area 13 of the Nevada Test Site. In: The Radioecology of Plutonium and Other Transuranics in Desert Environments, Report NVO-153, Oak Ridge National Laboratory, Environmental Sciences Division, Oak Ridge, TN.
Tamura, T., 1976. Plutonium Association in Soils. In: Transuranics in Natural Environments, Report NVO-178, Oak Ridge National Laboratory, Environmental Sciences Division, Oak Ridge, TN.
Tschanz, C.M., and Pampeyan. 1970. Geology and mineral deposits of Lincoln County, Nevada. Bulletin 73, Nevada Bureau of Mines and Geology, University of Nevada, Reno.
UNSCEAR, 2000. Sources and effects of ionizing radiation. Two volume report to the General Assembly prepared by the United Nations Scientific Committee on the Effects of Atomic Radiation.
USAF, 1999. Renewal of the Nellis Air Force Range Land Withdrawal: Department of the Air Force Legislative Environmental Impact Statement. U.S. Air Force, Nellis Air Force Range, Nevada.

APPENDIX A: METEOROLOGICAL AND CLIMATOLOGICAL PARAMETER DEFINITIONS

Observations – Instrument values recorded in temporary memory every three seconds (3-sec measurements) instantaneous (i.e., temperature) or integrated (i.e., precipitation) value for three-second period as appropriate.

Recorded observations – Average, maximum, minimum, or total of three-second measurements
are evaluated every 10 minutes (10-minute values). All plotted data in this report are based on
10-minute values. Ten-minute values are calculated in the data logger for intervals defined by the data logger program to start at three seconds after the start of the hour and after every 10 minute time interval.

10-minute maximum –
$10Mmax = MAX(3\text{-}sec_i)$ i = 1 to 200, for specified 10-minute period

10-minute minimum –
$10Mmin = MIN(3\text{-}sec_i)$ i = 1 to 200, for specified 10-minute period

10-minute average –
$10Mavg = \sum(3\text{-}sec_i)/200$ i = 1 to 200, for specified 10-minute period

10-minute total –
$10Mtot = \sum(3\text{-}sec_i)$ i = 1 to 200, for given 10-minute period

Transmitted observations – Average, maximum, minimum, or total of 3-second measurements are evaluated every 60 minutes (60-minute values). Sixty-minute values are transmitted via GOES once each hour and are used to update the WRCC data display until 10-minute data can be manually downloaded from the data logger, processed, and uploaded to the WRCC display.

Summary values – Summary values of electronically collected parameters are computed for various timescales from the included 10-minute observations. Values representing time intervals in excess of 10 minutes are calculated after 10-minute data is downloaded from the data logger.

Hourly maximum –
$Hmax = MAX(10Mmax_i)$ i = 1 to 6 for given hour

Hourly minimum –
$Hmin = MIN(10Mmin_i)$ i = 1 to 6 for given hour

Hourly average –
$Havg = \sum(10Mavg_i)/6$ i = 1 to 6 for given hour

Hourly total –
$Htot = \sum(10Mtot_i)$ i = 1 to 6 for given hour

Daily maximum (Equivalent to the daily maximum report for manually operated gage) –
$Dmax = MAX(10\text{-}min_i)$ i = 1 to 144 for given 00:00 to 23:59:59 period

Daily minimum (Equivalent to the daily minimum report for manually operated gage) –
$Dmin = MIN(10\text{-}min_i)$ i = 1 to 144 for given 00:00 to 23:59:59 period

Daily average –
$Davg = \sum(10\text{-}min_i)/144$ i = 1 to 144 for given 00:00 to 23:59:59 period

Daily total –
$Dtot = \sum(10\text{-}min_i)$ i = 1 to 144 for given 00:00 to 23:59:59 period

Monthly (extreme) maximum –
$Mmax = MAX(10\text{-}min_i)$ i = 1 to 144(# days in month) for given month

Monthly (extreme) minimum –
$Mmin = MIN(10\text{-}min_i)$ i = 1 to 144(# of days in month) for given month

Monthly average –
$Mavg = \sum(10\text{-}min_i)/(144(\text{\# days in month}))$
i = 1 to 144(# of days in month) for given month

Monthly total –
$Mtot = \sum(10\text{-}min_i)$ i = 1 to 144(# of days in month) for given month

Average of Daily Average for month = $\sum(Davg_i)/(\text{\# of days in month})$
i = 1 to # days in month

Average of Daily Maximum for month = $\sum(Dmax_i)/(\text{\# of days in month})$
i = 1 to # days in month

Highest Daily Maximum for month = $MAX(Dmax_i)$ $i = 1$ to # days in month

Average of Daily Minimum for month = $\sum(Dmin_i)$/(# of days in month)
$i = 1$ to # days in month

Lowest Daily Minimum for month = $MIN(Dmin_i)$ $i = 1$ to # days in month

APPENDIX B: MONTHLY CLIMATOLOGY SUMMARIES FOR TTR AIR MONITORING STATIONS 400, 401, AND 402

Table B-1. Station 400 monthly climatology summaries.

Average Mean Wind Speed (m/s)													
Year	**Jan**	**Feb**	**Mar**	**Apr**	**May**	**Jun**	**Jul**	**Aug**	**Sep**	**Oct**	**Nov**	**Dec**	**Annual**
2008						3.19	2.87	2.91	2.41d	2.69	2.68	2.40	2.74e
2009	2.66	2.62	3.85	3.91	2.81	2.94	2.86	3.01	2.63	3.39b	2.48	2.35	2.96
2010	2.20	2.09	3.40	4.08	4.00	3.30	3.02	3.42	2.73	2.48	3.35	2.53	3.05
2011	2.13	3.78	3.48	3.52	3.99	3.65	3.25	2.92	2.20	2.57	2.48	2.76	3.06
2012	2.33	3.25	4.00	3.89	3.79	4.37	4.04	3.10	2.53	2.63	3.03	3.62	3.38
Mean	2.33	2.93	3.68	3.85	3.65	3.49	3.21	3.07	2.50	2.75	2.80	2.73	3.11
S.D.	0.23	0.74	0.29	0.23	0.56	0.55	0.49	0.21	0.21	0.36	0.38	0.52	0.18
Skew	0.76	0.00	0.08	-0.69	-1.05	0.80	1.15	1.04	-0.43	1.33	0.54	1.19	0.94
Max	2.66	3.78	4.00	4.08	4.00	4.37	4.04	3.42	2.73	3.39	3.35	3.62	3.38
Min	2.13	2.09	3.40	3.52	2.81	2.94	2.86	2.91	2.20	2.48	2.48	2.35	2.96
# Yrs	4	4	4	4	4	5	5	5	5	5	5	5	4
a,b,c... = # of missing days/month or # missing months/year.													

Maximum Wind Gust (m/s)													
Year	**Jan**	**Feb**	**Mar**	**Apr**	**May**	**Jun**	**Jul**	**Aug**	**Sep**	**Oct**	**Nov**	**Dec**	**Annual**
2008						19.57	18.23	16.20	16.59d	17.38	15.03	20.61	17.66e
2009	16.17	17.74	18.98	19.67	16.46	17.64	19.17	16.30	16.66	17.74b	19.08	19.17	17.90
2010	19.53	14.47	21.49	23.52	19.70	20.25	15.48	19.37	17.87	15.52	20.05	17.18	18.70
2011	16.04	22.05	21.62	19.04	19.86	19.83	17.54	14.60	18.13	20.45	20.15	19.53	19.07
2012	19.14	17.64	20.05	19.34	17.93	21.13	18.85	17.18	13.07	19.79	18.19	18.23	18.38
Mean	17.72	17.98	20.54	20.39	18.49	19.68	17.85	16.73	16.46	18.18	18.50	18.94	18.51
S.D.	1.87	3.11	1.26	2.10	1.61	1.29	1.47	1.74	2.02	1.98	2.10	1.30	0.50
Skew	0.02	0.31	-0.33	1.10	-0.38	-0.70	-0.89	0.45	-1.07	-0.12	-1.01	-0.13	-0.17
Max	19.53	22.05	21.62	23.52	19.86	21.13	19.17	19.37	18.13	20.45	20.15	20.61	19.07
Min	16.04	14.47	18.98	19.04	16.46	17.64	15.48	14.60	13.07	15.52	15.03	17.18	17.90
# Yrs	4	4	4	4	4	5	5	5	5	5	5	5	4
a,b,c... = # of missing days/month or # missing months/year.													

Table B-1. Station 400 monthly climatology summaries (continued).

Average of Daily Average Air Temperature (Deg C)													
Year	**Jan**	**Feb**	**Mar**	**Apr**	**May**	**Jun**	**Jul**	**Aug**	**Sep**	**Oct**	**Nov**	**Dec**	**Annual**
2008						21.51	25.37	25.30	19.58d	11.97	7.23	-1.52	15.63e
2009	2.09	2.11	5.58	9.45	18.38	18.27	25.38	22.91	20.72	10.47b	5.46	-2.58	11.52
2010	0.53	2.39	4.45	7.87	11.32	21.27	25.71	23.00	19.49	11.87	3.70	2.42	11.17
2011	0.36	0.90	5.70	9.05	12.44	19.87	23.68	24.48	19.91	12.44	2.98	-0.58	10.94
2012	1.96	2.48	6.59	11.22	16.90	21.83	23.46	24.21	20.32	12.76	6.53	0.26	12.38
Mean	1.24	1.97	5.58	9.40	14.76	20.55	24.72	23.98	20.00	11.90	5.18	-0.40	11.50
S.D.	0.92	0.73	0.88	1.39	3.41	1.48	1.06	1.02	0.52	0.88	1.81	1.90	0.63
Skew	-0.01	-1.00	-0.24	0.35	0.04	-0.76	-0.37	0.07	0.38	-0.89	-0.13	0.45	0.70
Max	2.09	2.48	6.59	11.22	18.38	21.83	25.71	25.30	20.72	12.76	7.23	2.42	12.38
Min	0.36	0.90	4.45	7.87	11.32	18.27	23.46	22.91	19.49	10.47	2.98	-2.58	10.94
# Yrs	4	4	4	4	4	5	5	5	5	5	5	5	4
a,b,c… = # of missing days/month or # missing months/year.													

Average of Daily Maximum Air Temperature (Deg C)													
Year	**Jan**	**Feb**	**Mar**	**Apr**	**May**	**Jun**	**Jul**	**Aug**	**Sep**	**Oct**	**Nov**	**Dec**	**Annual**
2008						29.18	32.87	33.00	28.25c	21.22	15.37	6.22	23.73e
2009	10.18	8.24	13.10	17.04	26.18	25.03	33.18	30.50	29.09	18.26a	14.55	4.59	19.16
2010	7.10	8.58	11.60	14.75	18.44	28.32	32.95	30.67	28.86	19.26	11.08	8.68	18.36
2011	8.46	8.33	12.64	16.53	19.38	27.12	31.06	32.16	28.41	21.35	10.85	8.46	18.73
2012	11.30	9.46	14.23	18.33	24.15	29.10	30.86	31.79	28.02	20.80	14.77	5.61	19.87
Mean	9.26	8.66	12.89	16.66	22.04	27.75	32.18	31.62	28.53	20.18	13.32	6.71	19.03
S.D.	1.85	0.56	1.09	1.48	3.73	1.73	1.13	1.05	0.44	1.36	2.18	1.80	0.65
Skew	-0.08	0.94	0.07	-0.27	0.11	-0.80	-0.39	0.12	0.21	-0.54	-0.35	0.09	0.37
Max	11.30	9.46	14.23	18.33	26.18	29.18	33.18	33.00	29.09	21.35	15.37	8.68	19.87
Min	7.10	8.24	11.60	14.75	18.44	25.03	30.86	30.50	28.02	18.26	10.85	4.59	18.36
# Yrs	4	4	4	4	4	5	5	5	5	5	5	5	4
a,b,c… = # of missing days/month or # missing months/year.													

Table B-1. Station 400 monthly climatology summaries (continued).

Highest of Daily Maximum Air Temperature (Deg C)													
Year	**Jan**	**Feb**	**Mar**	**Apr**	**May**	**Jun**	**Jul**	**Aug**	**Sep**	**Oct**	**Nov**	**Dec**	**Annual**
2008						33.95	36.13	35.99	32.79d	27.85	23.09	18.24	29.72e
2009	18.51	16.49	20.10	27.40	31.65	33.98	36.33	35.47	33.90	26.25b	25.16	11.01	26.35
2010	14.49	15.40	19.42	22.36	26.39	34.42	36.89	35.10	34.03	27.85	24.98	16.65	25.67
2011	16.07	16.45	23.86	25.42	27.32	33.75	35.02	34.56	31.75	28.26	18.33	15.53	25.53
2012	18.47	16.57	21.73	28.38	30.90	33.24	37.32	35.41	31.57	29.57	22.23	12.85	26.52
Mean	16.88	16.23	21.28	25.89	29.06	33.87	36.34	35.31	32.81	27.96	22.76	14.86	26.02
S.D.	1.96	0.55	1.98	2.66	2.60	0.43	0.87	0.53	1.16	1.19	2.77	2.91	0.49
Skew	-0.31	-1.13	0.46	-0.52	-0.02	-0.28	-0.50	-0.19	0.01	-0.12	-0.82	-0.23	0.02
Max	18.51	16.57	23.86	28.38	31.65	34.42	37.32	35.99	34.03	29.57	25.16	18.24	26.52
Min	14.49	15.40	19.42	22.36	26.39	33.24	35.02	34.56	31.57	26.25	18.33	11.01	25.53
# Yrs	4	4	4	4	4	5	5	5	5	5	5	5	4
a,b,c... = # of missing days/month or # missing months/year.													

Average of Daily Minimum Air Temperature (Deg C)													
Year	**Jan**	**Feb**	**Mar**	**Apr**	**May**	**Jun**	**Jul**	**Aug**	**Sep**	**Oct**	**Nov**	**Dec**	**Annual**
2008						11.41	15.88	15.47	10.32c	2.99	0.06	-8.26	6.84e
2009	-5.05	-3.36	-2.82	0.86	9.59	10.64	16.46	13.56	11.45	2.43a	-3.00	-9.29	3.46
2010	-4.58	-2.68	-2.53	0.01	3.14	12.15	16.14	13.54	9.19	5.39	-2.80	-2.93	3.67
2011	-6.59	-6.54	-1.77	1.08	4.12	11.11	14.66	14.71	11.23	3.68	-3.98	-7.95	2.81
2012	-6.46	-4.52	-1.70	2.94	8.03	12.27	14.45	16.31	12.04	5.08	-0.36	-5.20	4.41
Mean	-5.67	-4.27	-2.21	1.22	6.22	11.52	15.52	14.72	10.85	3.91	-2.02	-6.73	3.59
S.D.	1.01	1.69	0.56	1.24	3.08	0.69	0.91	1.21	1.11	1.29	1.77	2.61	0.66
Skew	0.10	-0.54	-0.13	0.66	0.07	-0.05	-0.27	0.20	-0.55	0.09	0.23	0.57	0.12
Max	-4.58	-2.68	-1.70	2.94	9.59	12.27	16.46	16.31	12.04	5.39	0.06	-2.93	4.41
Min	-6.59	-6.54	-2.82	0.01	3.14	10.64	14.45	13.54	9.19	2.43	-3.98	-9.29	2.81
# Yrs	4	4	4	4	4	5	5	5	5	5	5	5	4
a,b,c... = # of missing days/month or # missing months/year.													

Table B-1. Station 400 monthly climatology summaries (continued).

Lowest of Daily Minimum Air Temperature (Deg C)													
Year	**Jan**	**Feb**	**Mar**	**Apr**	**May**	**Jun**	**Jul**	**Aug**	**Sep**	**Oct**	**Nov**	**Dec**	**Annual**
2008						3.36	12.59	12.50	7.02d	-6.68	-5.89	-19.36	0.51e
2009	-13.23	-10.64	-15.40	-5.90	5.47	5.02	13.37	9.32	3.13	-5.60b	-8.46	-21.67	-3.72
2010	-12.14	-8.03	-9.09	-6.95	-1.86	3.66	9.18	6.96	5.35	-4.69	-12.94	-14.27	-3.73
2011	-17.00	-12.81	-13.24	-5.76	-1.50	1.62	9.64	10.64	7.64	-3.70	-9.31	-13.51	-3.94
2012	-15.23	-8.67	-9.23	-6.28	0.16	4.61	10.95	12.75	8.28	-2.19	-10.10	-14.25	-2.43
Mean	-14.40	-10.04	-11.74	-6.22	0.57	3.65	11.15	10.43	6.28	-4.57	-9.34	-16.61	-3.46
S.D.	2.15	2.16	3.11	0.53	3.38	1.32	1.82	2.40	2.07	1.73	2.56	3.67	0.69
Skew	-0.19	-0.42	-0.23	-0.65	0.94	-0.61	0.14	-0.45	-0.67	0.20	-0.09	-0.53	1.08
Max	-12.14	-8.03	-9.09	-5.76	5.47	5.02	13.37	12.75	8.28	-2.19	-5.89	-13.51	0.00
Min	-17.00	-12.81	-15.40	-6.95	-1.86	1.62	9.18	6.96	3.13	-6.68	-12.94	-21.67	-3.94
# Yrs	4	4	4	4	4	5	5	5	5	5	5	5	4
a,b,c... = # of missing days/month or # missing months/year.													

Monthly Average Gamma Radiation (uR/hr)													
Year	**Jan**	**Feb**	**Mar**	**Apr**	**May**	**Jun**	**Jul**	**Aug**	**Sep**	**Oct**	**Nov**	**Dec**	**Annual**
2008						12.77	20.68	13.10	9.02d	20.83	20.89	20.88	16.88e
2009	20.54	20.45	21.66	22.08	21.66	20.85	20.76	20.77	20.90	21.04b	21.03	20.51	21.02
2010	20.34	20.45	20.35	20.48	20.61	20.72	20.78	19.76	19.25	18.99c	19.01a	18.98	19.98
2011	18.65	18.80	18.71	18.86	19.00	19.04	19.16	19.13	19.11	19.08	18.89	19.14	18.96
2012	19.00	18.98	18.88	18.41	17.82	17.89	17.73	17.83	17.81	17.80	17.86	17.81	18.15
Mean	19.63	19.67	19.90	19.96	19.77	18.25	19.82	18.12	17.22	19.55	19.54	19.46	19.53
S.D.	0.95	0.90	1.39	1.67	1.70	3.30	1.36	3.00	4.71	1.37	1.38	1.24	1.24
Skew	-0.05	-0.02	0.40	0.39	-0.05	-1.02	-0.80	-1.06	-1.30	-0.02	0.07	-0.10	0.13
Max	20.54	20.45	21.66	22.08	21.66	20.85	20.78	20.77	20.90	21.04	21.03	20.88	21.02
Min	18.65	18.80	18.71	18.41	17.82	12.77	17.73	13.10	9.02	17.80	17.86	17.81	18.15
# Yrs	4	4	4	4	4	5	5	5	5	5	5	5	4
a,b,c... = # of missing days/month or # missing months/year.													

Table B-1. Station 400 monthly climatology summaries (continued).

Monthly Average Soil Temperature - 4 Inches (Deg C)													
Year	**Jan**	**Feb**	**Mar**	**Apr**	**May**	**Jun**	**Jul**	**Aug**	**Sep**	**Oct**	**Nov**	**Dec**	**Annual**
2008						21.64	25.46	25.47	19.54d	11.75	6.82	-1.87	15.54e
2009	1.59	2.10	5.73	9.75	18.74	18.64	25.55	23.08	20.79	10.44b	4.91	-2.44	11.57
2010	0.75	3.97	6.92	11.19	15.85	25.55	30.10	28.29	23.46	14.39	4.82	2.83	14.01
2011	0.39	2.54	7.47	13.20	16.64	24.29	27.90	28.05	24.13	15.89	4.77	0.15	13.78
2012	2.05	4.18	8.69	14.63	22.00	26.64	27.50	28.52	25.61	17.44	9.94	3.20	15.87
Mean	1.19	3.20	7.20	12.19	18.31	23.35	27.30	26.68	22.71	13.98	6.25	0.37	13.81
S.D.	0.76	1.03	1.23	2.16	2.75	3.23	1.92	2.36	2.49	0.00	2.23	2.60	1.76
Skew	0.07	-0.07	0.02	0.00	0.57	-0.52	0.42	-0.76	-0.20	-0.08	1.05	0.06	-0.17
Max	2.05	4.18	8.69	14.63	22.00	26.64	30.10	28.52	25.61	17.44	9.94	3.20	15.87
Min	0.39	2.10	5.73	9.75	15.85	18.64	25.46	23.08	19.54	10.44	4.77	-2.44	11.57
# Yrs	4	4	4	4	4	5	5	5	5	5	5	5	4
a,b,c... = # of missing days/month or # missing months/year.													

Maximum Monthly Relative Humidity (%)													
Year	**Jan**	**Feb**	**Mar**	**Apr**	**May**	**Jun**	**Jul**	**Aug**	**Sep**	**Oct**	**Nov**	**Dec**	**Annual**
2008						59	91	80	92d	90	100	100	87e
2009	99	100	100	100	88	94	93	96	91	97b	97	100	96
2010	100	100	100	100	98	68	90	63	74	98	99	100	91
2011	99	100	100	98	100	70	94	97	95	89	100	95	95
2012	98	100	100	100	99	44	97	98	98	99	95	100	94
Mean	99	100	100	100	96	67	93	87	90	95	98	99	94
S.D.	1	0.1	0	0.9	5.55	18.18	2.84	15.1	9.43	0	0	0	2.37
Skew	-0.5	-1.15	0	-1.15	-1.05	0.35	0.33	-0.82	-1.22	-0.4	-0.48	-1.5	-0.56
Max	100	100	100	100	100	94	97	98	98	99	100	100	96
Min	98	100	100	98	88	44	90	63	74	89	95	95	91
# Yrs	4	4	4	4	4	5	5	5	5	5	5	5	4
a,b,c... = # of missing days/month or # missing months/year.													

Table B-1. Station 400 monthly climatology summaries (continued).

Minimum Monthly Relative Humidity (%)													
Year	**Jan**	**Feb**	**Mar**	**Apr**	**May**	**Jun**	**Jul**	**Aug**	**Sep**	**Oct**	**Nov**	**Dec**	**Annual**
2008						5	6	6	7d	6	13	13	8e
2009	10	12	9	8	7	7	7	7	6	8b	8	11	8
2010	19	23	9	7	8	7	6	6	5	7	9	9	10
2011	15	11	8	9	8	7	6	6	7	7	9	11	9
2012	8	6	7	4	4	4	3	6	5	9	12	22	7
Mean	13	13	8	7	7	6	6	6	6	8	10	13	8
S.D.	5.15	7.14	1.06	1.95	1.55	1.4	1.3	0.69	1.18	0	0	0	0.86
Skew	0.12	0.6	-0.08	-0.85	-0.84	-0.79	-1.07	0.8	0.25	-0.35	0.16	1.32	0.19
Max	19	23	9	9	8	7	7	7	7	9	13	22	10
Min	8	6	7	4	4	4	3	6	5	6	8	9	7
# Yrs	4	4	4	4	4	5	5	5	5	5	5	5	4
a,b,c… = # of missing days/month or # missing months/year.													

Average Monthly Barometric Pressure (mbar)													
Year	**Jan**	**Feb**	**Mar**	**Apr**	**May**	**Jun**	**Jul**	**Aug**	**Sep**	**Oct**	**Nov**	**Dec**	**Annual**
2008						831.90	832.60	831.60	833.40f	835.10	835.10	830.70	832.83f
2009	836.70	830.70	829.90	829.40	831.40	829.40	833.90	833.70	833.80	831.10b	833.00	830.40	831.95
2010	830.00	829.00	830.60	827.40	829.20	830.90	832.20	831.70	832.30	833.90	833.00	830.30	830.87
2011	834.90	830.80	830.10	829.40	828.60	829.50	832.20	833.10	834.60	833.80	832.40	835.30	832.06
2012	835.60	831.20	829.30	830.20	829.70	829.60	833.20	833.60	835.00	832.50	833.70	830.30	831.99
Mean	834.30	830.42	829.97	829.10	829.72	830.26	832.82	832.74	833.92	833.28	833.44	831.40	831.72
S.D.	2.96	0.97	0.54	1.19	1.20	1.10	0.73	1.02	1.19	0.00	0.00	0.00	0.56
Skew	-0.94	-0.98	-0.15	-0.80	0.69	0.69	0.60	-0.27	-0.62	-0.35	0.83	1.48	-1.13
Max	836.70	831.20	830.60	830.20	831.40	831.90	833.90	833.70	835.00	835.10	835.10	835.30	832.06
Min	830.00	829.00	829.30	827.40	828.60	829.40	832.20	831.60	832.30	831.10	832.40	830.30	830.87
# Yrs	4	4	4	4	4	5	5	5	4	5	5	5	4
a,b,c… = # of missing days/month or # missing months/year.													

Table B-1. Station 400 monthly climatology summaries (continued).

Total Precipitation (mm)													
Year	**Jan**	**Feb**	**Mar**	**Apr**	**May**	**Jun**	**Jul**	**Aug**	**Sep**	**Oct**	**Nov**	**Dec**	**Annual**
2008						1.02	21.08	0.51	5.59d	0.76	9.65	3.05	41.65e
2009	2.79	17.27	9.40	7.87	1.78	15.24	22.10	4.83	0.76	0.25b	2.54	14.99	99.83
2010	9.40	16.76	10.92	17.53	5.84	0.00	6.86	0.00	0.00	12.45	6.10	13.46	99.31
2011	2.54	5.84	20.07	4.32	21.08	0.00	32.77	0.00	2.79	1.78	5.59	0.00	96.78
2012	9.40	2.79	4.32	6.10	5.33	0.00	24.13	11.43	16.76	14.73	0.25	4.32	99.56
Mean	6.03	10.67	11.18	8.95	8.51	3.25	21.39	3.35	5.18	5.99	4.83	7.16	98.87
S.D.	3.89	7.44	6.57	5.90	8.57	6.72	9.34	4.95	6.82	0.00	0.00	0.00	1.41
Skew	0.00	-0.08	0.51	0.95	1.00	1.48	-0.54	1.00	1.16	0.43	0.04	0.25	-1.08
Max	9.40	17.27	20.07	17.53	21.08	15.24	32.77	11.43	16.76	14.73	9.65	14.99	99.83
Min	2.54	2.79	4.32	4.32	1.78	0.00	6.86	0.00	0.00	0.25	0.25	0.00	96.78
# Yrs	4	4	4	4	4	5	5	5	5	5	5	5	4
a,b,c… = # of missing days/month or # missing months/year.													

Table B-2. Station 401 monthly climatology summaries.

Average Mean Wind Speed (m/s)													
Year	**Jan**	**Feb**	**Mar**	**Apr**	**May**	**Jun**	**Jul**	**Aug**	**Sep**	**Oct**	**Nov**	**Dec**	**Annual**
2008						2.89f	2.89	2.76	2.45	2.55	2.67	2.28	2.60f
2009	2.49	3.20i	3.88f	4.20	2.78	3.12b	3.21g	2.85	2.48	3.39	2.45	2.33d	2.90c
2010	2.47i	2.45	3.93	4.44	4.45	3.49	3.21	3.59	2.77	2.74	3.61	2.83	3.41a
2011	2.10	4.04	3.80	3.90	4.38	3.92	3.58	3.19	2.34	2.75	2.66	2.94	3.30
2012	2.33	3.59	4.36	4.13	3.91	4.21	3.69	2.95	2.21	2.34	2.59	3.38	3.31
Mean	2.31	3.36	4.03	4.17	3.88	3.68	3.34	3.07	2.45	2.75	2.80	2.75	3.23
S.D.	0.19	0.82	0.29	0.22	0.77	0.48	0.37	0.33	0.21	0.39	0.46	0.46	0.23
Skew	-0.22	-0.47	0.55	0.02	-0.86	-0.11	-0.30	0.79	0.53	0.82	1.36	0.21	-0.98
Max	2.49	4.04	4.36	4.44	4.45	4.21	3.69	3.59	2.77	3.39	3.61	3.38	3.41
Min	2.10	2.45	3.80	3.90	2.78	3.12	2.89	2.76	2.21	2.34	2.45	2.28	2.90
# Yrs	3	3	3	4	4	4	4	5	5	5	5	5	4
a,b,c… = # of missing days/month or # missing months/year.													

Maximum Wind Gust (m/s)													
Year	**Jan**	**Feb**	**Mar**	**Apr**	**May**	**Jun**	**Jul**	**Aug**	**Sep**	**Oct**	**Nov**	**Dec**	**Annual**
2008						19.10f	20.15	15.20	15.35	16.85	15.05	19.70	17.05f
2009	14.15	16.85i	20.30f	23.15	17.45	19.55b	16.40g	17.00	17.60	15.65	17.15	20.42d	18.01c
2010	18.00i	15.62	20.28	25.38	20.28	18.00	18.16	17.90	18.62	16.33	17.28	17.35	18.65a
2011	14.00	22.57	20.05	19.86	19.20	21.65	17.35	15.74	18.42	19.70	18.45	25.05	19.34
2012	22.83	19.67	21.56	19.40	18.13	21.40	20.87	19.53	14.53	16.33	16.95	17.64	19.07
Mean	16.99	19.29	20.63	21.95	18.77	20.15	19.13	17.07	16.90	16.97	16.98	20.03	18.77
S.D.	5.06	3.49	0.81	2.83	1.24	1.71	1.65	1.73	1.86	1.58	1.23	3.10	0.58
Skew	0.71	-0.20	0.64	0.28	0.21	-0.37	-0.02	0.34	-0.36	1.23	-0.59	0.88	-0.45
Max	22.83	22.57	21.56	25.38	20.28	21.65	20.87	19.53	18.62	19.70	18.45	25.05	19.34
Min	14.00	15.62	20.05	19.40	17.45	18.00	17.35	15.20	14.53	15.65	15.05	17.35	18.01
# Yrs	3	3	3	4	4	4	4	5	5	5	5	5	4
a,b,c… = # of missing days/month or # missing months/year.													

Table B-2. Station 401 monthly climatology summaries (continued).

Average of Daily Average Air Temperature (Deg C)													
Year	**Jan**	**Feb**	**Mar**	**Apr**	**May**	**Jun**	**Jul**	**Aug**	**Sep**	**Oct**	**Nov**	**Dec**	**Annual**
2008						21.93f	24.37	24.07	17.63	9.96	5.44	-3.42	13.01f
2009	0.02	-0.47i	5.54f	8.31	17.19	18.14b	24.13g	21.64	19.15	8.62	3.33	-4.74d	10.19c
2010	-0.02i	1.47	3.42	6.96	10.38	20.18	24.56	21.70	17.42	10.59	2.09	1.05	10.89a
2011	-2.11	-0.41	4.60	7.99	11.59	18.73	22.71	23.22	18.48	10.66	1.05	-3.16	9.45
2012	-0.68	1.01	5.55	10.24	15.85	20.96	22.84	23.72	19.07	11.05	4.68	-0.57	11.14
Mean	-0.92	0.69	4.52	8.38	13.75	19.50	23.62	22.87	18.35	10.18	3.32	-2.17	10.42
S.D.	1.09	0.98	1.06	1.37	3.28	1.30	0.98	1.14	0.80	0.95	1.80	2.35	0.76
Skew	-0.39	-0.54	-0.13	0.54	0.02	0.07	0.01	-0.21	-0.16	-0.94	-0.07	0.38	-0.38
Max	0.02	1.47	5.55	10.24	17.19	20.96	24.56	24.07	19.15	11.05	5.44	1.05	11.14
Min	-2.11	-0.41	3.42	6.96	10.38	18.14	22.71	21.64	17.42	8.62	1.05	-4.74	9.45
# Yrs	3	3	3	4	4	4	4	5	5	5	5	5	4
a,b,c… = # of missing days/month or # missing months/year.													

Average of Daily Maximum Air Temperature (Deg C)													
Year	**Jan**	**Feb**	**Mar**	**Apr**	**May**	**Jun**	**Jul**	**Aug**	**Sep**	**Oct**	**Nov**	**Dec**	**Annual**
2008						30.66e	33.03	32.95	27.56	20.95	15.06	5.74	23.71e
2009	9.70	5.71h	14.31f	16.94	25.95	24.19	32.42g	30.42	28.91	17.93	14.09	2.66c	18.98c
2010	5.59c	7.71	11.24	14.60	18.47	28.56	33.15	30.74	28.74	18.89	10.62	8.01	18.03
2011	7.37	7.98	12.48	16.16	19.34	27.24	31.14	32.54	28.12	20.78	10.24	7.61	18.42
2012	10.54	9.10	14.24	18.27	24.38	29.57	31.26	32.14	27.96	20.58	14.44	5.62	19.84
Mean	8.30	8.26	12.65	16.49	22.04	28.04	32.15	31.76	28.26	19.83	12.89	5.93	18.82
S.D.	2.25	0.74	1.51	1.53	3.69	2.50	1.09	1.12	0.56	1.34	2.28	2.12	0.79
Skew	-0.23	0.59	0.21	-0.12	0.06	-0.65	0.00	-0.24	0.03	-0.57	-0.35	-0.62	0.42
Max	10.54	9.10	14.24	18.27	25.95	30.66	33.15	32.95	28.91	20.95	15.06	8.01	19.84
Min	5.59	7.71	11.24	14.60	18.47	24.19	31.14	30.42	27.56	17.93	10.24	2.66	18.03
# Yrs	4	3	3	4	4	5	4	5	5	5	5	5	4
a,b,c… = # of missing days/month or # missing months/year.													

Table B-2. Station 401 monthly climatology summaries (continued).

Highest of Daily Maximum Air Temperature (Deg C)													
Year	**Jan**	**Feb**	**Mar**	**Apr**	**May**	**Jun**	**Jul**	**Aug**	**Sep**	**Oct**	**Nov**	**Dec**	**Annual**
2008						33.95f	36.16	35.77	32.66	27.40	22.66	17.84	28.75f
2009	15.89	15.86i	20.37f	26.58	31.47	33.70b	35.35g	35.31	33.04	26.99	25.33	10.61d	26.55c
2010	11.20i	13.75	19.53	22.09	26.59	34.76	37.01	35.20	32.97	27.46	24.42	15.14	26.27a
2011	15.73	15.85	23.85	25.59	26.74	33.89	35.40	34.88	31.49	27.86	17.11	14.74	25.26
2012	17.02	16.47	21.85	28.81	31.31	33.23	37.85	35.72	31.79	29.02	22.53	12.72	26.53
Mean	16.21	15.36	21.74	25.77	29.03	33.90	36.60	35.38	32.39	27.75	22.41	14.21	26.15
S.D.	0.70	1.43	2.16	2.80	2.73	0.64	1.06	0.37	0.71	0.78	3.19	2.72	0.61
Skew	0.67	-0.56	-0.09	-0.37	0.00	0.51	0.05	-0.14	-0.36	0.94	-1.00	-0.02	-1.01
Max	17.02	16.47	23.85	28.81	31.47	34.76	37.85	35.77	33.04	29.02	25.33	17.84	26.55
Min	15.73	13.75	19.53	22.09	26.59	33.23	35.40	34.88	31.49	26.99	17.11	10.61	25.26
# Yrs	3	3	3	4	4	4	4	5	5	5	5	5	4
a,b,c… = # of missing days/month or # missing months/year.													

Average of Daily Minimum Air Temperature (Deg C)													
Year	**Jan**	**Feb**	**Mar**	**Apr**	**May**	**Jun**	**Jul**	**Aug**	**Sep**	**Oct**	**Nov**	**Dec**	**Annual**
2008						9.31e	13.39	12.24	5.94	-1.69	-3.45	-11.59	3.45e
2009	-8.35	-6.68h	-4.58f	-2.22	5.88	9.46	13.55g	10.47	7.97	-1.40	-7.00	-12.19c	0.29c
2010	-4.43c	-4.20	-4.52	-1.67	0.44	8.42	12.55	9.67	3.87	2.44	-6.11	-5.50	0.91
2011	-10.36	-9.14	-4.22	-1.60	1.64	7.32	12.44	11.07	7.67	0.03	-7.61	-11.82	-0.38
2012	-10.69	-7.73	-3.89	0.48	4.61	8.87	12.17	14.53	9.04	1.63	-4.20	-7.17	1.47
Mean	-8.46	-7.02	-4.21	-1.25	3.14	8.68	12.64	11.60	6.90	0.20	-5.67	-9.65	0.57
S.D.	2.88	2.54	0.32	1.19	2.53	0.86	0.53	1.89	2.03	1.82	1.79	3.09	0.80
Skew	0.76	0.47	0.08	0.96	0.01	-0.77	0.83	0.70	-0.58	0.15	0.22	0.50	-0.10
Max	-4.43	-4.20	-3.89	0.48	5.88	9.46	13.39	14.53	9.04	2.44	-3.45	-5.50	1.47
Min	-10.69	-9.14	-4.52	-2.22	0.44	7.32	12.17	9.67	3.87	-1.69	-7.61	-12.19	-0.38
# Yrs	4	3	3	4	4	5	4	5	5	5	5	5	4
a,b,c… = # of missing days/month or # missing months/year.													

Table B-2. Station 401 monthly climatology summaries (continued).

Lowest of Daily Minimum Air Temperature (Deg C)													
Year	**Jan**	**Feb**	**Mar**	**Apr**	**May**	**Jun**	**Jul**	**Aug**	**Sep**	**Oct**	**Nov**	**Dec**	**Annual**
2008						4.58f	8.80	8.20	-0.48	-9.64	-10.35	-21.98	-4.24f
2009	-18.57	-11.40i	-10.66f	-10.27	0.65	2.62b	7.97g	4.23	1.11	-8.96	-13.39	-25.29d	-7.54c
2010	-10.61i	-10.57	-14.87	-11.06	-5.53	0.49	4.34	3.03	0.14	-9.68	-16.51	-15.88	-6.92a
2011	-22.27	-14.17	-17.67	-8.79	-5.38	-3.13	8.00	7.89	3.54	-9.16	-13.84	-16.86	-7.65
2012	-19.48	-14.79	-11.64	-11.74	-1.49	1.65	6.79	8.22	4.35	-5.94	-12.69	-16.89	-6.14
Mean	-20.11	-13.18	-14.73	-10.46	-2.94	0.41	6.98	6.32	1.73	-8.67	-13.36	-19.38	-7.06
S.D.	1.93	2.28	3.02	1.27	3.03	2.52	1.95	2.49	2.12	1.56	2.22	4.08	0.70
Skew	-0.53	0.65	0.09	0.46	0.24	-0.77	-0.60	-0.49	0.26	1.36	-0.10	-0.62	0.54
Max	-18.57	-10.57	-11.64	-8.79	0.65	2.62	8.80	8.22	4.35	-5.94	-10.35	-15.88	-6.14
Min	-22.27	-14.79	-17.67	-11.74	-5.53	-3.13	4.34	3.03	-0.48	-9.68	-16.51	-25.29	-7.65
# Yrs	3	3	3	4	4	4	4	5	5	5	5	5	4
a,b,c… = # of missing days/month or # missing months/year.													

Monthly Average Gamma Radiation (uR/hr)													
Year	**Jan**	**Feb**	**Mar**	**Apr**	**May**	**Jun**	**Jul**	**Aug**	**Sep**	**Oct**	**Nov**	**Dec**	**Annual**
2008													
2009												20.92m	
2010	21.08i	20.85	20.56	20.77	21.14	21.37	21.56	21.63	21.86	21.54	21.75	21.71	21.34a
2011	21.46	21.37	20.93	21.09	21.27	21.26	21.17	21.35	21.41	21.57	21.71	22.09	21.39
2012	21.94	21.60	21.22	20.98	21.17	21.19	20.89	20.91	20.95	21.15	21.51	21.48	21.25
Mean	21.70	21.27	20.90	20.95	21.19	21.27	21.21	21.30	21.41	21.42	21.66	21.76	21.33
S.D.	0.34	0.38	0.33	0.16	0.07	0.09	0.34	0.36	0.46	0.23	0.13	0.31	0.07
Skew	0.00	-0.43	-0.15	-0.36	0.56	0.26	0.20	-0.26	-0.01	-0.69	-0.63	0.29	-0.34
Max	21.94	21.60	21.22	21.09	21.27	21.37	21.56	21.63	21.86	21.57	21.75	22.09	21.39
Min	21.46	20.85	20.56	20.77	21.14	21.19	20.89	20.91	20.95	21.15	21.51	21.48	21.25
# Yrs	2	3	3	3	3	3	3	3	3	3	3	3	3
a,b,c… = # of missing days/month or # missing months/year.													

Table B-2. Station 401 monthly climatology summaries (continued).

Monthly Average Soil Temperature - 4 Inches (Deg C)													
Year	**Jan**	**Feb**	**Mar**	**Apr**	**May**	**Jun**	**Jul**	**Aug**	**Sep**	**Oct**	**Nov**	**Dec**	**Annual**
2008													
2009												-0.98m	
2010	1.15i	3.67	5.91	10.56	15.44	24.25	28.66	27.27	22.75	15.19	6.11	3.39	14.84a
2011	0.36	3.03	7.41	12.82	16.29	22.74	26.63	27.30	23.18	15.14	5.19	0.10	13.35
2012	1.18	3.83	8.43	13.91	20.43	25.24	26.22	27.31	22.91	15.12	8.02	2.84	14.62
Mean	0.77	3.51	7.25	12.43	17.39	24.08	27.17	27.29	22.95	15.15	6.44	2.11	14.27
S.D.	0.58	0.42	1.27	1.71	2.67	1.26	1.31	0.02	0.22	0.00	1.44	1.76	0.80
Skew	0.00	-0.59	-0.23	-0.40	0.63	-0.25	0.63	-0.53	0.30	0.47	0.40	-0.63	-0.65
Max	1.18	3.83	8.43	13.91	20.43	25.24	28.66	27.31	23.18	15.19	8.02	3.39	14.84
Min	0.36	3.03	5.91	10.56	15.44	22.74	26.22	27.27	22.75	15.12	5.19	0.10	13.35
# Yrs	2	3	3	3	3	3	3	3	3	3	3	3	3
a,b,c... = # of missing days/month or # missing months/year.													

Maximum Monthly Relative Humidity (%)													
Year	**Jan**	**Feb**	**Mar**	**Apr**	**May**	**Jun**	**Jul**	**Aug**	**Sep**	**Oct**	**Nov**	**Dec**	**Annual**
2008						35f	91	81	93	90	97	95	91f
2009	93	96i	91f	95	93	93b	91g	94	95	96	94	97d	94c
2010	95i	97	96	95	93	73	90	80	76	96	93	97	90a
2011	94	96	95	95	95	74	96	97	93	89	94	90	92
2012	93	94	93	96	94	44	96	96	95	96	91	96	90
Mean	93	96	95	95	94	71	93	90	90	93	94	95	92
S.D.	0.55	1.67	1.72	0.43	0.83	20.17	3.37	8.36	7.92	0.00	0.00	0.00	2.20
Skew	0.11	-0.32	-0.28	0.60	0.33	-0.41	-0.07	-0.38	-1.43	-0.46	-0.07	-1.16	0.43
Max	94	97	96	96	95	93	96	97	95	96	97	97	94
Min	93	94	93	95	93	44	90	80	76	89	91	90	90
# Yrs	3	3	3	4	4	4	4	5	5	5	5	5	4
a,b,c... = # of missing days/month or # missing months/year.													

Table B-2. Station 401 monthly climatology summaries (continued).

Minimum Monthly Relative Humidity (%)													
Year	Jan	Feb	Mar	Apr	May	Jun	Jul	Aug	Sep	Oct	Nov	Dec	Annual
2008						1f	2	4	5	2	10	12	6f
2009	11	12i	7f	5	3	4b	3g	5	2	8	6	0d	5c
2010	18i	24	9	6	7	5	4	4	4	7	9	6	8a
2011	19	13	7	9	7	6	5	4	7	8	9	13	9
2012	7	5	7	3	4	3	3	6	5	11	10	23	7
Mean	13	14	8	6	5	5	3	4	4	7	9	11	7
S.D.	6.03	9.55	1.59	2.5	1.88	1.48	1.5	0.9	1.72	0	0	0	1.67
Skew	0.39	0.19	0.7	-0.02	-0.06	-0.28	0.11	0.91	0.09	-0.77	-1.06	0.23	-0.54
Max	19	24	9	9	7	6	5	6	7	11	10	23	9
Min	7	5	7	3	3	3	2	4	2	2	6	0	5
# Yrs	3	3	3	4	4	4	4	5	5	5	5	5	4
a,b,c… = # of missing days/month or # missing months/year.													

Average Monthly Barometric Pressure (mbar)													
Year	Jan	Feb	Mar	Apr	May	Jun	Jul	Aug	Sep	Oct	Nov	Dec	Annual
2008													
2009													
2010													
2011													
2012		No Data, No Sensor Installed											
Mean													
S.D.													
Skew													
Max													
Min													
# Yrs													
a,b,c… = # of missing days/month or # missing months/year.													

Table B-2. Station 401 monthly climatology summaries (continued).

Total Precipitation (mm)													
Year	**Jan**	**Feb**	**Mar**	**Apr**	**May**	**Jun**	**Jul**	**Aug**	**Sep**	**Oct**	**Nov**	**Dec**	**Annual**
2008													
2009												0.00m	0.00l
2010	0.00i	0.00	0.00	5.59	6.10	0.00	5.33	0.00	0.00	16.26	5.84	17.78	56.90a
2011	4.32	3.81	10.16	1.52	10.67	0.00	20.83	1.02	8.13	6.60	3.05	0.00	70.11
2012	4.06	2.03	5.33	9.40	5.08	0.00	45.21	27.69	33.78	19.05	0.00	3.81	155.45
Mean	4.19	1.95	5.16	5.50	7.28	0.00	23.79	9.57	13.97	13.97	2.96	7.20	94.15
S.D.	0.18	1.91	5.08	3.94	2.98	0.00	20.10	15.70	17.63	0.00	0.00	0.00	53.49
Skew	0.00	-0.08	-0.06	-0.04	0.62	0.00	0.26	0.70	0.54	-0.56	-0.05	0.58	0.66
Max	4.32	3.81	10.16	9.40	10.67	0.00	45.21	27.69	33.78	19.05	5.84	17.78	155.45
Min	4.06	0.00	0.00	1.52	5.08	0.00	5.33	0.00	0.00	6.60	0.00	0.00	56.90
# Yrs	2	3	3	3	3	3	3	3	3	3	3	3	3
a,b,c… = # of missing days/month or # missing months/year.													

Table B-3. Station 402 monthly climatology summaries.

Average Mean Wind Speed (m/s)													
Year	**Jan**	**Feb**	**Mar**	**Apr**	**May**	**Jun**	**Jul**	**Aug**	**Sep**	**Oct**	**Nov**	**Dec**	**Annual**
2011					5.10k	3.86	3.44	3.00	2.15	2.50	2.47	2.64	2.87e
2012	2.16	3.48	4.18	3.98	3.69	3.91	3.41	2.63	1.96	2.09	2.25	3.01	3.06
Mean	2.16	3.48	4.18	3.98	3.69	3.88	3.43	2.81	2.06	2.29	2.36	2.83	3.06
S.D.	0.00	0.00	0.00	0.00	0.00	0.03	0.02	0.26	0.13	0.29	0.16	0.26	
Skew	0.00	0.00	0.00	0.00	0.00	0.00	0.00	0.00	0.00	0.00	0.00	0.00	
Max	2.16	3.48	4.18	3.98	3.69	3.91	3.44	3.00	2.15	2.50	2.47	3.01	3.06
Min	2.16	3.48	4.18	3.98	3.69	3.86	3.41	2.63	1.96	2.09	2.25	2.64	3.06
Yrs	1	1	1	1	1	2	2	2	2	2	2	2	1
a,b,c… = # of missing days/month or # missing months/year.													

Maximum Wind Gust (m/s)													
Year	**Jan**	**Feb**	**Mar**	**Apr**	**May**	**Jun**	**Jul**	**Aug**	**Sep**	**Oct**	**Nov**	**Dec**	**Annual**
2011					21.17k	21.49	20.77	15.81	27.01	17.83	18.82	16.89	19.80e
2012	20.35	18.68	22.05	19.99	17.7	20.25	19.43	22.83	11.4	20.97	15.94	16.82	18.87
Mean	20.35	18.68	22.05	19.99	17.7	20.87	20.1	19.32	19.21	19.4	17.38	16.86	18.77
S.D.	0	0	0	0	0	0.88	0.95	4.96	11.04	2.22	2.04	0.05	0.58
Skew	0	0	0	0	0	0	0	0	0	0	0	0	-0.45
Max	20.35	18.68	22.05	19.99	17.7	21.49	20.77	22.83	27.01	20.97	18.82	16.89	18.87
Min	20.35	18.68	22.05	19.99	17.7	20.25	19.43	15.81	11.4	17.83	15.94	16.82	18.87
Yrs	1	1	1	1	1	2	2	2	2	2	2	2	1
a,b,c… = # of missing days/month or # missing months/year.													

Table B-3. Station 402 monthly climatology summaries (continued).

Average of Daily Average Air Temperature (Deg C)													
Year	**Jan**	**Feb**	**Mar**	**Apr**	**May**	**Jun**	**Jul**	**Aug**	**Sep**	**Oct**	**Nov**	**Dec**	**Annual**
2011					12.89k	19.39	23.07	23.55	18.94	11.21	1.64	-2.69	13.59e
2012	-0.17	1.62	5.93	10.77	16.47	21.31	23.15	23.98	19.19	11.36	4.83	-0.12	11.53
Mean	-0.17	1.62	5.93	10.77	16.47	20.35	23.11	23.77	19.07	11.29	3.24	-1.4	10.42
S.D.	0	0	0	0	0	1.36	0.06	0.3	0.18	0.11	2.26	1.82	0.76
Skew	0	0	0	0	0	0	0	0	0	0	0	0	-0.38
Max	-0.17	1.62	5.93	10.77	16.47	21.31	23.15	23.98	19.19	11.36	4.83	-0.12	11.53
Min	-0.17	1.62	5.93	10.77	16.47	19.39	23.07	23.55	18.94	11.21	1.64	-2.69	11.53
Yrs	1	1	1	1	1	2	2	2	2	2	2	2	1
a,b,c… = # of missing days/month or # missing months/year.													

Average of Daily Maximum Air Temperature (Deg C)													
Year	**Jan**	**Feb**	**Mar**	**Apr**	**May**	**Jun**	**Jul**	**Aug**	**Sep**	**Oct**	**Nov**	**Dec**	**Annual**
2011					19.90j	27.71	31.47	32.98	28.85	21.22	10.65	8.20	23.01e
2012	11.18	9.76	14.54	18.85	25.07	30.05	31.58	32.22	28.31	20.99	14.88	6.22	20.30
Mean	11.18	9.76	14.54	18.85	25.07	28.88	31.52	32.60	28.58	21.10	12.77	7.21	18.82
S.D.	0.00	0.00	0.00	0.00	0.00	1.65	0.08	0.54	0.38	0.16	2.99	1.40	0.79
Skew	0.00	0.00	0.00	0.00	0.00	0.00	0.00	0.00	0.00	0.00	0.00	0.00	0.42
Max	11.18	9.76	14.54	18.85	25.07	30.05	31.58	32.98	28.85	21.22	14.88	8.20	20.30
Min	11.18	9.76	14.54	18.85	25.07	27.71	31.47	32.22	28.31	20.99	10.65	6.22	20.30
Yrs	1	1	1	1	1	2	2	2	2	2	2	2	1
a,b,c… = # of missing days/month or # missing months/year.													

Table B-3. Station 402 monthly climatology summaries (continued).

Highest of Daily Maximum Air Temperature (Deg C)													
Year	**Jan**	**Feb**	**Mar**	**Apr**	**May**	**Jun**	**Jul**	**Aug**	**Sep**	**Oct**	**Nov**	**Dec**	**Annual**
2011					25.85k	34.42	36.07	35.24	32.25	28.59	17.23	15.51	28.47e
2012	17.68	17.01	21.98	29.38	32.30	33.91	38.28	35.93	31.87	29.59	22.67	13.16	26.98
Mean	17.68	17.01	21.98	29.38	32.30	34.16	37.17	35.59	32.06	29.09	19.95	14.34	26.15
S.D.	0.00	0.00	0.00	0.00	0.00	0.36	1.56	0.49	0.27	0.71	3.85	1.66	0.61
Skew	0.00	0.00	0.00	0.00	0.00	0.00	0.00	0.00	0.00	0.00	0.00	0.00	-1.01
Max	17.68	17.01	21.98	29.38	32.30	34.42	38.28	35.93	32.25	29.59	22.67	15.51	26.98
Min	17.68	17.01	21.98	29.38	32.30	33.91	36.07	35.24	31.87	28.59	17.23	13.16	26.98
Yrs	1	1	1	1	1	2	2	2	2	2	2	2	1
a,b,c… = # of missing days/month or # missing months/year.													

Average of Daily Minimum Air Temperature (Deg C)													
Year	**Jan**	**Feb**	**Mar**	**Apr**	**May**	**Jun**	**Jul**	**Aug**	**Sep**	**Oct**	**Nov**	**Dec**	**Annual**
2011					3.96j	8.13	12.65	11.33	7.90	0.99	-6.82	-11.28	3.27e
2012	-10.00	-7.06	-3.47	1.12	5.11	9.05	12.58	14.98	8.94	1.80	-4.28	-6.83	1.83
Mean	-10.00	-7.06	-3.47	1.12	5.11	8.59	12.62	13.16	8.42	1.39	-5.55	-9.06	0.57
S.D.	0.00	0.00	0.00	0.00	0.00	0.65	0.05	2.58	0.74	0.58	1.80	3.14	0.80
Skew	0.00	0.00	0.00	0.00	0.00	0.00	0.00	0.00	0.00	0.00	0.00	0.00	-0.10
Max	-10.00	-7.06	-3.47	1.12	5.11	9.05	12.65	14.98	8.94	1.80	-4.28	-6.83	1.83
Min	-10.00	-7.06	-3.47	1.12	5.11	8.13	12.58	11.33	7.90	0.99	-6.82	-11.28	1.83
Yrs	1	1	1	1	1	2	2	2	2	2	2	2	1
a,b,c… = # of missing days/month or # missing months/year.													

Table B-3. Station 402 monthly climatology summaries (continued).

Lowest of Daily Minimum Air Temperature (Deg C)													
Year	**Jan**	**Feb**	**Mar**	**Apr**	**May**	**Jun**	**Jul**	**Aug**	**Sep**	**Oct**	**Nov**	**Dec**	**Annual**
2011					-0.26k	-1.91	7.70	7.89	4.43	-8.71	-14.34	-16.16	-3.01e
2012	-18.86	-13.75	-12.90	-10.09	-1.15	1.65	8.03	8.28	4.24	-5.10	-11.79	-16.97	-5.70
Mean	-18.86	-13.75	-12.90	-10.09	-1.15	-0.13	7.86	8.09	4.33	-6.90	-13.06	-16.56	-7.06
S.D.	0.00	0.00	0.00	0.00	0.00	2.52	0.24	0.27	0.13	2.55	1.80	0.57	0.70
Skew	0.00	0.00	0.00	0.00	0.00	0.00	0.00	0.00	0.00	0.00	0.00	0.00	0.54
Max	-18.86	-13.75	-12.90	-10.09	-1.15	1.65	8.03	8.28	4.43	-5.10	-11.79	-16.16	0.00
Min	-18.86	-13.75	-12.90	-10.09	-1.15	-1.91	7.70	7.89	4.24	-8.71	-14.34	-16.97	-5.70
Yrs	1	1	1	1	1	2	2	2	2	2	2	2	1
a,b,c... = # of missing days/month or # missing months/year.													

Average Gamma Radiation (uR/hr)													
Year	**Jan**	**Feb**	**Mar**	**Apr**	**May**	**Jun**	**Jul**	**Aug**	**Sep**	**Oct**	**Nov**	**Dec**	**Annual**
2011												18.69h	
2012	18.58	18.37	18.09	17.97	18.14	18.18	17.80	17.71	17.93	18.16	18.40	18.30	18.14
Mean	18.58	18.37	18.09	17.97	18.14	18.18	17.80	17.71	17.93	18.16	18.40	18.30	21.33
S.D.	0.00	0.00	0.00	0.00	0.00	0.00	0.00	0.00	0.00	0.00	0.00	0.00	0.07
Skew	0.00	0.00	0.00	0.00	0.00	0.00	0.00	0.00	0.00	0.00	0.00	0.00	-0.34
Max	18.58	18.37	18.09	17.97	18.14	18.18	17.80	17.71	17.93	18.16	18.40	18.30	18.14
Min	18.58	18.37	18.09	17.97	18.14	18.18	17.80	17.71	17.93	18.16	18.40	18.30	18.14
Yrs	1	1	1	1	1	1	1	1	1	1	1	1	1
a,b,c... = # of missing days/month or # missing months/year.													

Table B-3. Station 402 monthly climatology summaries (continued).

Monthly Average Soil Temperature - 4 Inches (Deg C)													
Year	**Jan**	**Feb**	**Mar**	**Apr**	**May**	**Jun**	**Jul**	**Aug**	**Sep**	**Oct**	**Nov**	**Dec**	**Annual**
2011					16.09k	23.77	25.69	27.19	21.71	12.56	3.23	-1.32	16.12e
2012	0.06	2.53	6.82	13.43	20.97	25.72	25.58	26.06	21.01	12.71	6.39	1.72	13.58
Mean	0.06	2.53	6.82	13.43	20.97	24.74	25.63	26.62	21.36	12.64	4.81	0.20	14.27
S.D.	0.00	0.00	0.00	0.00	0.00	1.38	0.08	0.80	0.49	0.11	2.23	2.15	0.80
Skew	0.00	0.00	0.00	0.00	0.00	0.00	0.00	0.00	0.00	0.00	0.00	0.00	-0.65
Max	0.06	2.53	6.82	13.43	20.97	25.72	25.69	27.19	21.71	12.71	6.39	1.72	13.58
Min	0.06	2.53	6.82	13.43	20.97	23.77	25.58	26.06	21.01	12.56	3.23	-1.32	13.58
Yrs	1	1	1	1	1	2	2	2	2	2	2	2	1
a,b,c… = # of missing days/month or # missing months/year.													

Maximum Monthly Relative Humidity (%)													
Year	**Jan**	**Feb**	**Mar**	**Apr**	**May**	**Jun**	**Jul**	**Aug**	**Sep**	**Oct**	**Nov**	**Dec**	**Annual**
2011					100k	79	100	100	96	93	99	95	94e
2012	98	98	99	100	99	43	100	99	98	100	96	100	94
Mean	98	98	99	100	99	61	100	100	97	96	97	98	92
S.D.	0	0	0	0	0	25	0	0	1	5	2	3	2
Skew	0	0	0	0	0	0	0	0	0	0	0	0	0
Max	98	98	99	100	99	79	100	100	98	100	99	100	94
Min	98	98	99	100	99	43	100	99	96	93	96	95	94
Yrs	1	1	1	1	1	2	2	2	2	2	2	2	1
a,b,c… = # of missing days/month or # missing months/year.													

Table B-3. Station 402 monthly climatology summaries (continued).

Minimum Monthly Relative Humidity (%)												
Year	**Jan**	**Feb**	**Mar**	**Apr**	**May**	**Jun**	**Jul**	**Aug**	**Sep**	**Oct**	**Nov**	**Dec**	**Annual**
2011					4k	3	3	2	3	6	6	10	5e
2012	5	2	5	0	2	0	2	5	4	8	11	22	5
Mean	5	2	5	0	2	1	2	3	3	7	9	16	7
S.D.	0	0	0	0	0	2	1	2	1	2	4	9	2
Skew	0	0	0	0	0	0	0	0	0	0	0	0	-1
Max	5	2	5	0	2	3	3	5	4	8	11	22	5
Min	5	2	5	0	2	0	2	2	3	6	6	10	5
Yrs	1	1	1	1	1	2	2	2	2	2	2	2	1
a,b,c… = # of missing days/month or # missing months/year.													

Average Monthly Barometric Pressure (mbar)													
Year	**Jan**	**Feb**	**Mar**	**Apr**	**May**	**Jun**	**Jul**	**Aug**	**Sep**	**Oct**	**Nov**	**Dec**	**Annual**
2011					831.00k	832.80	835.40	836.30	838.10	837.40	836.40	836.70k	836.07f
2012				835.30k	833.80	833.50	837.20	837.70	839.10	836.80	838.00	834.00	836.26d
Mean					833.80	833.15	836.30	837.00	838.60	837.10	837.20	834.00	
S.D.					0	0.49	1.27	0.99	0.71	0.42	1.13	0	
Skew					0	0	0	0	0	0	0	0	
Max					833.80	833.50	837.20	837.70	839.10	837.40	838.00	834.00	
Min					833.80	832.80	835.40	836.30	838.10	836.80	836.40	834.00	
Yrs	0	0	0	0	1	2	2	2	2	2	2	1	0
a,b,c… = # of missing days/month or # missing months/year.													

Table B-3. Station 402 monthly climatology summaries (continued).

Total Precipitation (mm)													
Year	**Jan**	**Feb**	**Mar**	**Apr**	**May**	**Jun**	**Jul**	**Aug**	**Sep**	**Oct**	**Nov**	**Dec**	**Annual**
2011					5.08k	0.51	42.42	2.29	8.89	22.35	4.57	0.00	81.03e
2012	2.29	1.02	9.65	6.86	5.33	0.00	93.22	29.21	21.84	17.53	0.25	3.81	191.01
Mean	2.29	1.02	9.65	6.86	5.33	0.25	67.82	15.75	15.37	19.94	2.41	1.91	94.15
S.D.	0.00	0.00	0.00	0.00	0.00	0.36	35.92	19.04	9.16	3.41	3.05	2.69	53.49
Skew	0.00	0.00	0.00	0.00	0.00	0.00	0.00	0.00	0.00	0.00	0.00	0.00	0.66
Max	2.29	1.02	9.65	6.86	5.33	0.51	93.22	29.21	21.84	22.35	4.57	3.81	191.01
Min	2.29	1.02	9.65	6.86	5.33	0.00	42.42	2.29	8.89	17.53	0.25	0.00	191.01
Yrs	1	1	1	1	1	2	2	2	2	2	2	2	1
a,b,c… = # of missing days/month or # missing months/year.													

APPENDIX C: MONTHLY EXTREME TEMPERATURES FOR STATIONS 400, 401, AND 402

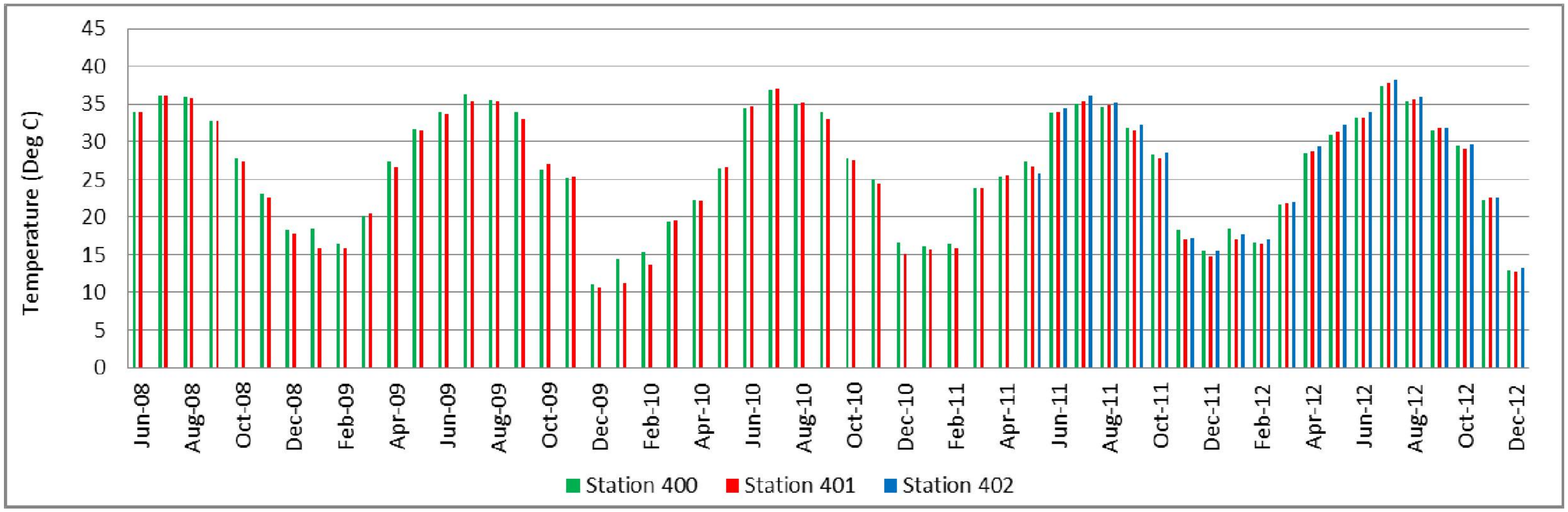

Figure C-1. Highest of daily maximum temperatures for TTR monitoring Stations 400, 401, and 402.

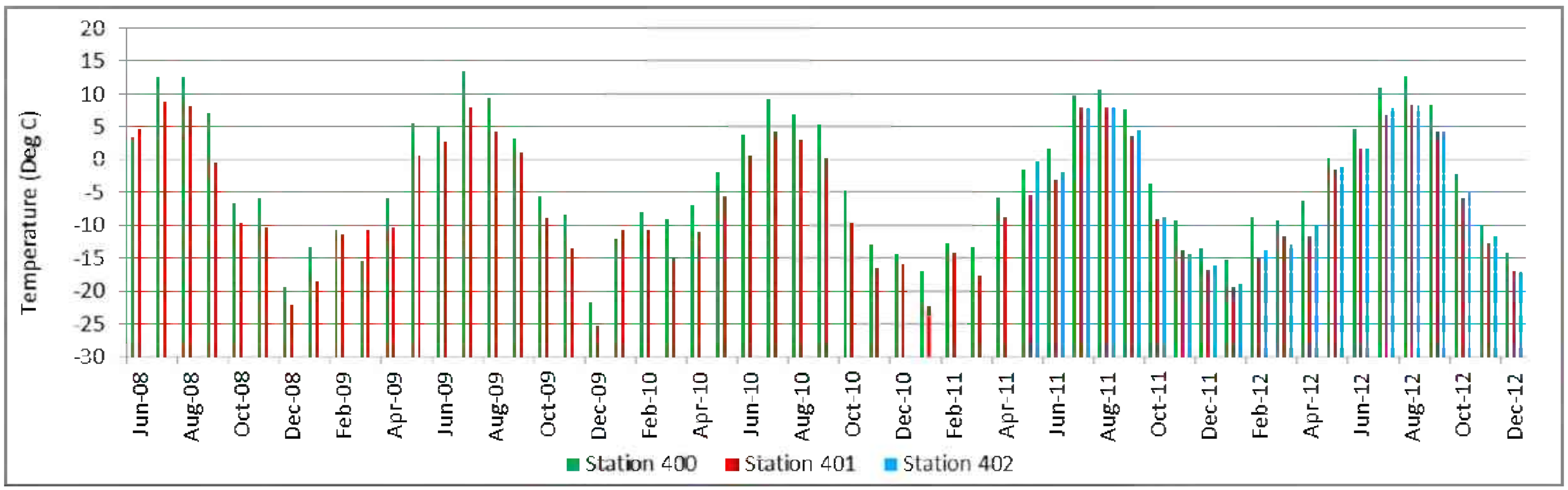

Figure C-2. Lowest of daily minimum temperatures for TTR monitoring Stations 400, 401, and 402.

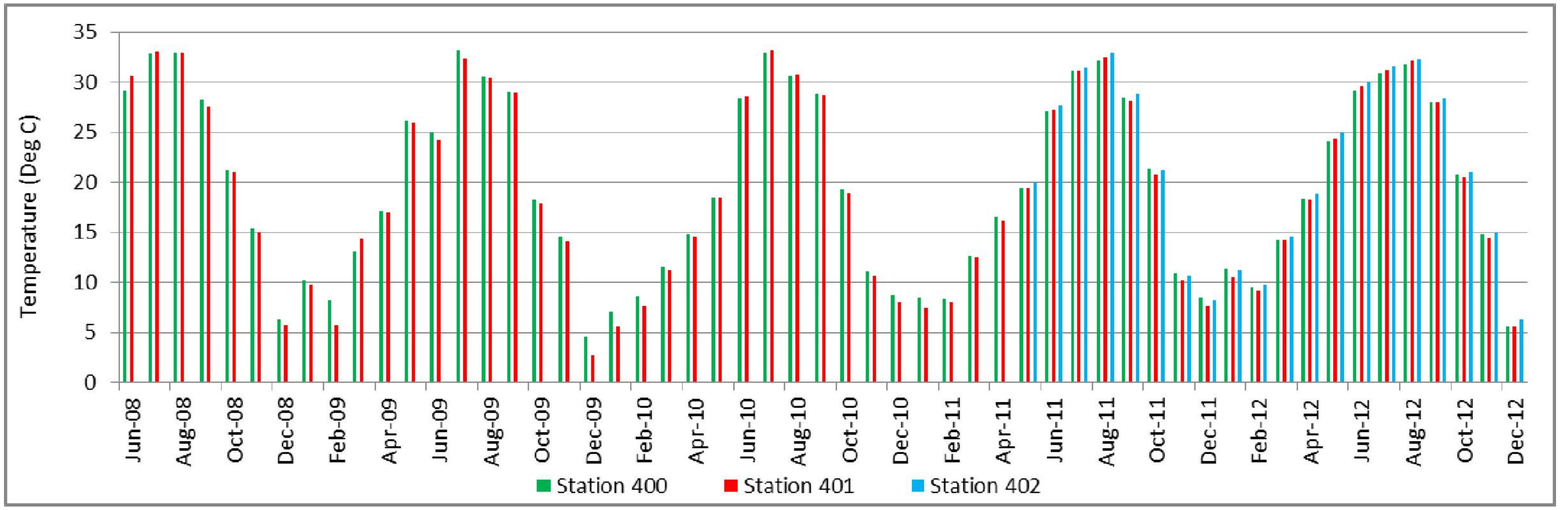

Figure C-3. Average of daily maximum temperatures for TTR monitoring Stations 400, 401, and 402.

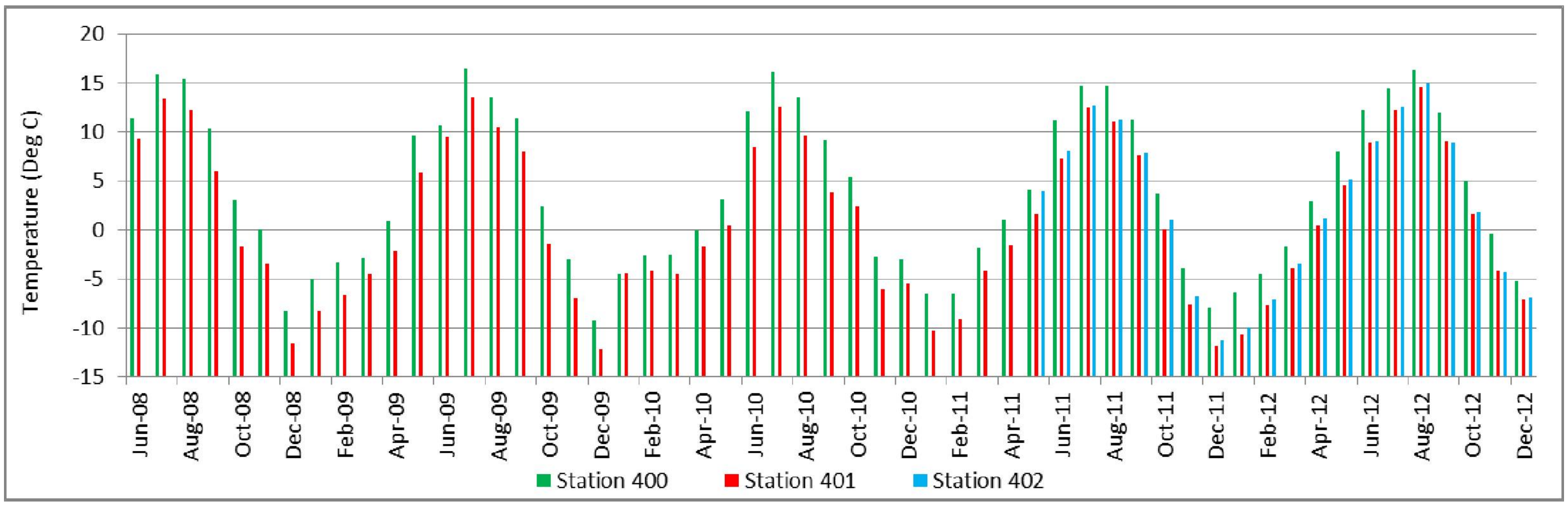

Figure C-4. Average of daily minimum temperatures for TTR monitoring Stations 400, 401, and 402.

APPENDIX D: GROSS ALPHA AND GROSS BETA RESULTS PRESENTED IN ANNUAL PLOTS FOR THE PERIOD OF RECORD AT EACH TONOPAH TEST RANGE MONITORING STATION

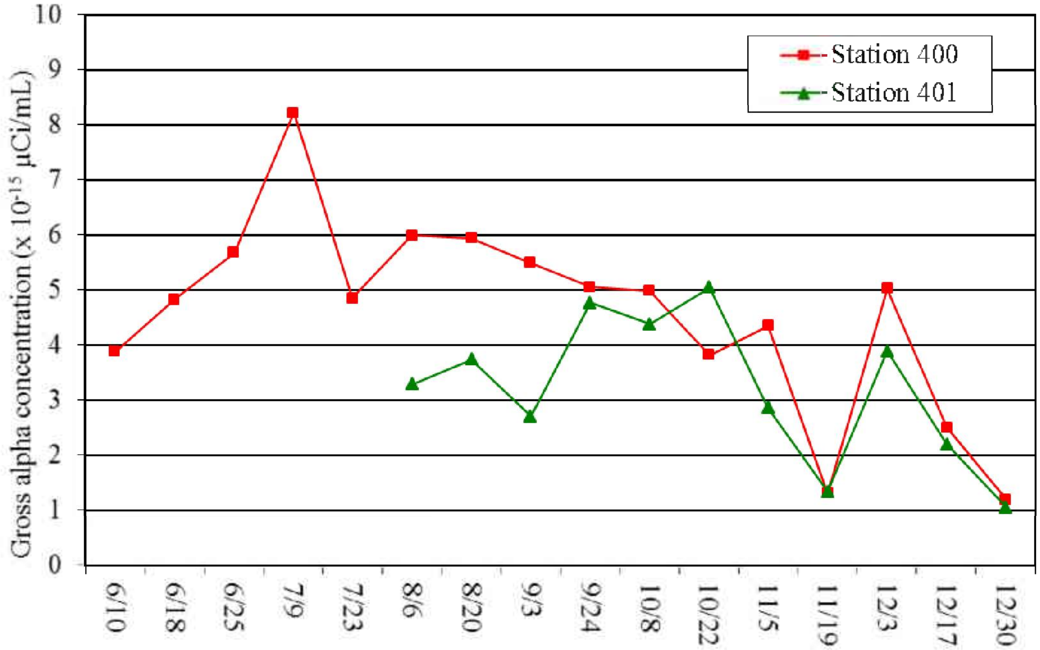

Figure D-1. Gross alpha results for TTR stations 400 and 401 for CY2008.

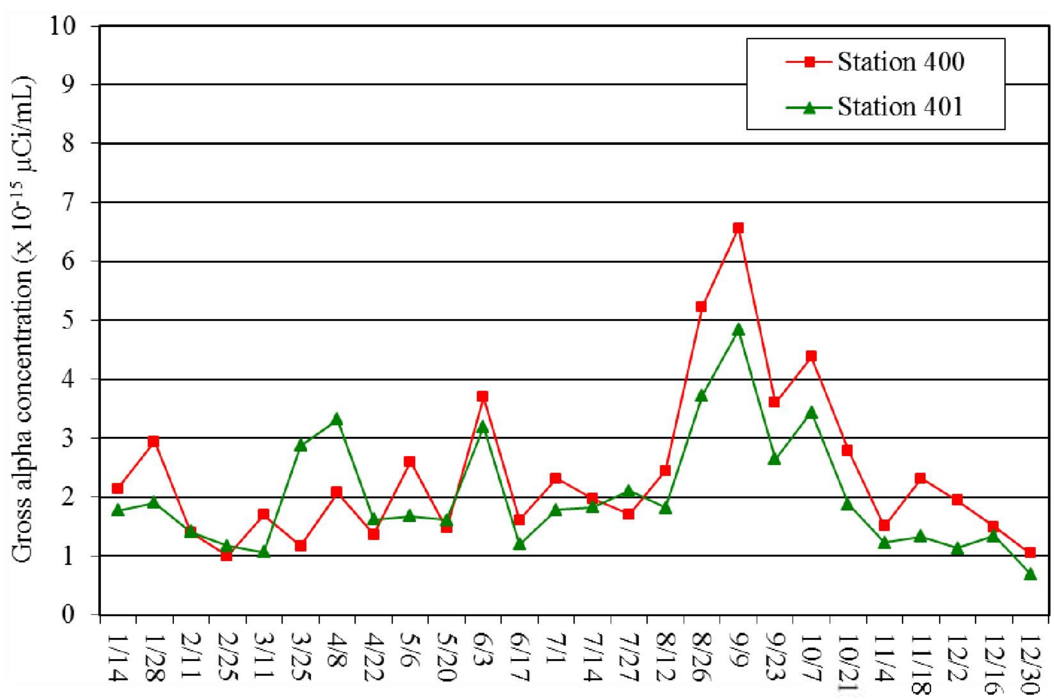

Figure D-2. Gross alpha results for TTR Stations 400 and 401 for CY2009.

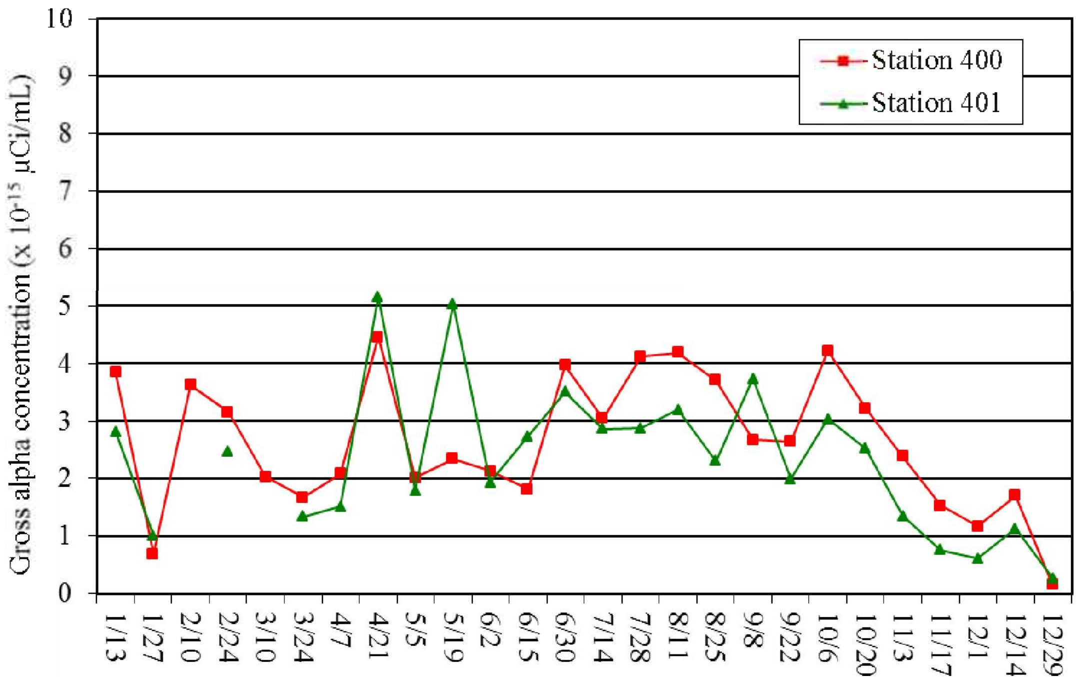

Figure D-3. Gross alpha results for TTR Stations 400 and 401 for CY2010.

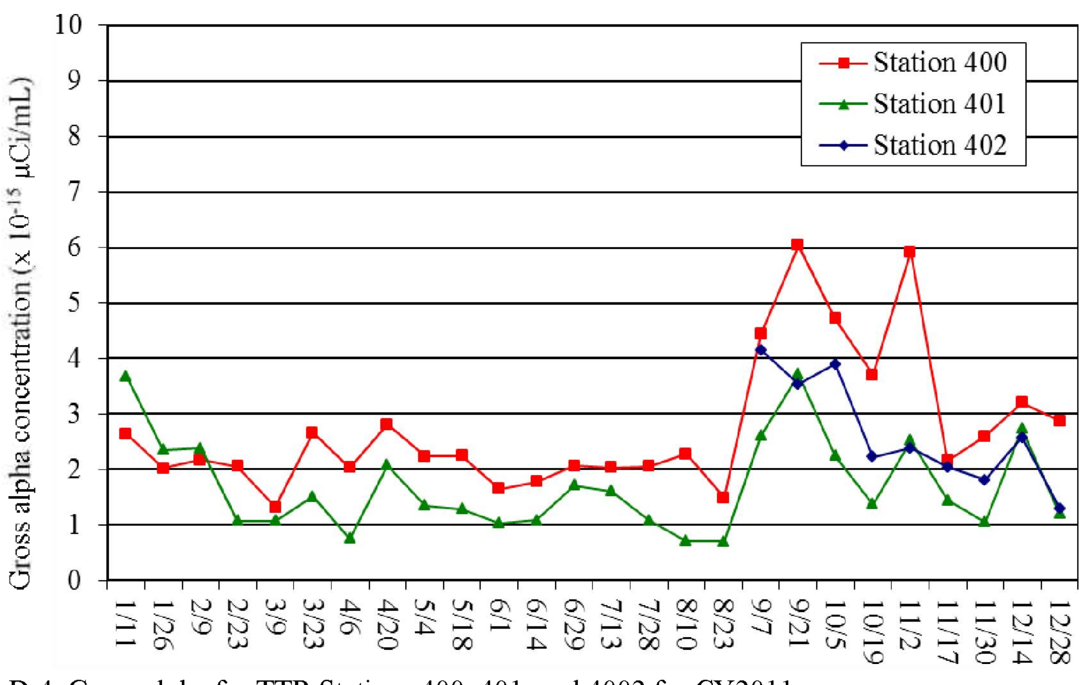

Figure D-4. Gross alpha for TTR Stations 400, 401, and 4002 for CY2011.

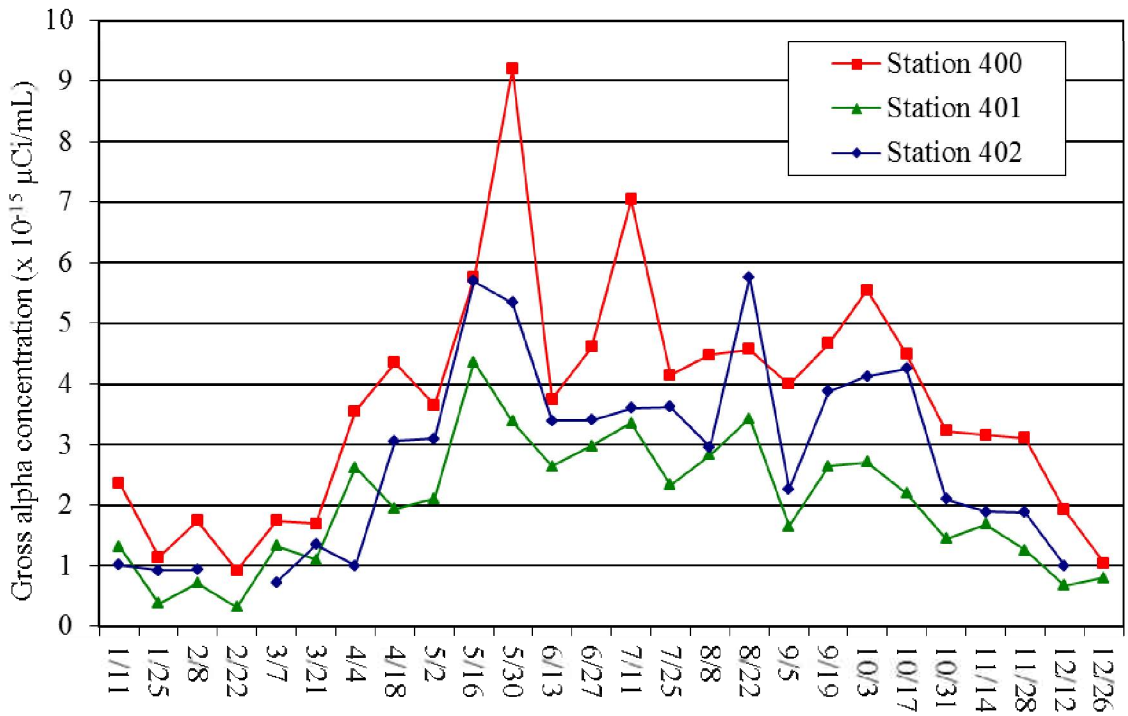

Figure D-5. Gross alpha results for TTR Stations 400, 401, and 402 for CY2012.

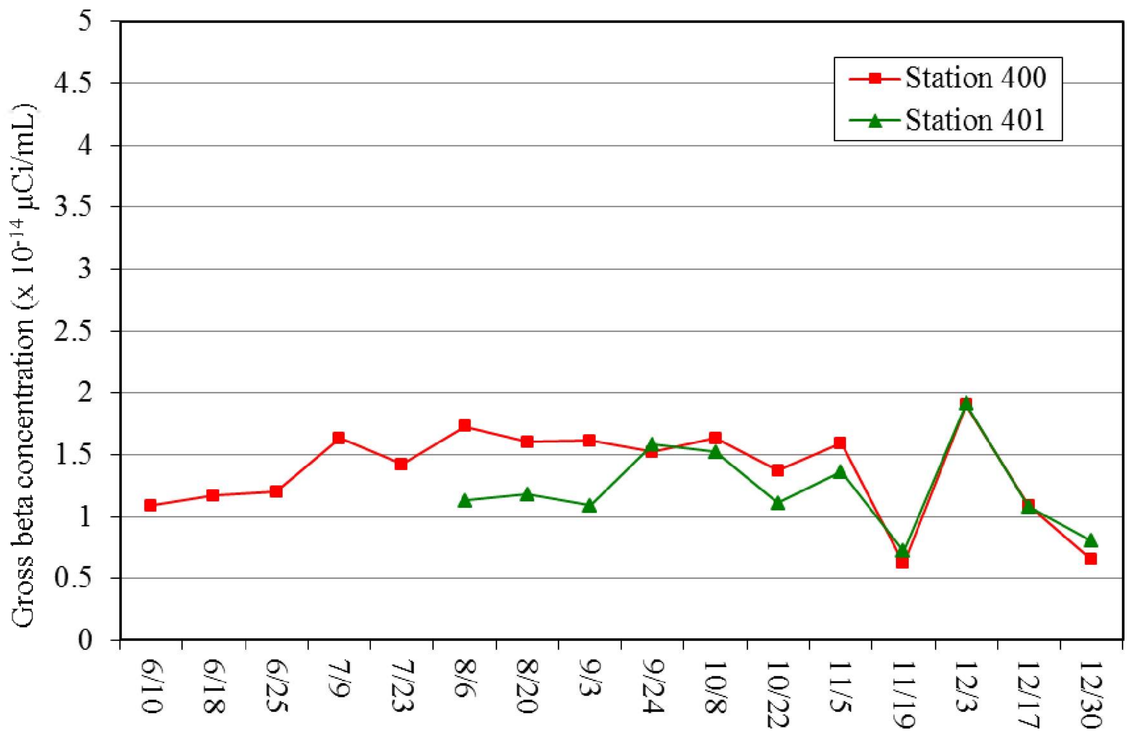

Figure D-6. Gross beta results for TTR Stations 400 and 401 for CY2008.

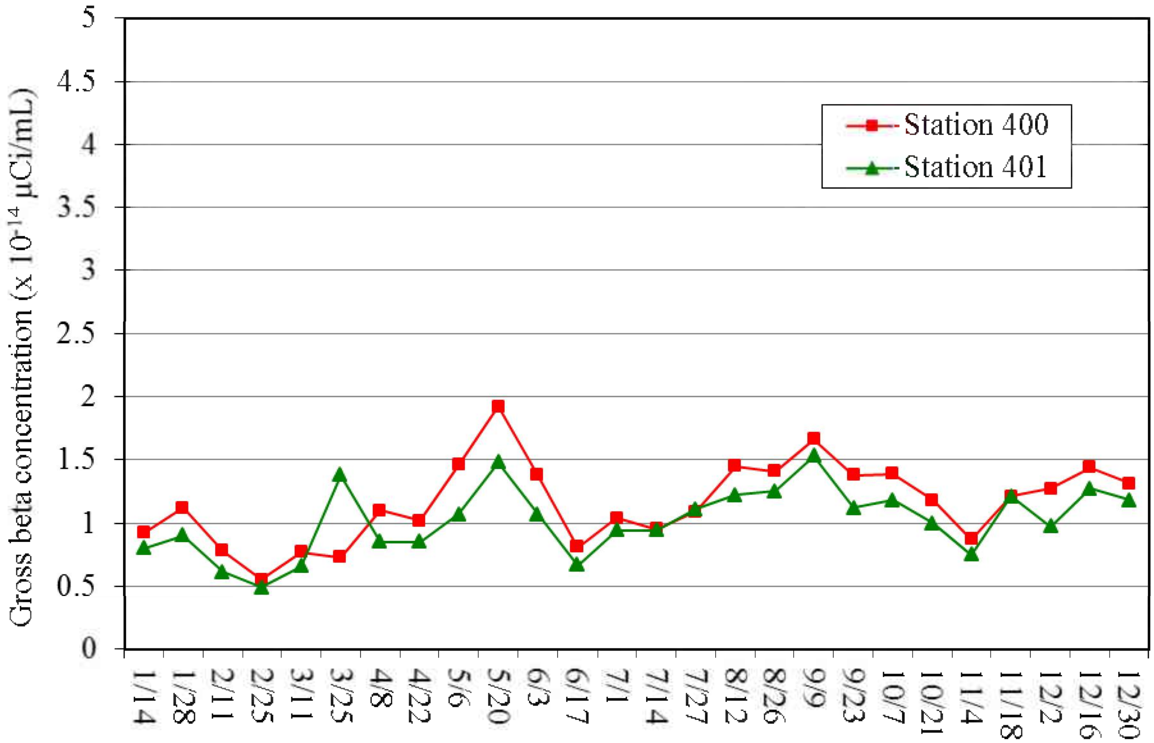

Figure D-7. Gross beta results for TTR Station 400 and 401 for CY2009.

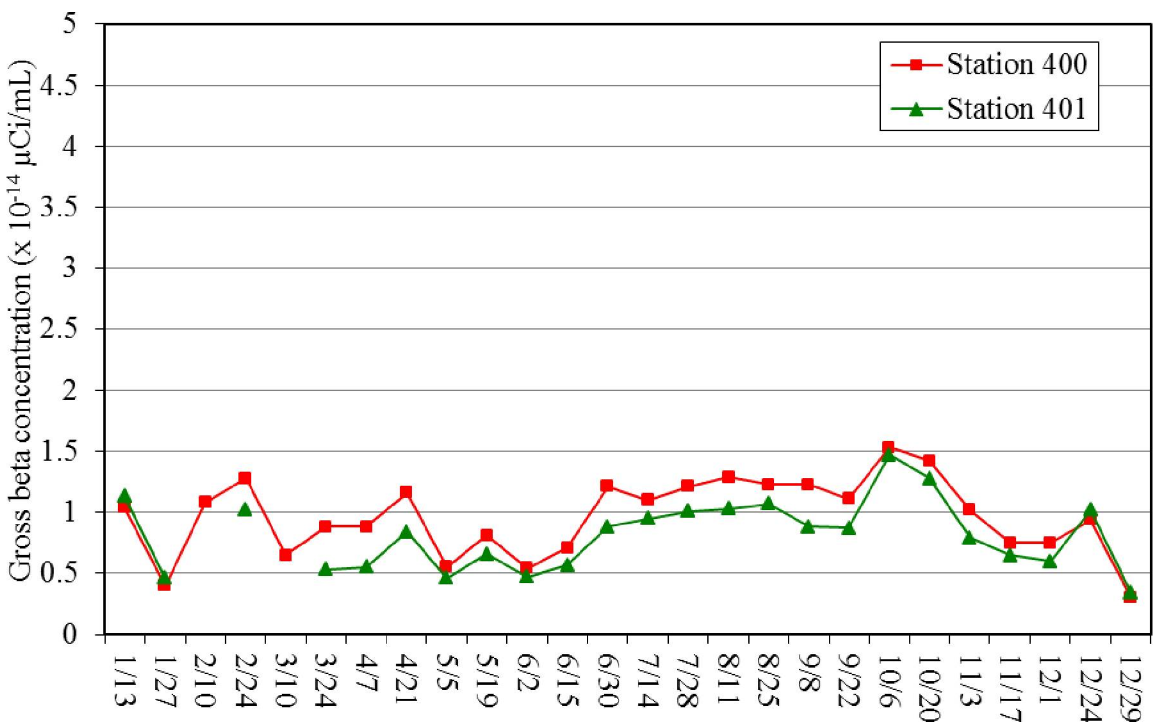

Figure D-8. Gross beta results for TTR Stations 400 and 401 for CY2010.

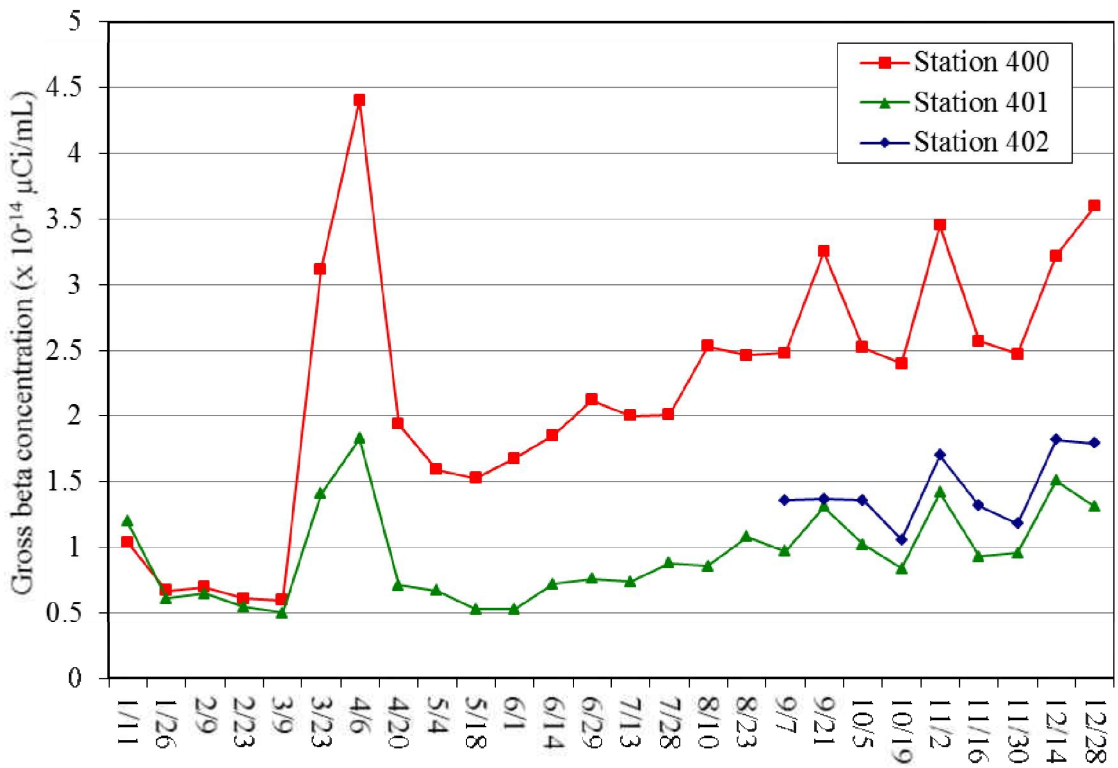

Figure D-9. Gross beta results for TTR Stations 400 and 401 for CY2011.

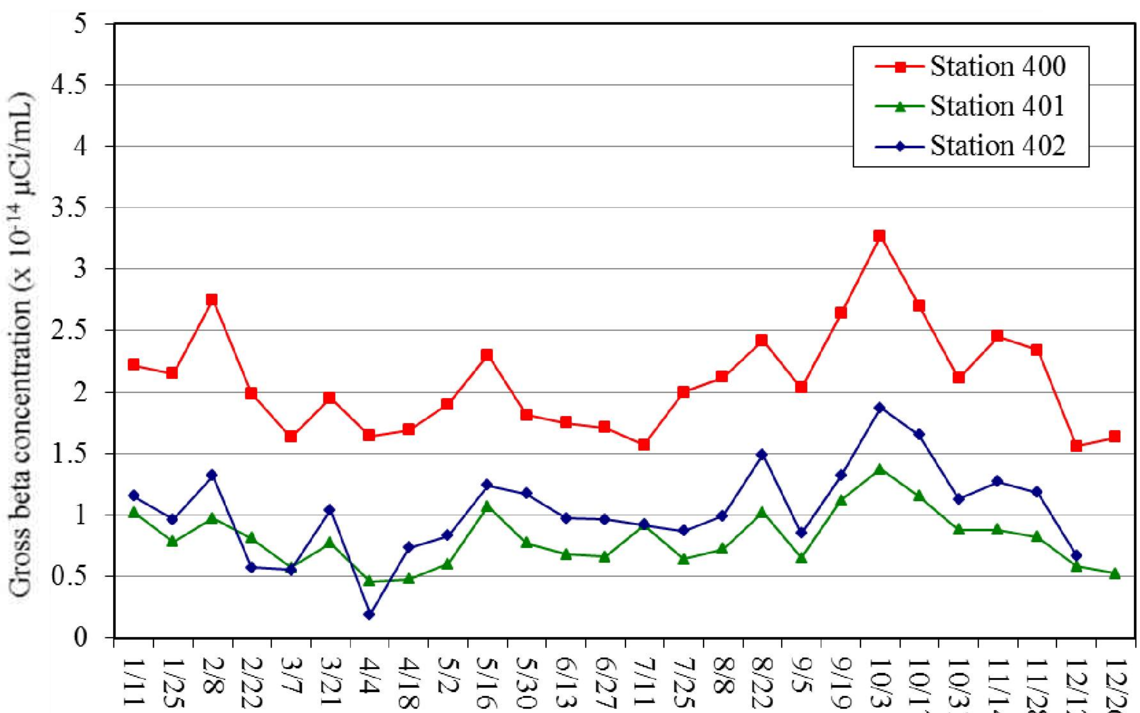

Figure D-10. Gross beta for TTR Stations 400, 401, and 402 for CY2012.

APPENDIX E: OBSERVED GAMMA VALUES THAT EXCEED STATION MAXIMUM BACKGROUND VALUE

Table E-1: Occasions when the observed PIC value exceeded the specified maximum background level at Station 400.

Table E-2: Occasions when the observed PIC value exceeded the specified maximum background level at Station 401.

Table E-3: Occasions when the observed PIC value exceeded the specified maximum background level at Station 402.

Table E-1. Observed PIC values of gamma exceeded the period-of-record defined maximum background level 47 times at Station 400.

Date (mm/dd/yyyy)	Start Time (hh:mm)	Duration (hh:mm)	Maximum Observed Gamma (μR/h)	Max Obs Gamma – Max Background Value (μR/h)
2/8/2009	0:50	3:10	23.41	0.89
3/15/2009	7:30	2:20	22.97	0.45
3/22/2009	11:30	3:20	23.77	1.25
3/29/2009	4:20	5:00	22.77	0.25
3/31/2009	4:00	0:10	22.57	0.05
4/2/2009	6:10	1:50	22.88	0.36
4/7/2009	7:10	0:50	22.83	0.31
4/8/2009	1:10	2:20	23.86	1.34
4/13/2009	7:20	1:00	22.69	0.17
4/14/2009	4:10	18:20	25.19	2.67
4/15/2009	0:10	6:00	22.69	0.17
4/22/2009	4:00	4:10	22.78	0.26
4/23/2009	0:50	7:40	22.82	0.3
5/10/2009	22:40	0:50	22.68	0.16
5/11/2009	0:00	7:50	22.89	0.37
5/18/2009	3:40	6:10	22.95	0.43
5/19/2009	3:50	3:50	22.82	0.3
5/19/2009	13:30	4:50	24.72	2.2
5/20/2009	3:30	3:20	23	0.48
5/29/2009	15:10	0:50	23.67	1.15
6/6/2009	17:40	0:40	22.96	0.44
6/15/2009	19:00	0:40	23.29	0.77
6/17/2009	15:10	0:20	22.64	0.12

Table E-1. Observed PIC values of gamma exceeded the period-of-record defined maximum background level 47 times at Station 400 (continued).

Date (mm/dd/yyyy)	Start Time (hh:mm)	Duration (hh:mm)	Maximum Observed Gamma (µR/h)	Max Obs Gamma – Max Background Value (µR/h)
6/20/2009	9:20	1:00	23.26	0.74
7/18/2009	16:20	0:10	22.69	0.17
7/19/2009	17:10	0:50	23	0.48
7/20/2009	18:10	3:20	26.5	3.98
7/28/2009	19:50	1:40	22.94	0.42
7/29/2009	14:50	0:10	22.57	0.05
7/31/2009	17:50	0:10	22.68	0.16
10/7/2009	13:10	1:50	23.59	1.07
10/19/2009	16:10	1:40	22.81	0.29
12/7/2009	18:00	3:00	23.46	0.94
12/13/2009	1:00	2:50	23.8	1.28
12/22/2009	5:30	1:10	24.38	1.86
1/21/2010	15:10	2:30	22.8	0.28
3/8/2010	22:40	1:10	23.5	0.98
3/18/2010	14:10	0:10	22.85	0.33
4/21/2010	5:30	1:40	23.23	0.71
4/22/2010	3:10	3:00	24.04	1.52
5/9/2010	17:40	3:30	23.02	0.5
5/23/2010	14:00	0:30	22.68	0.16
7/16/2010	17:50	1:10	23.56	1.04
7/26/2010	6:30	1:40	23.94	1.42
5/18/2011	12:20	0:20	22.88	0.36
7/7/2011	19:20	0:10	22.54	0.02
1/21/2012	9:10	1:20	24	1.48

Table E-2. Observed gamma values exceeded the period-of-record maximum background level 85 times at Station 401.

Date (mm/dd/yyyy)	Start Time (hh:mm)	Duration (hh:mm)	Maximum Observed Gamma (μR/h)	Max Obs Gamma – Max Background Value (μR/h)
2/7/2010	16:00	1:00	25.55	1.23
5/23/2010	14:10	1:30	24.79	0.47
7/26/2010	6:40	1:30	25.54	1.22
9/29/2010	7:20	1:00	24.37	0.05
9/30/2010	8:10	0:20	24.71	0.39
10/11/2010	6:50	0:50	25.05	0.73
10/17/2010	19:10	0:30	25.04	0.72
11/4/2010	8:00	0:30	24.54	0.22
11/8/2010	0:50	1:30	25.58	1.26
12/1/2010	7:50	0:20	24.37	0.05
12/2/2010	7:10	1:50	25.59	1.27
12/5/2010	8:10	1:10	24.61	0.29
12/10/2010	9:00	0:10	24.36	0.04
12/13/2010	8:20	0:50	25.17	0.85
12/14/2010	3:00	6:30	25.61	1.29
12/26/2010	0:40	0:20	24.67	0.35
1/7/2011	8:00	0:30	24.89	0.57
1/8/2011	8:40	0:30	25.71	1.39
1/28/2011	7:00	1:30	24.61	0.29
1/29/2011	7:10	1:30	24.82	0.5
3/7/2011	6:20	0:30	24.49	0.17
5/8/2011	14:10	0:10	24.37	0.05
7/7/2011	17:00	1:00	25.52	1.2
10/21/2011	7:50	0:10	24.71	0.39
10/24/2011	8:00	0:10	24.34	0.02
10/25/2011	7:50	0:10	24.43	0.11
10/28/2011	7:50	0:10	24.47	0.15
10/29/2011	7:30	1:00	25.01	0.69
10/31/2011	6:30	2:10	25.21	0.89
11/3/2011	8:10	0:10	24.37	0.05
11/14/2011	8:00	0:30	24.71	0.39
11/25/2011	8:00	1:10	25.08	0.76
11/29/2011	7:50	1:10	24.73	0.41
11/30/2011	7:30	1:40	26.59	2.27
12/7/2011	7:50	1:10	25.23	0.91
12/8/2011	5:30	3:30	25.75	1.43
12/9/2011	8:00	0:10	24.48	0.16

Table E-2. Observed gamma values exceeded the period-of-record maximum background level 85 times at Station 401 (continued).

Date (mm/dd/yyyy)	Start Time (hh:mm)	Duration (hh:mm)	Maximum Observed Gamma (μR/h)	Max Obs Gamma – Max Background Value (μR/h)
12/10/2011	7:50	1:40	24.82	0.5
12/11/2011	4:20	6:00	26.56	2.24
12/12/2011	4:40	6:00	25.96	1.64
12/13/2011	8:40	0:10	24.37	0.05
12/14/2011	7:50	1:30	25.88	1.56
12/18/2011	8:00	1:00	25.31	0.99
12/21/2011	8:10	0:10	24.48	0.16
12/25/2011	7:50	0:40	24.94	0.62
12/26/2011	5:40	3:10	25.25	0.93
12/27/2011	6:20	4:20	25.98	1.66
12/28/2011	7:50	1:10	24.89	0.57
12/29/2011	7:40	1:50	26.26	1.94
12/30/2011	7:30	2:20	25.69	1.37
1/1/2012	8:10	0:20	24.75	0.43
1/2/2012	8:10	0:20	24.46	0.14
1/3/2012	8:10	0:40	24.65	0.33
1/5/2012	8:30	1:50	24.76	0.44
1/6/2012	2:50	7:20	26.47	2.15
1/10/2012	7:00	2:30	25.88	1.56
1/13/2012	8:10	0:40	24.62	0.3
1/14/2012	7:10	2:30	25.41	1.09
1/15/2012	8:10	1:50	25.46	1.14
1/17/2012	8:20	0:10	24.68	0.36
1/20/2012	7:20	1:30	25.12	0.8
1/21/2012	10:00	1:00	25.54	1.22
1/26/2012	8:40	0:20	24.35	0.03
1/30/2012	6:30	3:00	26.41	2.09
1/31/2012	7:30	1:40	24.94	0.62
2/6/2012	8:10	1:00	24.98	0.66
2/10/2012	8:10	0:40	24.89	0.57
2/11/2012	8:20	0:30	24.73	0.41
2/13/2012	13:20	1:00	25.74	1.42
2/15/2012	14:30	0:40	24.83	0.51
2/18/2012	8:10	1:20	24.48	0.16
3/10/2012	7:40	0:10	24.39	0.07
4/14/2012	13:10	1:00	26.27	1.95
5/26/2012	9:20	0:10	24.44	0.12

Table E-2. Observed gamma values exceeded the period-of-record maximum background level 85 times at Station 401 (continued).

Date (mm/dd/yyyy)	Start Time (hh:mm)	Duration (hh:mm)	Maximum Observed Gamma (μR/h)	Max Obs Gamma – Max Background Value (μR/h)
8/14/2012	14:20	0:10	24.44	0.12
9/11/2012	6:50	1:10	25.18	0.86
11/3/2012	8:00	0:20	24.49	0.17
11/7/2012	7:50	0:50	24.66	0.34
11/14/2012	7:50	0:50	24.9	0.58
11/24/2012	8:00	0:30	24.49	0.17
11/25/2012	3:00	6:30	25.96	1.64
11/26/2012	8:00	0:20	24.64	0.32
12/5/2012	8:40	1:00	24.83	0.51
12/6/2012	8:50	0:10	24.37	0.05
12/8/2012	8:00	1:10	24.93	0.61

Table E-3. Observed gamma values exceeded the period-of-record maximum background level five times at Station 402.

Date (mm/dd/yyyy)	Start Time (hh:mm)	Duration (hh:mm)	Maximum Observed Gamma (μR/h)	Max Obs Gamma – Max Background Value (μR/h)
12/27/2011	5:00	0:10	21.33	0.17
12/29/2011	7:00	0:10	21.18	0.02
1/6/2012	7:30	1:40	21.49	0.33
5/26/2012	7:20	0:20	21.21	0.05
8/20/2012	23:40	0:40	22.54	1.38